ISSN 1948-5182 (online)

World Journal of *Hepatology*

World J Hepatol 2017 January 8; 9(1): 1-68

Published by Baishideng Publishing Group Inc

World Journal of Hepatology

A peer-reviewed, online, open-access journal of hepatology

Editorial Board

2014-2017

The *World Journal of Hepatology* Editorial Board consists of 474 members, representing a team of worldwide experts in hepatology. They are from 52 countries, including Algeria (1), Argentina (6), Armenia (1), Australia (2), Austria (4), Bangladesh (2), Belgium (3), Botswana (2), Brazil (13), Bulgaria (2), Canada (3), Chile (1), China (97), Czech Repoublic (1), Denmark (2), Egypt (12), France (6), Germany (20), Greece (11), Hungary (5), India (15), Indonesia (3), Iran (4), Israel (1), Italy (54), Japan (35), Jordan (1), Malaysia (2), Mexico (3), Moldova (1), Netherlands (3), Nigeria (1), Pakistan (1), Philippines (2), Poland (1), Portugal (2), Qatar (1), Romania (6), Russia (2), Saudi Arabia (4), Singapore (1), South Korea (12), Spain (20), Sri Lanka (1), Sudan (1), Sweden (1), Switzerland (1), Thailand (4), Turkey (21), Ukraine (3), United Kingdom (18), and United States (55).

Chile

Luis A Videla, *Santiago*

China

Guang-Wen Cao, *Shanghai*
En-Qiang Chen, *Chengdu*
Gong-Ying Chen, *Hangzhou*
Jin-lian Chen, *Shanghai*
Jun Chen, *Changsha*
Alfred Cheng, *Hong Kong*
Chun-Ping Cui, *Beijing*
Shuang-Suo Dang, *Xi'an*
Ming-Xing Ding, *Jinhua*
Zhi-Jun Duang, *Dalian*
He-Bin Fan, *Wuhan*
Xiao-Ming Fan, *Shanghai*
James Yan Yue Fung, *Hong Kong*
Yi Gao, *Guangzhou*
Zuo-Jiong Gong, *Wuhan*
Zhi-Yong Guo, *Guangzhou*
Shao-Liang Han, *Wenzhou*
Tao Han, *Tianjin*
Jin-Yang He, *Guangzhou*
Ming-Liang He, *Hong Kong*
Can-Hua Huang, *Chengdu*
Bo Jin, *Beijing*
Shan Jin, *Hohhot*
Hui-Qing Jiang, *Shijiazhuang*
Wan-Yee Joseph Lau, *Hong Kong*
Guo-Lin Li, *Changsha*
Jin-Jun Li, *Shanghai*
Qiang Li, *Jinan*
Sheng Li, *Jinan*
Zong-Fang Li, *Xi'an*
Xu Li, *Guangzhou*
Xue-Song Liang, *Shanghai*
En-Qi Liu, *Xi'an*
Pei Liu, *Shenyang*
Zhong-Hui Liu, *Changchun*
Guang-Hua Luo, *Changzhou*
Yi Lv, *Xi'an*
Guang-Dong Pan, *Liuzhou*
Wen-Sheng Pan, *Hangzhou*
Jian-Min Qin, *Shanghai*
Wai-Kay Seto, *Hong Kong*
Hong Shen, *Changsha*
Xiao Su, *Shanghai*
Li-Ping Sun, *Beijing*
Wei-Hao Sun, *Nanjing*
Xue-Ying Sun, *Harbin*
Hua Tang, *Tianjin*
Ling Tian, *Shanghai*
Eric Tse, *Hong Kong*
Guo-Ying Wang, *Changzhou*
Yue Wang, *Beijing*
Shu-Qiang Wang, *Chengdu*
Mary MY Waye, *Hong Kong*
Hong-Shan Wei, *Beijing*
Danny Ka-Ho Wong, *Hong Kong*
Grace Lai-Hung Wong, *Hong Kong*
Bang-Fu Wu, *Dongguan*
Xiong-Zhi Wu, *Tianjin*
Chun-Fang Xu, *Suzhou*
Rui-An Xu, *Quanzhou*
Rui-Yun Xu, *Guangzhou*
Wei-Li Xu, *Shijiazhuang*
Shi-Ying Xuan, *Qingdao*
Ming-Xian Yan, *Jinan*
Lv-Nan Yan, *Chengdu*
Jin Yang, *Hangzhou*
Ji-Hong Yao, *Dalian*
Winnie Yeo, *Hong Kong*
Zheng Zeng, *Beijing*
Qi Zhang, *Hangzhou*
Shi-Jun Zhang, *Guangzhou*
Xiao-Lan Zhang, *Shijiazhuang*
Xiao-Yong Zhang, *Guangzhou*
Yong Zhang, *Xi'an*
Hong-Chuan Zhao, *Hefei*
Ming-Hua Zheng, *Wenzhou*
Yu-Bao Zheng, *Guangzhou*
Ren-Qian Zhong, *Shanghai*
Fan Zhu, *Wuhan*
Xiao Zhu, *Dongguan*

Czech Repoublic

Kamil Vyslouzil, *Olomouc*

Denmark

Henning Gronbaek, *Aarhus*
Christian Mortensen, *Hvidovre*

Egypt

Ihab T Abdel-Raheem, *Damanhour*
NGB G Bader EL Din, *Cairo*
Hatem Elalfy, *Mansoura*
Mahmoud M El-Bendary, *Mansoura*
Mona El SH El-Raziky, *Cairo*
Mohammad El-Sayed, *Cairo*
Yasser M Fouad, *Minia*
Mohamed AA Metwally, *Benha*
Hany Shehab, *Cairo*
Mostafa M Sira, *Shebin El-koom*
Ashraf Taye, *Minia*
MA Ali Wahab, *Mansoura*

France

Laurent Alric, *Toulouse*
Sophie Conchon, *Nantes*
Daniel J Felmlee, *Strasbourg*
Herve Lerat, *Creteil*
Dominique Salmon, *Paris*
Jean-Pierre Vartanian, *Paris*

Germany

Laura E Buitrago-Molina, *Hannover*
Enrico N De Toni, *Munich*
Oliver Ebert, *Muenchen*
Rolf Gebhardt, *Leipzig*
Janine V Hartl, *Regensburg*
Sebastian Hinz, *Kiel*
Benjamin Juntermanns, *Essen*
Roland Kaufmann, *Jena*
Viola Knop, *Frankfurt*
Veronika Lukacs-Kornek, *Homburg*
Benjamin Maasoumy, *Hannover*
Jochen Mattner, *Erlangen*
Nadja M Meindl-Beinker, *Mannheim*
Ulf P Neumann, *Aachen*
Margarete Odenthal, *Cologne*
Yoshiaki Sunami, *Munich*
Christoph Roderburg, *Aachen*
Frank Tacke, *Aachen*
Yuchen Xia, *Munich*

Greece

Alex P Betrosian, *Athens*
George N Dalekos, *Larissa*
Ioanna K Delladetsima, *Athens*
Nikolaos K Gatselis, *Larissa*
Stavros Gourgiotis, *Athens*
Christos G Savopoulos, *Thessaloniki*
Tania Siahanidou, *Athens*
Emmanouil Sinakos, *Thessaloniki*
Nikolaos G Symeonidi, *Thessaloniki*
Konstantinos C Thomopoulos, *Larissa*
Konstantinos Tziomalos, *Thessaloniki*

Hungary

Gabor Banhegyi, *Budapest*
Peter L Lakatos, *Budapest*
Maria Papp, *Debrecen*
Ferenc Sipos, *Budapest*
Zsolt J Tulassay, *Budapest*

India

Deepak N Amarapurkar, *Mumbai*
Girish M Bhopale, *Pune*
Sibnarayan Datta, *Tezpur*
Nutan D Desai, *Mumbai*
Sorabh Kapoor, *Mumbai*
Jaswinder S Maras, *New Delhi*
Nabeen C Nayak, *New Delhi*
C Ganesh Pai, *Manipal*
Amit Pal, *Chandigarh*
K Rajeshwari, *New Delhi*
Anup Ramachandran, *Vellore*
D Nageshwar Reddy, *Hyderabad*
Shivaram P Singh, *Cuttack*
Ajith TA, *Thrissur*
Balasubramaniyan Vairappan, *Pondicherry*

Indonesia

Pratika Yuhyi Hernanda, *Surabaya*
Cosmas RA Lesmana, *Jakarta*
Neneng Ratnasari, *Yogyakarta*

Iran

Seyed M Jazayeri, *Tehran*
Sedigheh Kafi-Abad, *Tehran*
Iradj Maleki, *Sari*
Fakhraddin Naghibalhossaini, *Shiraz*

Israel

Stephen DH Malnick, *Rehovot*

Italy

Francesco Angelico, *Rome*
Alfonso W Avolio, *Rome*
Francesco Bellanti, *Foggia*
Marcello Bianchini, *Modena*
Guglielmo Borgia, *Naples*
Mauro Borzio, *Milano*
Enrico Brunetti, *Pavia*
Valeria Cento, *Roma*
Beatrice Conti, *Rome*
Francesco D'Amico, *Padova*
Samuele De Minicis, *Fermo*
Fabrizio De Ponti, *Bologna*
Giovan Giuseppe Di Costanzo, *Napoli*
Luca Fabris, *Padova*
Giovanna Ferraioli, *Pavia*
Matteo Garcovich, *Rome*
Edoardo G Giannini, *Genova*
Rossano Girometti, *Udine*
Alessandro Granito, *Bologna*
Alberto Grassi, *Rimini*
Alessandro Grasso, *Savona*
Francesca Guerrieri, *Rome*
Quirino Lai, *Aquila*
Andrea Lisotti, *Bologna*
Marcello F Maida, *Palermo*
Lucia Malaguarnera, *Catania*
Andrea Mancuso, *Palermo*
Luca Maroni, *Ancona*
Francesco Marotta, *Milano*
Pierluigi Marzuillo, *Naples*
Sara Montagnese, *Padova*
Giuseppe Nigri, *Rome*
Claudia Piccoli, *Foggia*
Camillo Porta, *Pavia*
Chiara Raggi, *Rozzano (MI)*
Maria Rendina, *Bari*
Maria Ripoli, *San Giovanni Rotondo*
Kryssia I Rodriguez-Castro, *Padua*
Raffaella Romeo, *Milan*
Amedeo Sciarra, *Milano*
Antonio Solinas, *Sassari*
Aurelio Sonzogni, *Bergamo*
Giovanni Squadrito, *Messina*
Salvatore Sutti, *Novara*
Valentina Svicher, *Rome*
Luca Toti, *Rome*
Elvira Verduci, *Milan*
Umberto Vespasiani-Gentilucci, *Rome*
Maria A Zocco, *Rome*

Japan

Yasuhiro Asahina, *Tokyo*
Nabil AS Eid, *Takatsuki*
Kenichi Ikejima, *Tokyo*
Shoji Ikuo, *Kobe*
Yoshihiro Ikura, *Takatsuki*
Shinichi Ikuta, *Nishinomiya*
Kazuaki Inoue, *Yokohama*
Toshiya Kamiyama, *Sapporo*
Takanobu Kato, *Tokyo*
Saiho Ko, *Nara*
Haruki Komatsu, *Sakura*
Masanori Matsuda, *Chuo-city*
Yasunobu Matsuda, *Niigata*
Yoshifumi Nakayama, *Kitakyushu*
Taichiro Nishikawa, *Kyoto*
Satoshi Oeda, *Saga*
Kenji Okumura, *Urayasu*
Michitaka Ozaki, *Sapporo*
Takahiro Sato, *Sapporo*
Junichi Shindoh, *Tokyo*
Ryo Sudo, *Yokohama*
Atsushi Suetsugu, *Gifu*
Haruhiko Sugimura, *Hamamatsu*
Reiji Sugita, *Sendai*
Koichi Takaguchi, *Takamatsu*
Shinji Takai, *Takatsuki*
Akinobu Takaki, *Okayama*
Yasuhito Tanaka, *Nagoya*
Takuji Tanaka, *Gifu City*
Atsunori Tsuchiya, *Niigata*
Koichi Watashi, *Tokyo*
Hiroshi Yagi, *Tokyo*
Taro Yamashita, *Kanazawa*
Shuhei Yoshida, *Chiba*
Hitoshi Yoshiji, *Kashihara*

Jordan

Kamal E Bani-Hani, *Zarqa*

Malaysia

Peng Soon Koh, *Kuala Lumpur*
Yeong Yeh Lee, *Kota Bahru*

Mexico

Francisco J Bosques-Padilla, *Monterrey*
María de F Higuera-de la Tijera, *Mexico City*
José A Morales-Gonzalez, *México City*

Moldova

Angela Peltec, *Chishinev*

Netherlands

Wybrich R Cnossen, *Nijmegen*
Frank G Schaap, *Maastricht*
Fareeba Sheedfar, *Groningen*

Nigeria

CA Asabamaka Onyekwere, *Lagos*

Pakistan

Bikha Ram Devrajani, *Jamshoro*

Philippines

Janus P Ong, *Pasig*
JD Decena Sollano, *Manila*

Poland

Jacek Zielinski, *Gdansk*

Portugal

Rui T Marinho, *Lisboa*
Joao B Soares, *Braga*

Qatar

Reem Al Olaby, *Doha*

Romania

Bogdan Dorobantu, *Bucharest*
Liana Gheorghe, *Bucharest*
George S Gherlan, *Bucharest*
Romeo G Mihaila, *Sibiu*
Bogdan Procopet, *Cluj-Napoca*
Streba T Streba, *Craiova*

Russia

Anisa Gumerova, *Kazan*
Pavel G Tarazov, *St.Petersburg*

Saudi Arabia

Abdulrahman A Aljumah, *Riyadh*
Ihab MH Mahmoud, *Riyadh*
Ibrahim Masoodi, *Riyadh*
Mhoammad K Parvez, *Riyadh*

Singapore

Ser Yee Lee, *Singapore*

South Korea

Young-Hwa Chung, *Seoul*
Jeong Heo, *Busan*
Dae-Won Jun, *Seoul*
Bum-Joon Kim, *Seoul*
Do Young Kim, *Seoul*
Ji Won Kim, *Seoul*
Moon Young Kim, *Wonu*
Mi-Kyung Lee, *Suncheon*
Kwan-Kyu Park, *Daegu*
Young Nyun Park, *Seoul*
Jae-Hong Ryoo, *Seoul*
Jong Won Yun, *Kyungsan*

Spain

Ivan G Marina, *Madrid*

Juan G Acevedo, *Barcelona*
Javier Ampuero, *Sevilla*
Jaime Arias, *Madrid*
Andres Cardenas, *Barcelona*
Agustin Castiella, *Mendaro*
Israel Fernandez-Pineda, *Sevilla*
Rocio Gallego-Duran, *Sevilla*
Rita Garcia-Martinez, *Barcelona*
José M González-Navajas, *Alicante*
Juan C Laguna, *Barcelona*
Elba Llop, *Madrid*
Laura Ochoa-Callejero, *La Rioja*
Albert Pares, *Barcelona*
Sonia Ramos, *Madrid*
Francisco Rodriguez-Frias, *Córdoba*
Manuel L Rodriguez-Peralvarez, *Córdoba*
Marta R Romero, *Salamanca*
Carlos J Romero, *Madrid*
Maria Trapero-Marugan, *Madrid*

Sri Lanka

Niranga M Devanarayana, *Ragama*

Sudan

Hatim MY Mudawi, *Khartoum*

Sweden

Evangelos Kalaitzakis, *Lund*

Switzerland

Christoph A Maurer, *Liestal*

Thailand

Taned Chitapanarux, *Chiang mai*
Temduang Limpaiboon, *Khon Kaen*
Sith Phongkitkarun, *Bangkok*
Yong Poovorawan, *Bangkok*

Turkey

Osman Abbasoglu, *Ankara*
Mesut Akarsu, *Izmir*
Umit Akyuz, *Istanbul*
Hakan Alagozlu, *Sivas*
Yasemin H Balaban, *Istanbul*
Bulent Baran, *Van*
Mehmet Celikbilek, *Yozgat*
Levent Doganay, *Istanbul*
Fatih Eren, *Istanbul*
Abdurrahman Kadayifci, *Gaziantep*
Ahmet Karaman, *Kayseri*
Muhsin Kaya, *Diyarbakir*
Ozgur Kemik, *Van*
Serdar Moralioglu, *Uskudar*
A Melih Ozel, *Gebze - Kocaeli*
Seren Ozenirler, *Ankara*
Ali Sazci, *Kocaeli*
Goktug Sirin, *Kocaeli*
Mustafa Sunbul, *Samsun*
Nazan Tuna, *Sakarya*
Ozlem Yonem, *Sivas*

Ukraine

Rostyslav V Bubnov, *Kyiv*
Nazarii K Kobyliak, *Kyiv*
Igor N Skrypnyk, *Poltava*

United Kingdom

Safa Al-Shamma, *Bournemouth*
Jayantha Arnold, *Southall*
Marco Carbone, *Cambridge*
Rajeev Desai, *Birmingham*
Ashwin Dhanda, *Bristol*
Matthew Hoare, *Cambridge*
Stefan G Hubscher, *Birmingham*
Nikolaos Karidis, *London*
Lemonica J Koumbi, *London*
Patricia Lalor, *Birmingham*
Ji-Liang Li, *Oxford*
Evaggelia Liaskou, *Birmingham*
Rodrigo Liberal, *London*
Wei-Yu Lu, *Edinburgh*
Richie G Madden, *Truro*
Christian P Selinger, *Leeds*
Esther Una Cidon, *Bournemouth*
Feng Wu, *Oxford*

United States

Naim Alkhouri, *Cleveland*
Robert A Anders, *Baltimore*
Mohammed Sawkat Anwer, *North Grafton*
Kalyan Ram Bhamidimarri, *Miami*
Brian B Borg, *Jackson*
Ronald W Busuttil, *Los Angeles*
Andres F Carrion, *Miami*
Saurabh Chatterjee, *Columbia*
Disaya Chavalitdhamrong, *Gainesville*
Mark J Czaja, *Bronx*
Jonathan M Fenkel, *Philadelphia*
Catherine Frenette, *La Jolla*
Lorenzo Gallon, *Chicago*
Kalpana Ghoshal, *Columbus*
Hie-Won L Hann, *Philadelphia*
Shuang-Teng He, *Kansas City*
Wendong Huang, *Duarte*
Rachel Hudacko, *Suffern*
Lu-Yu Hwang, *Houston*
Ijaz S Jamall, *Sacramento*
Neil L Julie, *Bethesda*
Hetal Karsan, *Atlanta*
Ahmed O Kaseb, *Houston*
Zeid Kayali, *Pasadena*
Timothy R Koch, *Washington*
Gursimran S Kochhar, *Cleveland*
Steven J Kovacs, *East Hanover*
Mary C Kuhns, *Abbott Park*
Jiang Liu, *Silver Spring*
Li Ma, *Stanford*
Francisco Igor Macedo, *Southfield*
Sandeep Mukherjee, *Omaha*
Natalia A Osna, *Omaha*
Jen-Jung Pan, *Houston*
Christine Pocha, *Minneapolis*
Yury Popov, *Boston*
Davide Povero, *La Jolla*
Phillip Ruiz, *Miami*
Takao Sakai, *Cleveland*
Nicola Santoro, *New Haven*
Eva Schmelzer, *Pittsburgh*
Zhongjie Shi, *Philadelphia*
Nathan J Shores, *New Orleans*
Siddharth Singh, *Rochester*
Shailendra Singh, *Pittsburgh*
Veysel Tahan, *Iowa City*
Mehlika Toy, *Boston*
Hani M Wadei, *Jacksonville*
Gulam Waris, *North Chicago*
Ruliang Xu, *New York*
Jun Xu, *Los Angeles*
Matthew M Yeh, *Seattle*
Xuchen Zhang, *West Haven*
Lixin Zhu, *Buffalo*
Sasa Zivkovic, *Pittsburgh*

World Journal of Hepatology

Contents

Three issues per month Volume 9 Number 1 January 8, 2017

ABOUT COVER

Editorial Board Member of *World Journal of Hepatology*, Dr. Ferenc Sipos, MD, PhD, Assistant Professor, Senior Scientist, 2nd Department of Internal Medicine, Semmelweis University, 1088 Budapest, Hungary

AIM AND SCOPE

World Journal of Hepatology (*World J Hepatol*, *WJH*, online ISSN 1948-5182, DOI: 10.4254), is a peer-reviewed open access academic journal that aims to guide clinical practice and improve diagnostic and therapeutic skills of clinicians.

WJH covers topics concerning liver biology/pathology, cirrhosis and its complications, liver fibrosis, liver failure, portal hypertension, hepatitis B and C and inflammatory disorders, steatohepatitis and metabolic liver disease, hepatocellular carcinoma, biliary tract disease, autoimmune disease, cholestatic and biliary disease, transplantation, genetics, epidemiology, microbiology, molecular and cell biology, nutrition, geriatric and pediatric hepatology, diagnosis and screening, endoscopy, imaging, and advanced technology. Priority publication will be given to articles concerning diagnosis and treatment of hepatology diseases. The following aspects are covered: Clinical diagnosis, laboratory diagnosis, differential diagnosis, imaging tests, pathological diagnosis, molecular biological diagnosis, immunological diagnosis, genetic diagnosis, functional diagnostics, and physical diagnosis; and comprehensive therapy, drug therapy, surgical therapy, interventional treatment, minimally invasive therapy, and robot-assisted therapy.

We encourage authors to submit their manuscripts to *WJH*. We will give priority to manuscripts that are supported by major national and international foundations and those that are of great basic and clinical significance.

INDEXING/ABSTRACTING

World Journal of Hepatology is now indexed in PubMed, PubMed Central, and Scopus.

FLYLEAF

EDITORS FOR THIS ISSUE

NAME OF JOURNAL
World Journal of Hepatology

ISSN
ISSN 1948-5182 (online)

LAUNCH DATE
October 31, 2009

FREQUENCY
36 Issues/Year (8th, 18th, and 28th of each month)

EDITORIAL OFFICE
Xiu-Xia Song, Director
World Journal of Hepatology
Baishideng Publishing Group Inc
8226 Regency Drive, Pleasanton, CA 94588, USA
Telephone: +1-925-2238242
Fax: +1-925-2238243
E-mail: editorialoffice@wjgnet.com
Help Desk: http://www.wjgnet.com/esps/helpdesk.aspx
http://www.wjgnet.com

PUBLISHER
Baishideng Publishing Group Inc
8226 Regency Drive,
Pleasanton, CA 94588, USA
Telephone: +1-925-2238242
Fax: +1-925-2238243
E-mail: bpgoffice@wjgnet.com
Help Desk: http://www.wjgnet.com/esps/helpdesk.aspx
http://www.wjgnet.com

PUBLICATION DATE
January 8, 2017

INSTRUCTIONS TO AUTHORS
http://www.wjgnet.com/bpg/gerinfo/204

ONLINE SUBMISSION
http://www.wjgnet.com/esps/

World Journal of Hepatology

Submit a Manuscript: http://www.wjgnet.com/esps/
Help Desk: http://www.wjgnet.com/esps/helpdesk.aspx
DOI: 10.4254/wjh.v9.i1.1

World J Hepatol 2017 January 8; 9(1): 1-17
ISSN 1948-5182 (online)

REVIEW

Disease monitoring of hepatocellular carcinoma through metabolomics

Asem I Fitian, Roniel Cabrera

Asem I Fitian, School of Medicine, Virginia Commonwealth University, Richmond, VA 23298, United States

Roniel Cabrera, Department of Medicine, Division of Gastroenterology, Hepatology and Nutrition, Section of Hepatobiliary Diseases, University of Florida, Gainesville, FL 32610, United States

Author contributions: Fitian AI and Cabrera R conceptualized the study, searched and reviewed the literature, and drafted the manuscript; both authors reviewed and approved the final version of the manuscript.

Conflict-of-interest statement: Authors declare no conflicts of interest for this article.

Manuscript source: Invited manuscript

Correspondence to: Roniel Cabrera, MD, MS, Department of Medicine, Division of Gastroenterology, Hepatology and Nutrition, Section of Hepatobiliary Diseases, University of Florida, 1600 SW Archer Rd M440, Gainesville, FL 32610, United States. roniel.cabrera@medicine.ufl.edu
Telephone: +1-352-2739500
Fax: +1-352-3927393

Received: June 30, 2016
Peer-review started: June 30, 2016
First decision: August 18, 2016
Revised: September 20, 2016
Accepted: October 22, 2016
Article in press: October 24, 2016
Published online: January 8, 2017

Abstract

We elucidate major pathways of hepatocarcinogenesis and accurate diagnostic metabolomic biomarkers of hepatocellular carcinoma (HCC) identified by contemporary HCC metabolomics studies, and delineate a model HCC metabolomics study design. A literature search was carried out on Pubmed for HCC metabolomics articles published in English. All relevant articles were accessed in full text. Major search terms included "HCC", "metabolomics", "metabolomics", "metabonomic" and "biomarkers". We extracted clinical and demographic data on all patients and consolidated the lead candidate biomarkers, pathways, and diagnostic performance of metabolomic expression patterns reported by all studies in tables. Where reported, we also extracted and summarized the metabolites and pathways most highly associated with the development of cirrhosis in table format. Pathways of lysophospholipid, sphingolipid, bile acid, amino acid, and reactive oxygen species metabolism were most consistently associated with HCC in the cited works. Several studies also elucidate metabolic alterations strongly associated with cirrhosis, with γ-glutamyl peptides, bile acids, and dicarboxylic acids exhibiting the highest capacity for stratifying cirrhosis patients from appropriately matched controls. Collectively, global metabolomic profiles of the referenced works exhibit a promising diagnostic capacity for HCC at a capacity greater than that of conventional diagnostic biomarker alpha-fetoprotein. Metabolomics is a powerful strategy for identifying global metabolic signatures that exhibit potential to be leveraged toward the screening, diagnosis, and management of HCC. A streamlined study design and patient matching methodology may improve concordance among metabolomic datasets in future works.

Key words: Metabolomics; Hepatocellular carcinoma; Biomarkers; Metabolic profiling; Chromatography/mass spectrometry; Noninvasive biomarkers; Cirrhosis

Core tip: The high-throughput, validated nature of metabolomics makes it an ideal methodology for rapidly identifying the global metabolic alterations associated with hepatocarcinogenesis - alterations that not only enhance our understanding of the metabolic underpinnings of cirrhosis and hepatocellular carcinoma (HCC), but that can be leveraged to improve HCC diagnostic, therapeutic, and disease monitoring efficacy. Indeed, contemporary HCC metabolomics works time and again demonstrate this promise that metabolomics platforms hold in serving as standalone non-invasive HCC diagnostic and disease monitoring modalities.

Fitian AI, Cabrera R. Disease monitoring of hepatocellular carcinoma through metabolomics. *World J Hepatol* 2017; 9(1): 1-17 Available from: URL: http://www.wjgnet.com/1948-5182/full/v9/i1/1.htm DOI: http://dx.doi.org/10.4254/wjh.v9.i1.1

INTRODUCTION

Hepatocellular carcinoma (HCC) is the world's third most lethal cancer, possessing a five-year survival rate of 10% that results in between 250000 to 1000000 deaths per year[1,2]. HCC culminates from a preexisting long-term condition of cirrhosis in 90% of cases[3] and cirrhosis patients are among the best characterized individuals at high risk for developing cancer. Notwithstanding the opportunity for clinical surveillance of these patients, the dismal survival rate persists and HCC has now emerged as the fastest rising cause of cancer related death in the United States[4,5]. HCC patients in Asia and sub-Saharan Africa face a particularly grim outlook, with > 90% of patients in rural areas of these regions progressing within the first year of HCC onset[6]. A major hindrance to successful early diagnosis of HCC stems from the substandard accuracy of the principal HCC diagnostic modalities. Alpha-fetoprotein (AFP) is the principal biomarker for HCC and despite the inexpensive and reproducible nature of the AFP blood test, its sensitivity of 25%-65%[7,8] for HCC has exacerbated early detection of this cancer. The low sensitivity of AFP can be explained by the fact that up to 40% of HCC and cirrhosis patients have normal AFP levels, and that AFP is often elevated in patients without HCC[9-11]. Moreover, only 10%-20% of patients with early-stage HCC have elevated AFP levels[12]. Exclusion of AFP as an HCC diagnostic modality in the AASLD guidelines for HCC surveillance underscores AFP's unreliability to accurately screen for early HCC[13]. Efforts to overcome this substandard performance have resulted in the identification and commercialization of novel HCC biomarkers des-gamma-carboxyprothrombin and lectin-bound AFP (AFP-L3). These markers are ineffective when used alone as HCC biomarkers, however, and even when combined with AFP still demonstrate poor sensitivity for HCC, particularly in the detection of lesions < 3 cm[14]. While magnetic resonance imaging and computed tomography offer better accuracy in HCC diagnosis, these sophisticated diagnostic modalities are both economically and logistically incompatible with the resource-poor areas experiencing the brunt of HCC's mortality rate[15-17]. Improving early HCC detection and patient outcome globally requires fulfilling of the urgent need for a reproducible, inexpensive, and accurate HCC diagnostic test.

Metabolomics as an HCC biomarker discovery tool

Numerous genomic and proteomic screening studies have been employed to identify potential biomarkers of HCC[18-24] but to date the markers identified in these studies have not been clinically fruitful. Because the liver is the hub of carbohydrate, amino acid, and lipid metabolism[25,26], chronic liver diseases undoubtedly disrupt normal metabolic function. A metabolomics analysis of HCC and cirrhotic tissue can therefore elucidate not just the metabolic pathways most relevant to the hepatocarcinogenic process, thereby identifying metabolites showing promise as HCC biomarkers, but also global metabolic patterns that serve as comprehensive disease signatures and which may therefore be used to stratify cases from controls. Metabolomics is the comprehensive identification of all small metabolites < 2 kD in a tissue sample. Through combined gas or liquid chromatography/mass spectrometry, surface-enhanced laser desorption/ionization time-of-flight mass spectrometry (SELDI TOF-MS) or nuclear magnetic resonance instrumentation, metabolomics platforms enable investigators to rapidly screen hundreds of metabolites in a large series of biofluid or solid tissue samples and are capable of simultaneously detecting metabolites belonging to a diverse array of pathways including amino acids, lipids, carbohydrates, and nucleotides. Metabolomics platforms are translationally optimal and hold potential for clinical implementation because they reveal global metabolite expression pattern differences among cases and controls in an automated, rapid, high-throughput, quality controlled, and reproducible manner. Metabolomics facilitates rapid identification of diagnostic markers, prognostic markers, and lead drug target pathways and their implementation in drug discovery divisions of pharmaceutical giants underscores their important role in the lead target generation realm[27].

Nearly two dozen HCC metabolomics studies have been reported[28-46]. These studies illustrate the key pathways involved in stepwise hepatocarcinogenesis and reveal metabolites that may have utility as biomarkers of HCC and cirrhosis. The findings of these studies are summarized in Tables 1 and 2. These works reveal deregulation of bile acid metabolism, fatty acid β-oxidation by way of the carnitine palmitoyltransferase (CPT) shuttle system, amino acid metabolism, and glycerophospholipid metabolism in HCC *vs* cirrhosis,

Table 1 Significantly altered metabolites in hepatocellular carcinoma patients *vs* cirrhosis controls

Ref.	Platform	Tissue (organism)	HCC etiology	Significantly altered metabolites in HCC patients *vs* cirrhosis controls	Main pathways distinguishing HCC from cirrhosis
Patterson *et al*[29]	UPLC/QTOF-MS; UPLC/ESI-TQMS; GC/MS	Plasma (human)	HCC *n* = 20: EtOH *n* = 6 HBV *n* = 3 HCV *n* = 5 NASH *n* = 3 NASH/alcoholic steatohepatitis *n* = 1 HH *n* = 2	LPC (14:0) ↓ LPC (18:1) ↓ LPC (20:4) ↓ LPC (20:3) ↓ LPC (22:6) ↓ FFA (24:0) - lignoceric acid ↓ FFA (24:1) - nervonic acid ↓ Bilirubin ↑ Biliverdin ↑	LPC metabolism Very long chain fatty acid metabolism Hemoglobin metabolism
Xiao *et al*[37]	UPLC/QTOF-MS	Serum (human)	HCV	3β, 6β-dihydroxy-5β-cholan-24-oic acid ↓ 3α, 7β-dihydroxy-5β-cholest-24-en-26-oic acid ↓ GCA ↓ GDCA ↓ GCDCA ↓ TCDCA ↓ Linoelaidyl carnitine ↓ Oleoylcarnitine ↓ Palmitoyl carnitine ↓ O-octanoyl-R-carnitine ↓ LPC (20:1) ↓ LPC (20:4) ↓ PE (20:4/18:1) ↓ 4E;15Z-Bilirubin IXa ↓ 15,16-dihydrobiliverdin ↓ 3-ganidinopropionicacid ↓ Tetracosahexaenoic acid ↓ 3-hydroxy-eicosanoic acid ↓ Oleamide ↓ Phe-Phe ↑	Bile acid biosynthesis CPT shuttle system LPC metabolism Hemoglobin metabolism Eicosanoid metabolism
Wang *et al*[38]	UPLC/MS-MS; LC/QTOF-MS	Serum (human)	HCC *n* = 82: HBV-cirrhosis *n* = 41 HBV-only *n* = 41	LPC-16:0 ↑ LPC-18:0 ↑ 16:0/18:1-PC ↑ 16:0/18:2-PC ↑ 16:0/20:4-PC ↑ 16:0/22:6-PC ↑ 18:0/18:2-PC ↑ Phenylalanine ↓ GCDCA ↓ Canavaninosuccinate ↑↑	LPC metabolism Gut flora metabolism Bile acid metabolism Organic acid metabolism
Zhou *et al*[39]	UPLC/QTOF-MS	Serum (human)	HCC *n* = 69: HBV-HCC (HCC-B) *n* = 38 HCV-HCC (HCC-C) *n* = 31	LPC (14:0) HCC-C ↓ LPC (16:1) HCC-C ↓ LPC (18:3) HCC-B ↓ HCC-C ↓ LPC (18:2) HCC-B ↓ HCC-C ↓ LPC (18:1) HCC-B ↓ HCC-C ↓ LPC (18:0) HCC-C ↓ LPC (20:5) HCC-C ↓ LPC (20:4) HCC-B ↓ HCC-C ↓ LPC (20:3) HCC-B ↓ HCC-C ↓ LPC (20:2) HCC-C ↓ LPC (20:0) HCC-B ↓ HCC-C ↓ LPC (22:6) HCC-C ↓ LPC (22:5) HCC-B ↓ HCC-C ↓ LPC (22:4) HCC-B ↓ HCC-C ↓	LPC metabolism
Wu *et al*[31]	SELDI-TOF-MS; HPLC/MS	Serum (human)	HBV	GRO-α ↑ Thrombin light chain ↑	Cytokine Protease cleavage
Ressom *et al*[36]	UPLC/QTOF-MS	Serum (human)	HCC *n* = 78: → HCV 67%	GDCA ↓ TCA ↓	Bile acid metabolism

			→ HBV 15% → Alcoholism 29% → NASH 13% → Cryptogenic (8%) → Autoimmune (3%)	TCDCA ↓ Sphingosine 1-phosphate ↑ LPC (16:0) ↑ LPC (17:0) ↑ LPC (18:0) ↑ LPC (15:0) ↑ LPC (22:6) ↑ LPE (22:6) ↑ LPE (20:4) ↑ LPE (20:3) ↑ PS ↑	Sphingolipid metabolism LPC metabolism
Yang *et al*[28]	HRMAS 1H NMR	Biopsy (human)	HCC *n* = 17: → Cirrhosis *n* = 9 → No cirrhosis *n* = 8	Glucose ↓ Creatine ↓ PE ↑ Glutamine ↑ Glutamate ↑ PC + GPC ↑	Glycolysis LPC metabolism Amino acid metabolism Bile acid metabolism
Nahon *et al*[40]	NMR	Serum (human)	EtOH cirrhosis	High density lipoproteins Acetate ↑ N-acetyl-glycoproteins ↑ Glutamate ↑ Glutamine ↓	HDL biosynthesis Ketone body metabolism N-acetylglycoprotein Amino acid metabolism
Budhu *et al*[43]	GC/MS, UPLC/MS-MS	Biopsy samples (human)	HCC *n* = 356 Training cohort *n* = 30 Testing cohort *n* = 217 Validation cohort *n* = 139	Study reported on markers involved in cancer aggressivity through comparison of stem-like HCC to less benign mature hepatocyte HCC	N/A
Beyoğlu *et al*[44]	GC/MS	Biopsy samples (human)	Six HCC subtypes, liver fibrosis status unknown	Glucose ↓ Glycerol 3-phosphate ↓ Glycerol 2-phosphate ↓ Malate ↓ Alanine ↓ Myo-inositol ↓ Linoleic acid ↓	Glycolysis PI3K pathway Prostaglandin biosynthesis
Fitian *et al*[45]	UPLC/MS-MS and GC/MS	Serum (human)	HCV cirrhosis-associated HCC *n* = 30 HCV-cirrhosis *n* = 27 Healthy volunteers *n* = 30	Sphingosine ↑ Xanthine ↑ 2-Pyrrolidinone ↑ 2-Hydroxybutyrate ↑ Serine ↑ Glycine ↑ Aspartate ↑ 12-HETE ↑ 15-HETE ↑ Isovalerate ↑	Sphingolipid Oxidative stress metabolism GABA metabolism Oxidative stress metabolism Amino acid Inflammation pathway Gut microflora metabolism
Gao *et al*[46]	GC-TOF/MS	Serum (human)	HBV cirrhosis-associated HCC *n* = 39 HBV-cirrhosis (*n* = 52)	Dihomo-linolenate ↑ Stearic acid Heptadecanoic acid Palmitic acid 5-Aminovaleric acid Cholesterol ↑ 3-hydroxybutyric acid ↑ Malic acid ↑ Glutamine ↑ Asparagine ↓ Alanine ↑ Threonine ↓ Leucine ↓ Glutamic acid ↑ β-glutamate ↑ 5-oxoproline ↓ 1,2,4-cyclopropranodicarboxylic acid ↓	Inflammation pathway Fatty acid biosynthesis Gut microflora metabolism Cholesterol metabolism Ketogenesis TCA metabolism Amino acid Glutathione metabolism Dicarboxylic acid metabolism

Pathways of importance in the comparison of (1A) HCC *vs* cirrhosis and (2) cirrhosis *vs* healthy controls are shown. Arrows indicate the metabolite's expression in cases *vs* appropriate controls. $P < 0.05$ was used as the significance level and metabolites reported in table are those which were most significantly upregulated or downregulated in each study. EtOH: Alcohol; TOCSY: Total correlation spectroscopy; HH: Hereditary hemochromatosis; TCA: Tricarboxylic acid; UPLC: Ultrahigh-performance liquid chromatography; QTOF: Quadrupole time of flight; SELDI: Surface-enhanced laser desorption/ionization; HRMAS: High-resolution magic angle spinning; LPE: Lysophosphatidyethanolamine; LPC: Lysophosphatidylcholine; HCC: Hepatocellular carcinoma; MS: Mass spectrometry; TOF: Time-of-flight; GC: Gas chromatography; LC: Liquid chromatography; NMR: Nuclear magnetic resonance; HBV: Hepatitis B virus; HCV: Hepatitis C virus; NASH: Non-alcoholic steatohepatitis; FFA: Free fatty acids; PE: Phosphorylethanolamine; GABA: γ-aminobutyric acid.

Table 2 Significantly altered metabolites in cirrhosis patients *vs* healthy volunteers

Ref.	Platform	Tissue (organism)	Significantly altered metabolites in cirrhosis patients *vs* healthy volunteers	Main pathways distinguishing cirrhosis from healthy volunteers
Gao *et al*[33]	^{1}H NMR	Serum (human)	Isoleucine ↓	Amino acid metabolism
			Leucine ↓	
			Valine ↓	
			Glutamine ↑	
			Tyrosine ↑	
			Phenylalanine ↑	
			1-methylhistidine ↑	
			N-acetylglycoproteins ↑	
			Acetate ↑	N-acetylglycoprotein
			Acetoacetate ↓	Ketonogenesis
			Pyruvate ↑	
			α-ketoglutarate ↑	Glycolysis
			Choline ↓	TCA cycle
			Taurine ↑	
			Glycerol ↑	Bile acid metabolism
Li *et al*[42]	UPLC/QTOF-MS	Serum (mouse)	Leucine ↓	Amino acid metabolism
			Phenylpyruvic acid ↓	
			Phenylalanine ↓	
			Tryptophan ↓	
			LPE (16:0) ↓	LPE metabolism
			LPE (18:0) ↓	
			LPC (16:0) ↓	LPC metabolism
			LPC (20:1) ↓	
			LPC (22:6) ↑	
			PC (16:0/18:3) ↑	Phosphatidylcholine metabolism
			PC (12:1/24:3) ↑	
			PC (16:0/20:4) ↑	
			PC (16:0/22:6) ↑	
			PC (18:0/20:4) ↑	Sphingomyelin metabolism
			SM (d18:0/16:1) ↓	
Soga *et al*[35]	Capillary elecrtophore-sis/TOF-MS	Serum (human)	γ-glutamylalanine ↑	Glutathione metabolism
			γ-glutamylvaline ↑	
			γ-glutamylglutamine ↑	
			γ-glutamylphenyl-	
			γ-glutamylcitrulline ↑	
			Alanine ↑	Amino acid metabolism
			Methionine sulfoxide ↑	
Wang *et al*[38]	UPLC/MS-MS; LC/QTOF-MS	Serum (human)	LPC-16:0 ↓	LPC metabolism
			LPC-18:0 ↓	
			16:0/18:1-PC ↓	
			16:0/18:2-PC ↓	
			16:0/20:4-PC ↓	
			16:0/22:6-PC ↓	
			18:0/18:2-PC ↓	
			Oleamide ↑	Fatty acid metabolism
			Phenylalanine ↑	
			GCDCA ↑	Bile acid metabolism
			Canavaninosuccinate ↓	Arginosuccinate synthetase pathway
Zhou *et al*[39]	UPLC/QTOF-MS	Serum (human)	Phenylalanine ↑	Amino acid metabolism
			GCA ↑	Bile acid metabolism
			GDCA ↑	
			Bilirubin ↑	Hemoglobin metabolism
			LPE (18:2) ↓	Lysolipid metabolism
			LPC (22:6) ↓	
			LPC (18:2) ↓	
			LPC (20:4) ↓	
			LPC (16:0) ↓	
			LPC (18:0) ↓	
			C18:1-CN ↑	CPT shuttle system
Chen *et al*[30]	UPLC/QTOF-MS	Serum (human); Urine (human)	Inositol ↓	TCA cycle
			2,2-bipyridine ↓	
			Methionine ↓	Amino acid metabolism
			Tyrosine ↓	
			Arginine ↓	Fatty acid metabolism
			Stearic acid ↓	
			Palmitic acid ↓	
			Citric acid ↓	

Cao *et al*[32]	UPLC/MS	Fecal (human)	2-piperidine carboxylic acid ↓ 5-Hydroxy-tryptophan ↓ Chenodeoxycholic Acid dimeride ↓ Urobilin ↓ Urobilinogen ↓ 7-ketolithocholic acid ↓	 Bile acid metabolism Hemoglobin metabolism Microbiome metabolism
Yin *et al*[41]	RPLC/MS	Serum (human)	LPC C18:0 ↑ LPC C16:0 ↑ Hypoxanthine ↓ Inosine ↓ Bilirubin ↑ GCA ↑ GCDCA ↑ Taurine ↓ LPC C18:2 ↓ LPC C18:3 ↓ LPC C16:1 ↓ LPC C18:0 ↓ LPC C16:1 ↓	LPC metabolism Purine synthesis Hemoglobin metabolism Bile acid metabolism LPC metabolism
Fitian *et al*[45]	Integrated UPLC/MS-MS and GC/MS	Serum (human)	L-acetylcarnitine ↑ 6-Methylnicotinic acid ↓ Glycocholate (GCA) ↑ Tauroursodeoxycholate ↑ Glychochemodeoxycholate ↑ Azelate (nonanedioate) ↑ Undecanedioate ↑ Sebacate (decanedioate) ↑ Hexadecanedioate↑ Tetradecanedioate↑ DSGEGDFXAEGGGVR ↑ ADSGEGDFXAEGGGVR ↑ Bilirubin (Z,Z) ↑ Biliverdin ↑ 1,2-propanediol ↑ Succinylcarnitine ↑ Acetylcarnitine ↑ Glutarylcarnitine ↑	CPT shuttle system Nicotine metabolism Bile acid metabolism Dicarboxylic acid metabolism Fibrinogen cleavage peptide Hemoglobin catabolism metabolite Ketogenesis CPT shuttle system
Gao *et al*[46]	GC-TOF/MS	Serum (human)	Palmitic acid ↑ Stearic acid ↑ Oleic acid ↑ Arachidic acid ↑ Aminomalonic acid ↑ Phenylalanine ↑ Cysteine ↑ Leucine ↑ Citric acid ↑ Oxoproline ↑	Fatty acid metabolism Arachidonic acid metabolism Dicarboxylic acid metabolism Amino acid metabolism

EtOH: Alcohol; TOCSY: Total correlation spectroscopy; HH: Hereditary hemochromatosis; TCA: Tricarboxylic acid; UPLC: Ultrahigh-performance liquid chromatography; QTOF: Quadrupole time of flight; SELDI: Surface-enhanced laser desorption/ionization; HRMAS: High-resolution magic angle spinning; LPE: Lysophosphatidyethanolamine; LPC: Lysophosphatidylcholine; MS: Mass spectrometry; TOF: Time-of-flight; NMR: Nuclear magnetic resonance; LC: Liquid chromatography; GC: Gas chromatography; CPT: Carnitine palmitoyltransferase; TCA: Tricarboxylic acid.

and further delineate metabolites with potential utility in stratifying patients with cirrhosis from the healthy population.

Pathways of importance in hepatocarcinogenesis

Glycerophospholipids: The liver is the principal organ of lipid metabolism and the presence of cirrhosis and hepatocellular carcinoma results in a dramatic shift in the normal metabolism of fatty acids. Among the first HCC metabolomics studies to elucidate this massive deregulation of lipid metabolism in HCC was the Yang *et al*[28] work in 2007 which employed high resolution magic angle-spinning ^{1}H nuclear magnetic resonance to delineate the metabolomic profile differences in low-grade HCC, high-grade HCC, and non-involved adjacent cirrhosis patient biopsy specimens. The group reported higher levels of several phospholipids in HCC *vs* cirrhosis, including glycerophosphocholine, phosphatidylcholine, choline and the phosphorylethanolamine. Increases in phosphatidylcholine were further observed in low-grade HCC *vs* uninvolved cirrhotic tissue, suggesting possible deregulation of glycerophospholipid metabolism at the early phases of HCC development. These phospholipids also exhibited a direct, positive relationship to tumor burden.

In Yang *et al*[28], the elevation of choline, the head

group of many phospholipids that comprise the plasma membrane, not only reflects increased plasma membrane synthesis demand by the growing tumor but is also consistent with the observed elevations in bile (cholic) acid concentration in HCC *vs* control tissue.

Lysophospholipids, free fatty acids, and acylcarnitines: Significant alterations in the expression of a subtype of glycerophospholipids known as lysophosphatidylcholines (LPC) have routinely been observed in HCC metabolomics studies[29,36-39]. Still other classes of lipids observed to be significantly altered in HCC *vs* cirrhosis include free fatty acids (FFA)[29,45], very long chain fatty acids[29], and acylcarnitines[37,45]. Downregulated LPCs and FFA in HCC *vs* cirrhosis were among the major metabolomic trends reported by Patterson *et al*[29], with LPC (14:0), LPC (20:3), LPC (22:6) and very long chain fatty acids FFA (24:0) (lignoceric acid) and FFA (24:1) (nervonic acid) all trending lower in HCC *vs* cirrhosis. The decreases of lignoceric and nervonic acid in HCC *vs* cirrhosis were especially patent and may reflect peroxisome proliferator-activated receptor-alpha (PPAR-α) induced enhancement of peroxisomal β-oxidation. Previous reports implicating heightened PPAR-α activity in HCC support this hypothesis[47,48]. Decreases in these FFAs may also be related to increased activity of lignoceryl-CoA ligase, the enzyme responsible for very long chain fatty acid catabolism and one acted upon by PPAR-α[49]. LPCs are the glycerophospholipid building blocks of cell membranes and elevation of these metabolites may reflect the heightened metabolic needs of growing HCCs. LPCs are also major lipids bound to human albumin[50]. Decreased serum albumin is a signature of liver cirrhosis and liver cancer and elevations of systemic LPCs may be attributed to the shortage of appropriate albumin binding sites that results in increased circulating levels of these metabolites.

Further metabolomics work by Xiao *et al*[37] also identified this downregulation of LPCs and LPEs in 40 hepatitis C virus (HCV)-associated HCC patients and 49 cirrhosis controls. Among the novel findings of this investigation included decreased levels of acylcarnitines in HCC *vs* cirrhosis. Results also showed that as tumor burden worsened, the expression of acylcarnitines and bile acids trended significantly downward. Stage Ⅱ and Ⅲ HCC exhibited lower levels of these metabolites in comparison to stage 1 [staging based on the American Joint Committee on Cancer Tumor Lymph Node Metastatic Disease (TNM) system]. The downregulation of fatty acids, acylcarnitines, and bile acids in HCC *vs* cirrhosis supports the cancer Warburg effect involving a metabolic shift from tricarboxylic acid (TCA) cycle and mitochondrial β-oxidation to a heightened reliance on glycolysis for energy production. To undergo β-oxidation in the mitochondrial matrix, free fatty acids (fatty acyl-CoA) must link with cytosolic carnitine *via* CPT shuttle system enzymes to form acylcarnitines. Acylcarnitines are capable of penetrating the inner mitochondrial membrane and once inside the matrix, CPT enzymes liberate fatty acyl-CoA allowing β-oxidation to ensue. Decreased concentration of acylcarnitines in HCC *vs* cirrhosis suggests impairment of CPT1-mediated formation of these compounds from FFA and carnitine.

Sphingolipids: One major lipid expression alteration in HCC reported in HCC metabolomics is a perturbation of sphingosine metabolism, with overexpressed sphingosine-1-phosphate (S1P) and sphingosine reported in HCC *vs* cirrhosis. The overexpression of LPCs is in agreement with the Patterson study while the upregulation of S1P, a signaling lipid, was a novel finding in HCC metabolomics. S1P has been heavily implicated in promoting the progression of several cancers including HCC[51,52] and building the case for this pathway's involvement in HCC development, our HCC metabolomics work identified S1P's precursor sphingosine as one of the most strongly upregulated metabolites in HCC *vs* cirrhosis[45]. Sphingosine is produced *via* acid ceramidase (AC) activity on ceramide. Ceramides are shown to possess apoptotic effects, while sphingosine 1-phosphate is demonstrated as an anti-apoptotic and angiogenic molecule[53]. This cell turnover control mechanism is known as the "sphingosine rheostat", and AC is an important modulator of cell death homeostasis. Higher S1P in HCC may also reflect an independent enhancement of sphingosine kinase (SPHK) activity. One study demonstrated the antitumor property of a selective SPHK2 inhibitor in HCC xenografts[54], implicating SPHK as a promoter of HCC progression. Heightened AC activity that results in increased sphingosine may lead to a larger reservoir of S1P *via* sphingosine kinase and may promote the establishment of a microenvironment conducive to HCC initiation.

Bile acids

Bile acids are synthesized in the liver and aid in fatty acid absorption and digestion. Bile acid elevations in HCC have been reported previously[55] and may be explained by HCC invasion and obstruction of the bile duct. Bile duct blockage can impede adequate transfer of bile acids to the small intestine thereby impairing sufficient absorption and digestion of fats and leading to a buildup of both bile acids and cholinergic lipids in the hepatic tumor microenvironment. The majority of studies comparing HCC and cirrhosis metabolomes did not uncover a significant differential expression of bile acids, but where a significant trend was seen[36-38], the metabolites collectively trended downward, in contrast to the aforementioned previous reports[55,56]. A significant negative correlation between bile acid levels and tumor burden was also observed[37]. Similar to the Yang *et al*'s work, our metabolomics investigation[45] identified a significant elevation of choline in HCC *vs* cirrhosis, and bile acids in our study were strongly elevated in cirrhosis patients *vs* healthy subjects. The elevation of choline, a building block of bile acids, is consistent with an impairment of bile acid synthesis. Bile acid down-

regulation in HCC may also reflect a metabolic shift away from β-oxidation and the reduced *de novo* bile acid production caused by the obliteration of healthy hepatocytes during chronic liver disease. Diminished bile acids may also reflect constitutive activation of farnesyl X receptor (FXR), a bile acid-activated nuclear receptor that is also activated by a variety of other lipids including eicosanoids[57]. FXR silences Cyp7A1-catalyzed production of bile acids and is implicated in promoting progression of HCC by multiple studies[58,59]. In the Fujino study of FXR-induced promotion of HCC progression[58], siR-mediated supplementation of FXR enhanced HepG2, Huh7, and HLE HCC cell line progression while FXR knockdown halted this progression.

Oxidative stress metabolism

Among the other pathways found to be significantly associated with HCC in metabolomics investigations are pathways of reactive oxygen species metabolism, notable metabolites of which include the γ-glutamyl peptides. A recent capillary electrophoresis-time of flight mass spectrometry analysis involving sera obtained from HCV-associated HCC patients, cirrhosis patients, hepatitis B virus (HBV) and chronic hepatitis C (HCV) patients, and healthy volunteers showed markedly significant variations in γ-glutamyl expression among these groups[35]. No differences in γ-glutamyl peptide expression were observed between HCC and cirrhosis controls, but several significant alterations were witnessed in the HCC *vs* viral hepatitis, HCC *vs* normal healthy controls (NHC), cirrhosis *vs* viral hepatitis, and cirrhosis *vs* NHC comparisons. In general, HCC γ-glutamyl expression was increased in comparison to healthy controls, while γ-glutamyl peptides were decreased in HCC *vs* viral hepatitis. γ-glutamylglycine, γ-glutamylalanine, γ-glutamylvaline and γ-glutamylserine, γ-glutamyltaurine, γ-glutamylleucine, and γ-glutamyllysine were all strongly ($0.0001 < P < 0.001$) downregulated in HCC *vs* viral hepatitis B (HBV) and C infection. γ-glutamyl peptides are precursors to glutathione, the chief antioxidant compound primarily synthesized in the liver. The respective elevation of these intermediates in HCC and cirrhosis patients *vs* NHC suggests that increased oxidative stress contributing to liver dysfunction calls for heighted production of these precursors to combat this deteriorative process. This is consistent with reports implicating oxidative damage as a key pathway in HCC progression and one that increases patient vulnerability for HCC recurrence[60,61]. γ-glutamyl peptides are also liberated in free form by gamma-glutamyl transpeptidase (GGT) mediated breakdown of glutathione. GGT is an enzymatic signature of liver disease and a marker routinely used in the clinic to assess the severity of liver dysfunction. Excess breakdown of glutathione may explain the relative elevation of γ-glutamyl peptides in cirrhosis *vs* NHC and the impaired oxidative stress neutralization commonly witnessed in HCC.

The Wang *et al*[38] study also found an oxidative stress signature in HCC, showed a striking 677-fold elevation in canavaninosuccinate (CSA) level in HCC patients *vs* their cirrhosis counterparts ($P < 0.01$). Subsequent receiver operator characteristic (ROC) analysis revealed that the sensitivity and specificity of AFP and CSA for distinguishing the HCC patients from cirrhosis controls were: $AFP_{20\ ng/mL}$ 74% and 38%; $AFP_{200\ ng/mL}$ 52% and 90%; CSA 79.3% and 100%; combined CSA and $AFP_{20\ ng/mL}$ 96.4% and 100%. CSA is the precursor to fumarate, a key metabolite of the TCA cycle, and elevation of CSA may reflect impairment in the formation of TCA intermediates and promotes the above referenced Warburg theory involving a metabolic shift from oxidative to anaerobic energy production in cancer microenvironments, which are often more hypoxic than healthy tissue[62].

In our work[45], a strong oxidative stress signature in HCC was also observed, with xanthine, 2-hydroxybutyrate and several γ-glutamylpeptides trending significantly higher in HCC *vs* cirrhosis. Still, the work of Gao *et al*[46] uncovered trends suggestive of an opposite phenomenon: Elevations of glutamic acid, lysine and cysteine in HCC compared with healthy controls were observed and are curious in the context of reactive oxygen species (ROS) given that these amino acids are precursors of glutathione (GSH). Increased levels of these amino acids suggest a possible enhancement of GSH production that establishes a microenvironment conducive for tumor survival[46].

Protein metabolites

The liver is the major organ of protein metabolism and not surprisingly, HCC metabolomics shows that the expression profiles of patients with advanced liver disease exhibit major differences in amino acid expression when compared to metabolic profiles of appropriate diseased or healthy controls. In the Yang *et al*[28] study, significant increases in creatine, glutamine, and glutamate were found in HCC *vs* cirrhosis, and these trends were juxtaposed by decreases in lactate, alanine, leucine, glutamate, glutamine in HCC *vs* cirrhosis. The finding of increased amino acids in HCC *vs* cirrhosis is consistent with numerous studies implicating elevated amino acids and the enzymes responsible for their production in cancer initiation and progression[63-66]. In one large scale metabolomics analysis of 60 cancer cell lines, Jain *et al*[66] identified glycine as the most significantly and consistently upregulated metabolite in cancer cells *vs* healthy lines. Enhanced amino acid production is consistent with the metabolic remodeling hallmark of cancer known as the Warburg effect, which involves a shift from TCA cycle and β-oxidation to a heightened reliance on glycolysis for energy production[67]. Amino acids are important glycolytic enzyme activators, and one recent study demonstrated that serine was an activator of pyruvate kinase M2[68], the cancer isoform of glycolytic enzyme pyruvate kinase responsible for conversion of phosphoenolpyruvic acid (PEP) to pyruvate. The group's concomitant observation of elevated lactate in HCC *vs* cirrhosis is consistent with the Warburg hypothesis.

Gao *et al*[46] propose that their observed elevation of pyruvate, which would seem to counteract the tumor's reliance on the lower-activity PKM2 compared to PKM1, is due to enhanced production of glutamine which is used as an alternative pyruvate precursor. Our study identified a strong amino acid signature associated with HCC with serine, glycine and aspartate being the most significantly upregulated metabolites in HCC *vs* cirrhosis. These elevations are corroborated by a recent metabolomic analysis of HBV-associated HCC showing a strong upregulation of serine, alanine, glycine, cysteine, aspartic acid, methionine, tyrosine, tryptophan, and phenylalanine in HCC *vs* healthy controls. Upregulated amino acids in HCC may be explained by the greater protein turnover that transpires in rapidly dividing tumors *vs* the surrounding non-cancerous tissue along with impaired amino acid utilization in liver.

In addition to very small molecular weight amino acids, metabolomics is also useful for detecting larger protein metabolites weighing near 10 kDa. SELDI TOF-MS metabolomics is a highly versatile methodology for large-scale identification and quantification of these larger metabolites. Wu *et al*[31] tapped this technology to investigate the metabolomic expression profiles of HBV-associated HCC patients, cirrhosis patients, and healthy controls. Their results reveal the upregulation of two proteins, growth related oncogene-alpha (GRO-α) and thrombin light chain (TLC), in HCC patients *vs* cirrhosis controls. To validate these putative markers, serum from an alternative series of HCC, cirrhosis, healthy, and cancer control patients was subjected to SephdexTM Peptide 10/300 GL, HitrapTM CM, and Mono Q 5/50 GL liquid chromatography for protein separation. The separated products were purified using SDS-PAGE and their identities were confirmed using electrospray ionization mass spectrometry. In this alternative series of patients, GRO-α was upregulated four-fold in HCC patients *vs* cirrhosis controls and its level directly correlated with HCC tumor burden. GRO-α also trended higher in gastric, nasopharyngeal and lung cancers relative to cirrhosis patients, but the magnitude of GRO-α elevation in cancer controls *vs* cirrhosis was smaller than the elevation witnessed in HCC *vs* cirrhosis, suggesting that GRO-α may play a more prominent role in HCC progression. Interestingly, TLC was 1.4 times more elevated in HCC patients *vs* cirrhosis controls but downregulated in the cancer control patients *vs* cirrhosis, suggesting that TLC is a unique signature of HCC. The combined sensitivity and specificity of GRO-α + TLC + AFP for discriminating HCC patients from cirrhosis and healthy controls was 91.7% and 92.7% respectively. At the 400 ng/mL cutoff for HCC diagnosis, AFP had a sensitivity of 69% and a specificity of 83%.

GRO-α is a chemokine involved in invoking leukocyte cell migration and is associated with pro-inflammatory processes, angiogenesis, and cancer[69-71]. Its elevation may be a signature of a viral hepatitis-associated HCC immune deregulation involving heightened monocyte migration and increased inflammation, and a subsequent increased likelihood for successful host evasion of tumor prophylactic mechanisms[72]. TLC is a protein cleavage fragment that is generated from matrix metalloproteinase-associated (MMP) peptide cleavage[31]. Its upregulation may be explained by simultaneous E-cadherin loss and MMP activation by Twist1 which has been shown to promote HCC expansion[73]. Its utility as a cancer biomarker was also shown in a SELDI TOF-MS study of gastric cancer by Ebert *et al*[74], where TLC accurately distinguished gastric cancer patients from patients without cancer with a sensitivity of 89.9% and a specificity of 90%.

The destruction of cholinergic receptors in amyloid plaques and neurofibrillary tangles of the brain has also been linked to encephalopathy, a common neurological disorder witnessed in HCC patients[75]. The molecular mechanisms linking hepatic encephalopathy (HE) and HCC are not fully understood, but the parallel elevations of choline and glutamine in HCC patients *vs* cirrhosis controls may partially be associated with a cataclysmic loss in cholinergic receptor concentration and the initial stages of HE onset, respectively[76]. A possible neurological metabolic signature was one of the most strongly correlated trends observed in HCC patients *vs* cirrhosis and *vs* healthy controls in our study, with 2-pyrrolidinone, a γ-aminobutyric acid (GABA) metabolite, was strongly elevated in HCC when compared to levels in both the cirrhosis controls and the healthy volunteers. GABA is a major inhibitory chemical messenger in the brain, and the sharp elevation of its metabolic byproducts in HCC may reflect heightened production of GABA and may coincide with the neurodegenerative hallmarks of advanced liver disease.

Two previously unidentified fibrinogen cleavage peptides, denoted by amino acid sequence as DSGEGD FXAEGGGVR and ADSGEGDFXAEGGGVR, were observed to be significantly overexpressed in HCC in our study. While they trended higher in HCC *vs* cirrhosis, their elevation in cirrhosis *vs* healthy controls was more patent and these metabolites exhibited a better diagnostic utility for cirrhosis. Taken together, the aberrations in protein and amino acid expression in HCC revealed by metabolomics may be harnessed toward the development of clinically fruitful HCC diagnostics.

Markers of cirrhosis

A number of HCC metabolomics studies report significant alterations between cirrhosis patients and healthy volunteers[30,32,33,35,38,39,41,42,45,46] and within these findings are opportunities for development of biomarkers for cirrhosis. Currently, the best cirrhosis diagnostic is liver biopsy, a procedure that by virtue of its invasive nature is not a gold standard diagnostic approach[77]. Identification of accurate cirrhosis diagnostic biomarkers can streamline development of a less invasive diagnostic that minimizes patient discomfort and the expenses associated with biopsy while simultaneously enabling early detection of cirrhosis in both industrialized nations and in resource poor areas of the globe. Among the putative markers

of cirrhosis identified in these works include the purine metabolites hypoxanthine[41,45] and inosine[41], both significantly downregulated five and six-fold respectively in cirrhosis *vs* NHC. γ-glutamylalanine, γ-glutamylvaline, γ-glutamylglutamine, γ-glutamylphenylalanine and γ-glutamylcitrulline were also significantly elevated in cirrhosis *vs* NHCs[41,45]. Increases in the γ-glutamyl peptides in cirrhosis *vs* NHC and HCC *vs* NHC indicates heighted production of glutathione to combat the oxidative damage process commonly implicated as a promoter of tumor initiation and progression. γ-glutamyl peptides are also liberated in free form by GGT mediated breakdown of glutathione. The elevation of γ-glutamyl peptides in cirrhosis *vs* NHC may therefore conversely be explained by excessive breakdown of glutathione resulting in impaired oxidative stress neutralization that is commonly witnessed in HCC.

Other promising markers of cirrhosis include bile acids[45] and dicarboxylic acids[45,46], with these metabolite classes exhibiting the strongest and most significant fold-differences among all markers significantly altered between cirrhotics and healthy controls in the references metabolomic studies.

Etiological metabolomic differences

Because HCC is linked to a variety of diverse etiologies including viral hepatitis, alcoholic cirrhosis, non-alcoholic fatty liver disease, steatohepatitis, and aflatoxin B1, metabolomics is useful for revealing the variation in metabolism these etiologies cause. The majority of studies have focused on characterizing the metabolomic signatures of single HCC etiologies, or have not accounted for etiology. Studies to date have not queried the metabolomic expression pattern differences between the various etiologies of HCC and as the metabolic underpinnings of each etiology are better characterized, HCC etiology metabolome comparison studies will prove vital in establishing the utility for metabolomics as an accurate diagnostic modality of different HCC subtypes. Only one study, by Zhou *et al*[39], compared the serum metabolomic expression patterns of HCV cirrhosis-associated HCC and HBV cirrhosis-HCC. The group also looked at whether metabolomic alterations in HCV-HCC and HBV-HCC were significantly different from cirrhosis and healthy control metabolomes. The study revealed a greater magnitude decrease of LPC expression in HBV-infected HCC patients *vs* cirrhosis controls than the magnitude decrease of LPCs HCV-HCC *vs* cirrhosis. The analysis also showed significant elevation of bile acids, heme pigmentation compounds bilirubin and biliverdin, upregulation of acylcarnitines and downregulation of glycerophospholipids in cirrhosis patients *vs* healthy controls, suggesting that these metabolites were signatures of the onset of cirrhosis. Metabolomic profile comparison between HBV-cirrhosis patients *vs* patients with HBV-only revealed a similar global downregulation of LPCs in the cirrhosis cohort *vs* viral hepatitis controls. The findings of this study suggest a progressive downregulation of LPCs during the course of progression from viral hepatitis to cirrhosis and a bottomed out expression occurring with HCC. The downregulation of LPC in HCC may be explained by their well-known anti-tumor roles that include induction of apoptosis, anti-invasive effects, and a direct effect on tumor sensitization to treatment. This trend of diminished LPCs may reflect first the substantial cell death that occurs during cirrhosis resulting in diminished LPC levels, followed by a subsequent massive turnover of residual LPCs by the growing HCC that further exhausts the LPC reservoir. The magnitude of LPC decrease in HBV-HCC *vs* cirrhosis was greater than HCV-HCC *vs* cirrhosis, suggesting that HBV exerts a more prominent influence on LPC metabolism than HCV.

Integrated "omics" approaches

As the above studies demonstrate, metabolomics is a powerful strategy for identifying a large panel of metabolites that exhibit promise in accurately diagnosing HCC. What is unclear from these works, however, are the genomic and proteomic synergies that culminate in these metabolic manifestations. Integrating two or more "omics" approaches can unveil the complex genomic-proteomic-metabolomic network galvanizing cancer development. Two recent studies tapped the power of such an approach, coupling metabolomics with transcriptomics to identify the genetic underpinnings of metabolomic disruptions. The first study by Budhu *et al*[43] investigated the network of metabolic pathways and corresponding genes involved in HCC aggressivity. Patient demographic and clinical characteristics, including body mass index, were extensively characterized for 356 HCC cases, which were divided into a training set (n = 30), a testing set (n = 217), and a validation cohort (n = 139). The training cohort consisted of 15 epithelial cell adhesion molecule-positive/AFP-positive (EpCAM+AFP+) HpSC-HCC patients, representing aggressive stem-like HCC, and 15 less aggressive (EpCAM-AFP-) mature hepatocyte MH-HCC patients. Analysis of tumor specimens and uninvolved healthy tissue by principal component analysis revealed clear demarcation between tumor and non-tumor metabolomes. Non-targeted metabolic profiling of tumor and non-tumor specimens identified 48 markers that were significantly altered between HpSC-HCC patients and patients with MH-HCC. This metabolite panel resolved aggressive HCC from the less subtype at a sensitivity of 72% and a specificity of 83% ($P < 0.05$). The group further demonstrated that within the subset of 48 metabolites associated with HCC aggressivity, 28 were significantly associated with overall survival. Subsequent microarray gene expression profiling of the paired tumor specimens identified 169 genes that could significantly distinguish the two HCC subtypes. The group then gauged the correlation between this genetic signature and the panel of 28 metabolites that were associated with both HCC aggressivity and overall survival and found that each of the 28 metabolites were associated with at least one of the 169 genes identified by microarray analysis. To determine the principal metabolite-gene

pairs potentially influencing HCC aggressivity, the group performed correlation analysis with randomization and found 15 metabolites and 121 genes most highly associated with the tumor and stem-like HCC genes. Validation of the genetic signature in an independent testing cohort (n = 217) revealed a panel of 273 genes that distinguished HpSC-HCC from MH-HCC with a sensitivity of 72% and a specificity of 91% (P < 0.01), and this genetic signature was also strongly (P < 0.0001) associated with overall survival. This gene set was also a significant independent predictor of overall survival, progression free survival and recurrence, highlighting its utility as a prognostic panel of aggressive HCC. Many of the genes were associated with fatty acid metabolism and the phosphatidylinositide 3-kinase signaling pathway. Elevated palmitoleate expression in HpSC-HCC tumor *vs* paired non-tumor specimens reflected overexpression or enhanced activity of stearoyl-CoA dehydrogenase (SCD), an important cell turnover regulatory pathway. Significant downregulation of arachidonate and linoleate, the parent molecules of the eicosanoid signaling cascade, suggested overconsumption of these metabolites from hyperactivity of cycloxygenase, lipoxygenase, and/or cytochrome P450c in aggressive HCC. SCD, which converts saturated palmitic acid to palmitoleic acid, was among the gene set. To validate the possible role of SCD in cancer aggressivity, *in vitro* and *in vivo* analysis was done and showed that selective SCD inhibitor CGX0168 abrogated Huh7 cell migration and invasion. Supplementation of Huh7 with palmitoleate, the end product of SCD activity, enhanced cell migration and invasion. Xenografted tumors in nude mice showed that SCD-siRNA inhibited tumor migration and colony formation and increased apoptosis, likely owing to the accumulation of pro-apoptotic palmitate. Taken together, this approach showed a strong lipid signature associated with HCC aggressivity. Elevated palmitoleate reflected upregulated SCD, a key regulator of the ratio between saturated and unsaturated fatty acids. A tilt in the delicate balance between saturated and unsaturated fatty acids toward unsaturated has been implicated in cancer aggressiveness.

Remarkably, the integrated metabolomics-transcriptomics study by Beyoğlu *et al*[44] also revealed a consistent role for palmitate, linoleate, and the PI3K pathway in HCC. Microarray analysis found that 11 genes involved in fatty acid were associated with HBV-positive HCC cases. More broadly, the comparison of tumor *vs* paired non-tumor tissues identified a metabolic shift toward glycolysis reflective of the Warburg effect implicated in other HCC metabolomics works. Levels of glucose, glycerol 3-phosphate, glycerol 2-phosphate, malate, alanine, and myo-inositol were all significantly decreased in tumor *vs* non-tumor specimens, indicating both impaired mitochondrial respiration and enhanced glycolysis. Myo-inositol is the metabolic precursor of the messenger molecule inositol triphosphate (PI3) required by PI3K-AKT-mTOR, and its downregulation in tumor *vs* non-tumor specimens is consistent with the hyperactivity of this pathway implicated in numerous cancers. Furthermore, the group showed that 1-stearoylglycerol and 1-palmitoylglycerol were decreased in tumor *vs* non-tumor. 1-acylglycerols are synthesized by phospholipase activity on LPCs and the routinely reported decrease in LPCs in HCC *vs* controls may explain the reduced 1-acylglycerols in this study. Through integration of metabolomics and transcriptomics, these groups together show a possible role for SCD in HCC, implicate the PI3K pathway as important to HCC progression, and show a strong lipid signature associated with HCC, in agreement with other HCC metabolomics works. More broadly, these works demonstrate that the achievement of consistent trends in independent, integrated "omics" studies can be achieved and lay important groundwork for future studies of this nature.

Sensitivity and specificity of metabolomics in HCC diagnosis

To evaluate the utility for metabolomic profiles to distinguish between patients with cirrhosis and patients with HCC, these studies primarily employed principal component analysis, orthogonal projection to latent structures, supervised projection to latent structures discriminant analysis, the random forest machine learning algorithm, or ROC curve class prediction analyses. Reported sensitivity/specificity/area under the curve values reflecting the accuracy of metabolomics in distinguishing HCC from cirrhosis are shown in Table 3. In general, metabolomics was a highly accurate diagnostic method and clear demarcation between healthy controls and/or cirrhosis controls *vs* HCC patients were realized. Where metabolomics profile class prediction was compared with AFP, the metabolomics approach showed greater class prediction power. In general, the focus of these works was the potential standardization of metabolomics as a high-throughput clinical diagnostic platform-big-data biomarkers rather than single metabolite alterations-which may explain the lack of emphasis on the sensitivity and specificity of individual metabolites for diagnosing HCC. Just two studies verified the metabolite expression patterns *in vitro*, and with the exception of the *in vivo* validation performed by Budhu *et al*[43], no studies used *in vivo* models to validate their metabolomics data. It is therefore recommended that future validation of HCC metabolomics data include preliminary information on metabolite concentrations in HCC cases *vs* cirrhosis controls as measured *in vitro* or *in vivo* to reveal their utility as potential biomarkers that can be employed in a rapid *in vitro* diagnostic.

DISCUSSION

Summary of major findings

The results of these studies show that aberrations in bile acid, LPC, acylcarnitine, ROS, and protein metabolism may be signatures of HCCs emerging in the setting of cirrhosis. Bile acids trended lower in HCC *vs* cirrhosis controls in all studies reporting a significant difference in expression of these metabolites[36-38]. In general, LPCs were shown

Table 3 Utility of significantly altered ($P < 0.05$) metabolites in accurately predicting hepatocellular carcinoma (hepatocellular carcinoma cases *vs* patients with cirrhosis)

Ref.	Platform	Comparison	Class prediction methodology	Classification accuracy or sensitivity/specificity	AFP sensitivity /specificity
Patterson *et al*[29]	UPLC/ESI-QTOF-MS	HCC (n = 20) *vs* cirrhosis (n = 7)	Random forest	96.3	-
Chen *et al*[30]	Integrated GC/QTOF-MS + UPLC/QTOF-MS	HCC (n = 82) *vs* healthy (n = 71)	OPLS-DA	100.0	-
Wu *et al*[31]	SELDI-TOF MS	HCC (n = 48) *vs* cirrhosis (n = 54) or healthy (n = 42)	GRO-α + thrombin light chain PS20 Protein immunoassay	89.6/89.6	69/83
Cao *et al*[32]	UPLC/QTOF-MS	HCC (n = 23) *vs* cirrhosis (n = 22)	PLS-DA	67.0	-
Gao *et al*[33]	NMR	HCC (n = 39) *vs* cirrhosis (n = 36)	PLS-DA	45.7	-
Wu *et al*[34]	GC/MS	HCC (n = 20) *vs* healthy (n = 20)	PCA with ROC curve analysis	AUC=88.3; AUCAFP = 92.5 when combined with AFP	-
Soga *et al*[35]	LC/MS-MS	HCC (n = 32) *vs* HCV-only (n = 35) or cirrhosis (n = 18)	Multiple logistic regression; ROC curve analysis	88.1	0.760
Wang *et al*[38]	UPLC-MS	HCC (59) *vs* cirrhosis (20) or NHC (20)	PLS-DA, ROC curve analysis	CSA 79.3/100 CSA + AFP20 96.4/100 UPLC-MS 100/100	AFP20 74/38 AFP200 52/90
Zhou *et al*[39]	UPLC-QTOF-MS	HCC (n = 69) *vs* cirrhosis (n = 28)	PLS-DA, ROC curve analysis	AEA 88.0 PEA 82.0 AEA + PEA 88.0	-
Nahon *et al*[40]	NMR	Small HCC (n = 28) *vs* cirrhosis (n = 93); Large HCC (n = 33) *vs* cirrhosis (n = 93)	OPLS	Small HCC: 61.0/100.0 Large HCC: 100.0/100.0	-
Yin *et al*[41]	RPLC/QTOF-MS; HILIC/QTOF-MS	HCC (n = 25) *vs* cirrhosis (n = 24) or healthy (n = 25)	OPLS	RPLC: 61.8 HILIC: 57.0 RPLC + HILIC = 63.6	-
Li *et al*[42]	UPLC/QTOF-MS	HCC (n = 8) *vs* cirrhosis (n = 6) or healthy (n = 6) (murine samples)	OPLS-DA	88.2	-
Budhu *et al*[43]	Training set1: GC/MS + UPLC/MS-MS; Testing set2: Affymetrix GeneChip	Training set: Stem-like aggressive HpSC-HCC (n = 15) *vs* Mature hepatocyte less aggressive MH-HCC (n = 15); Testing set: HpSC-HCC and MH-HCC (n = 217)	Multivariate analysis	172.0/83.0, AUC = 0.830 272.0/91.0, AUC = 0.860	-
Fitian *et al*[45]	UPLC/MS-MS + GC/MS	HCC (n = 30) *vs* HCV-cirrhosis (n = 27)	Random forest ROC analysis	72% 12-HETE 73.3/69.2 15-HETE 83.3/59.3 Aspartate 100/51.9 Glycine 83.3/63.0 Serine 73.3/85.2 Phenylalanine 73.3/81.5 Homoserine 70.0/85.2 Sphingosine 58.3/86.7 Xanthine 63.3/88.9 2-Hydroxybutyrate 76.7/77.8	AFP20 63.3/83.6
Gao *et al*[46]	GC-TOF/MS	HCC (n = 39) *vs* HBV-cirrhosis (n = 52)	Random forest (validation set) ROC analysis (validation set) Bayes discriminant function model (validation set)	96.8% in HCC *vs* HBV-cirrhosis 100% in HBV-cirrhosis *vs* HBV 100% in HBV *vs* NHC 100/95.2 HBV *vs* NC 83.3/100 HBV-cirrhosis *vs* HBV 76.9/83.3 HCC *vs* HBV-cirrhosis 76.9% HCC 100% HBV-cirrhosis 94.1% HBV 100% NHC	-

Classification accuracy describes the capacity of the metabolomic classification technique to accurately predict the group of each study subject. UPLC: Ultrahigh-performance liquid chromatography; AEA: Anandamide; OPLS: Orthogonal projection to latent structure; PCA: Principal component analysis; PEA: Palmitylethanolamide; PLS-DA: Partial least squares-discriminant analysis; MS: Mass spectrometry; TOF: Time-of-flight; GC: Gas chromatography; HCC: Hepatocellular carcinoma; HBV: Hepatitis B virus; GRO-α: Growth related oncogene-alpha; ROC: Receiver operator characteristic; NHC: Normal healthy controls; AFP20: AFP performance at the cutoff of 20 ng/mL; AFP200: AFP performance at the cutoff of 200 ng/mL.

to be downregulated in HCC *vs* cirrhosis[37-39,45]. But the works by Ressom *et al*[36] and Wang *et al*[38] found that LPCs and LPEs were consistently elevated in the HCC *vs* cirrhosis comparison. Acylcarnitines, which function as liaisons of fatty acid β-oxidation by enabling fatty acid importation to the mitochondrial matrix, were significantly downregulated in HCC *vs* cirrhosis. Amino acids also trended higher in HCC in all studies reporting significant expression differences between HCC and cirrhosis. The hemoglobin metabolite bilirubin was also consistently elevated in HCC *vs* cirrhosis[29,39,41,45], consistent with the clinical utility this metabolite possesses for diagnosing advanced liver disease. Biliverdin, another heme catabolite, was significantly upregulated in HCC *vs* cirrhosis in two studies[29,45] and a metabolic derivative of biliverdin downregulated in a third[37].

The elevation of LPCs in HCC *vs* cirrhosis seen by Ressom *et al*[36] is consistent with increased demand of glycerophospholipids by the growing tumor. LPCs comprise only 3% of the total phospholipids in plasma membranes, however, and a better explanation for their elevation may be that LPCs are major lipids bound to albumin. The loss of albumin commonly witnessed in chronic liver disease and HCC may mean a shortage of docking sites for LPCs, resulting in increased systemic levels of these glycerophospholipids. Diminished bile acids in HCC *vs* cirrhosis reinforces the Warburg effect commonly witnessed in cancer studies involving a shift in energy production away from oxidative processes like β-oxidation and the TCA cycle toward anaerobic glycolysis, which is more suitable to the hypoxic or anoxic tumor microenvironment. The loss of bile acids in HCC significantly impairs fatty acid absorption and digestion and is consistent with the general trend of increased circulating lipids in HCC *vs* cirrhosis and cirrhosis *vs* appropriate controls. The elevation of bile acids has historically served as a clinical indicator of chronic liver disease and specifically cirrhosis and consistent with this function, our metabolomics work showed a global upregulation of bile acids in cirrhosis *vs* healthy volunteers[45]. Decreased acylcarnitines further reflects diminished reliance on β-oxidation, and it may also signify impairment of the mitochondrial carnitine palmitoyltransferase shuttle system.

Metabolomic heterogeneity attributed to differences in study design

While perturbations in phospholipid, bile acid, hemoglobin, acylcarnitine and amino acid metabolism were routinely encountered in these studies, the referenced works did not achieve uniform conclusions regarding the directional shifts of the metabolites' expression in HCC *vs* cirrhosis, with examples including contradictory patterns of LPC[36,39] and amino acid[28,46] expression in HCC *vs* cirrhosis. The heterogeneity among these studies' metabolomes is likely due to differences in study design. Although some studies matched patients by age and gender, the majority of the referenced HCC metabolomics studies did not extensively characterize HCC and cirrhosis patients by demographic and clinical characteristic parameters. Only four studies reported MELD scores for HCC and cirrhosis patients[36,37,40,45], and just three studies indicated the Child-Pugh status of their HCC or cirrhosis cohorts[29,40,45]. This lack of information on whether liver function of the study participants is compensated or decompensated complicates interpretation of metabolomic data. Body mass index (BMI) also went unreported for HCC, cirrhosis, and healthy study subjects in all but two studies[43,45] referenced in this review. BMI can have a significant influence on the relative metabolite expression differences between patients, particularly with regard to adiposity. Because these studies did not control for BMI, is likely that the patients recruited for these metabolomics studies had wide-ranging BMIs that may further explain the noticeably different trends of LPC, FFA, and acylcarnitine expression in HCC *vs* controls. To limit the influence of potential cofounders such as comorbidity, BMI, age or gender, and etiology on HCC metabolomes, patient clinical characteristics should be controlled for more conscientiously in future HCC metabolomics studies.

There was also marked variation in how each group diagnosed and staged their HCC patients. Three studies[29,43,45] staged according to the Barcelona Clinic for Liver Cancer staging criteria. The TNM Classification of Malignant Tumors (TNM) was used to diagnose HCC in five studies[28,30,37,38,43], imaging in two, histopathology in one[36], and six studies made no mention of their HCC diagnosis method[31,33,35,39,41,42]. Differences in HCC diagnosis and staging among these studies likely contributed to the discordant global metabolomic alterations in HCC *vs* cirrhosis among these studies and further confounded the interpretation of these metabolomic trends.

Lack of emphasis on HCC vs cirrhosis comparison

The critical metabolomic comparison between HCC patients and cirrhosis controls was reported in just ten out of the twenty studies referenced in this review[28,29,31,35-39,45,46], with half of the cited works instead focusing on the metabolomic profile differences between HCC patients and NHC subjects. While this comparison sheds light on altered pathways during hepatocarcinogensis, it may not be as applicable from a clinical standpoint as the trends elucidated through a comparison of HCC *vs* cirrhosis. This owes to the fact that the majority of primary liver cancer cases occur in patients with a preexisting condition of cirrhosis. Therefore, the metabolomic comparison between HCC and cirrhosis is more clinically informative and potentially translational than the comparison of HCC *vs* NHC. HCC is a complex heterogeneous disease and HCC patients often present with multiple comorbidities. It is therefore likely that marked metabolomic differences will be observed between HCC patients and healthy subjects. Differences between HCC patients and cirrhosis controls are subtler than HCC *vs* NHC[45,46] and it would be expected that conspicuous metabolomic differences

exist between HCC/NHC and cirrhosis/NHC. Given that HCC arose in the background of cirrhosis in all reported HCC metabolomics studies, it is impossible to determine whether the alterations witnessed in HCC *vs* NHC are related to HCC or cirrhosis, further reinforcing the need for future metabolomic comparisons between HCC and cirrhosis.

CONCLUSION

Bile acids, acylcarnitines, amino acids, free fatty acids, LPCs, and heme pigmentation molecules exhibited utility in stratifying HCC patients from patients with cirrhosis. Canavaninosuccinate, which showed a striking 680-fold elevation in HCC patients *vs* cirrhosis controls and outperformed AFP in sensitivity and specificity. Sphingosine 1-phosphate (↑), sphingosine (↑), GRO-α (↑), and thrombin light chain (↑) were other putative HCC biomarkers that had superior predictive utility for HCC than AFP. Bile acids, fibrinogen cleavage byproducts, dicarboxylic fatty acids, and ROS-related γ-glutamyl peptides exhibited strong association with cirrhosis and the further development of these metabolites as diagnostic markers of cirrhosis may be valuable. In addition to individual metabolites, global patient metabolomes exhibited superior sensitivity for diagnosis of HCC *vs* AFP where a comparison was made[31,35,38,45].

Although these data are preliminary in nature, they reflect the early promise that metabolomics platforms hold in potential clinical implementation for disease diagnosis. Future metabolomics studies with larger, better demographically and clinically characterized patient cohorts may resolve the heterogeneous metabolomic expression patterns in HCC *vs* cirrhosis.

Given that > 90% of HCCs emerge in the setting of cirrhosis, future HCC metabolomics studies will be most impactful and clinically relevant if they compare the expression patterns of HCC patients *vs* cirrhosis controls. Moreover, patients with HCC and cirrhosis should be matched by etiology (viral *vs* non-viral), liver function, and BMI to limit the influence of data confounders. Furthermore, it is paramount the appropriate metabolomic profile comparisons are made, namely HCC *vs* cirrhosis, cirrhosis *vs* etiology of cirrhosis (viral or non-viral), and cirrhosis *vs* NHC. In a recent study, the entire stepwise hepatocarcinogenic process from NHC to HBV, through cirrhosis, and culminating in HCC was analyzed. Appropriately, Gao *et al*[46] focused their expression profile comparisons on HCC *vs* cirrhosis, and cirrhosis *vs* HBV/NHC. This approach enables investigators to make adequate conclusions about the interval at which putative biomarkers become relevant in the hepatocarcinogenic process and demonstrates the relevance of the dataset comparisons. Moreover, investigation of the pathways involved in the progression from the initial liver insult to cirrhosis remains a largely untapped realm of biomarker discovery within metabolomics, and may streamline the identification of potential cirrhosis diagnostic markers. More broadly, metabolomics is well-suited for clarifying the entirety of the metabolic remodeling that occurs throughout hepatocarcinogensis, and can hence streamline biomarker discovery efforts at each pathological interval.

The findings of these works demonstrate the powerful resource that is metabolomics for identifying potential novel diagnostic biomarkers of HCC. The translational optimality of metabolomics is underscored by its capability to simultaneously process high volumes of patient specimens and interpret metabolic expression profiles through robust, validated and automated software. Still greater, metabolomics holds promise as a novel disease screening and diagnostic modality that, through characterization of a patient's global metabolic profile, can in a more sophisticated and comprehensive fashion accurately predict the presence of disease.

REFERENCES

1 **Altekruse SF**, McGlynn KA, Reichman ME. Hepatocellular carcinoma incidence, mortality, and survival trends in the United States from 1975 to 2005. *J Clin Oncol* 2009; **27**: 1485-1491 [PMID: 19224838 DOI: 10.1200/JCO.2008.20.7753]

2 **El-Serag HB**. Hepatocellular carcinoma. *N Engl J Med* 2011; **365**: 1118-1127 [PMID: 21992124 DOI: 10.1056/NEJMra1001683]

3 **Hussain SM**, Semelka RC, Mitchell DG. MR imaging of hepatocellular carcinoma. *Magn Reson Imaging Clin N Am* 2002; **10**: 31-52, v [PMID: 11998574 DOI: 10.1016/S1064-9689(03)00048-5]

4 **El-Serag HB**, Rudolph KL. Hepatocellular carcinoma: epidemiology and molecular carcinogenesis. *Gastroenterology* 2007; **132**: 2557-2576 [PMID: 17570226 DOI: 10.1053/j.gastro.2007.04.061]

5 **El-Serag HB**, Mason AC. Rising incidence of hepatocellular carcinoma in the United States. *N Engl J Med* 1999; **340**: 745–750

6 **Kew MC**. Epidemiology of hepatocellular carcinoma in sub-Saharan Africa. *Ann Hepatol* 2013; **12**: 173-182 [PMID: 23396727]

7 **Cedrone A**, Covino M, Caturelli E, Pompili M, Lorenzelli G, Villani MR, Valle D, Sperandeo M, Rapaccini GL, Gasbarrini G. Utility of alpha-fetoprotein (AFP) in the screening of patients with virus-related chronic liver disease: does different viral etiology influence AFP levels in HCC? A study in 350 western patients. *Hepatogastroenterology* 2000; **47**: 1654-1658 [PMID: 11149026]

8 **Gupta S**, Bent S, Kohlwes J. Test characteristics of alpha-fetoprotein for detecting hepatocellular carcinoma in patients with hepatitis C. A systematic review and critical analysis. *Ann Intern Med* 2003; **139**: 46-50 [PMID: 12834318 DOI: 10.7326/0003-4819-139-1-200307010-00012]

9 **Tateishi R**, Yoshida H, Matsuyama Y, Mine N, Kondo Y, Omata M. Diagnostic accuracy of tumor markers for hepatocellular carcinoma: a systematic review. *Hepatol Int* 2008; **2**: 17-30 [PMID: 19669276 DOI: 10.1007/s12072-007-9038-x]

10 **Bialecki ES**, Di Bisceglie AM. Diagnosis of hepatocellular carcinoma. *HPB* (Oxford) 2005; **7**: 26-34 [PMID: 18333158 DOI: 10.1080/13651820410024049]

11 **Chen CH**, Lin ST, Kuo CL, Nien CK. Clinical significance of elevated alpha-fetoprotein (AFP) in chronic hepatitis C without hepatocellular carcinoma. *Hepatogastroenterology* 2008; **55**: 1423-1427 [PMID: 18795704]

12 **Lai Q**, Melandro F, Pinheiro RS, Donfrancesco A, Fadel BA, Levi Sandri GB, Rossi M, Berloco PB, Frattaroli FM. Alpha-fetoprotein and novel tumor biomarkers as predictors of hepatocellular carcinoma recurrence after surgery: a brilliant star raises again. *Int J Hepatol* 2012; **2012**: 893103 [PMID: 22792474 DOI: 10.1155/2012/893103]

13 **Bruix J**, Sherman M. Management of hepatocellular carcinoma.

Hepatology 2005; **42**: 1208-1236 [PMID: 16250051 DOI: 10.1002/hep.20933]
14 **Weitz IC**, Liebman HA. Des-gamma-carboxy (abnormal) prothrombin and hepatocellular carcinoma: a critical review. *Hepatology* 1993; **18**: 990-997 [PMID: 8406374 DOI: 10.1002/hep.1840180434]
15 **Wild CP**, Hall AJ. Primary prevention of hepatocellular carcinoma in developing countries. *Mutat Res* 2000; **462**: 381-393 [PMID: 10767647 DOI: 10.1016/S1383-5742(00)00027-2]
16 **El-Serag HB**, Davila JA. Surveillance for hepatocellular carcinoma: in whom and how? *Therap Adv Gastroenterol* 2011; **4**: 5-10 [PMID: 21317990 DOI: 10.1177/1756283X10385964]
17 **Venook AP**, Papandreou C, Furuse J, de Guevara LL. The incidence and epidemiology of hepatocellular carcinoma: a global and regional perspective. *Oncologist* 2010; **15** Suppl 4: 5-13 [PMID: 21115576 DOI: 10.1634/theoncologist.2010-S4-05]
18 **Qiao B**, Wang J, Xie J, Niu Y, Ye S, Wan Q, Ye Q. Detection and identification of peroxiredoxin 3 as a biomarker in hepatocellular carcinoma by a proteomic approach. *Int J Mol Med* 2012; **29**: 832-840 [PMID: 22344546]
19 **Marshall A**, Lukk M, Kutter C, Davies S, Alexander G, Odom DT. Global gene expression profiling reveals SPINK1 as a potential hepatocellular carcinoma marker. *PLoS One* 2013; **8**: e59459 [PMID: 23527199 DOI: 10.1371/journal.pone.0059459]
20 **Lok AS**, Sterling RK, Everhart JE, Wright EC, Hoefs JC, Di Bisceglie AM, Morgan TR, Kim HY, Lee WM, Bonkovsky HL, Dienstag JL. Des-gamma-carboxy prothrombin and alpha-fetoprotein as biomarkers for the early detection of hepatocellular carcinoma. *Gastroenterology* 2010; **138**: 493-502 [PMID: 19852963 DOI: 10.1053/j.gastro.2009.10.031]
21 **Woo HG**, Park ES, Thorgeirsson SS, Kim YJ. Exploring genomic profiles of hepatocellular carcinoma. *Mol Carcinog* 2011; **50**: 235-243 [PMID: 21465573 DOI: 10.1002/mc.20691]
22 **Shang S**, Plymoth A, Ge S, Feng Z, Rosen HR, Sangrajrang S, Hainaut P, Marrero JA, Beretta L. Identification of osteopontin as a novel marker for early hepatocellular carcinoma. *Hepatology* 2012; **55**: 483-490 [PMID: 21953299 DOI: 10.1002/hep.24703]
23 **Rodrigues RR**, Barry CT. Gene pathway analysis of hepatocellular carcinoma genomic expression datasets. *J Surg Res* 2011; **170**: e85-e92 [PMID: 21601879 DOI: 10.1016/j.jss.2011.04.004]
24 **Pleguezuelo M**, Lopez-Sanchez LM, Rodriguez-Ariza A, Montero JL, Briceno J, Ciria R, Muntane J, de la Mata M. Proteomic analysis for developing new biomarkers of hepatocellular carcinoma. *World J Hepatol* 2010; **2**: 127-135 [PMID: 21160983]
25 **Nguyen P**, Leray V, Diez M, Serisier S, Le Bloc'h J, Siliart B, Dumon H. Liver lipid metabolism. *J Anim Physiol Anim Nutr* (Berl) 2008; **92**: 272-283 [PMID: 18477307 DOI: 10.1111/j.1439-0396.2007.00752.x]
26 **Mitra V,** Metcalf J. Metabolic functions of the liver. *Anaes Inten Care Med* 2009; **10**: 334-335 [DOI: 10.1016/j.mpaic.2009.03.011]
27 **Xu EY**, Schaefer WH, Xu Q. Metabolomics in pharmaceutical research and development: metabolites, mechanisms and pathways. *Curr Opin Drug Discov Devel* 2009; **12**: 40-52 [PMID: 19152212]
28 **Yang Y**, Li C, Nie X, Feng X, Chen W, Yue Y, Tang H, Deng F. Metabonomic studies of human hepatocellular carcinoma using high-resolution magic-angle spinning 1H NMR spectroscopy in conjunction with multivariate data analysis. *J Proteome Res* 2007; **6**: 2605-2614 [PMID: 17564425 DOI: 10.1021/pr070063h]
29 **Patterson AD**, Maurhofer O, Beyoglu D, Lanz C, Krausz KW, Pabst T, Gonzalez FJ, Dufour JF, Idle JR. Aberrant lipid metabolism in hepatocellular carcinoma revealed by plasma metabolomics and lipid profiling. *Cancer Res* 2011; **71**: 6590-6600 [PMID: 21900402 DOI: 10.1158/0008-5472.CAN-11-0885]
30 **Chen T**, Xie G, Wang X, Fan J, Qiu Y, Zheng X, Qi X, Cao Y, Su M, Wang X, Xu LX, Yen Y, Liu P, Jia W. Serum and urine metabolite profiling reveals potential biomarkers of human hepatocellular carcinoma. *Mol Cell Proteomics* 2011; **10**: M110.004945 [PMID: 21518826]
31 **Wu FX**, Wang Q, Zhang ZM, Huang S, Yuan WP, Liu JY, Ban KC, Zhao YN. Identifying serological biomarkers of hepatocellular carcinoma using surface-enhanced laser desorption/ionization-time-of-flight mass spectroscopy. *Cancer Lett* 2009; **279**: 163-170 [PMID: 19268439 DOI: 10.1016/j.canlet.2009.01.034]
32 **Cao H**, Huang H, Xu W, Chen D, Yu J, Li J, Li L. Fecal metabolome profiling of liver cirrhosis and hepatocellular carcinoma patients by ultra performance liquid chromatography-mass spectrometry. *Anal Chim Acta* 2011; **691**: 68-75 [PMID: 21458633 DOI: 10.1016/j.aca.2011.02.038]
33 **Gao H**, Lu Q, Liu X, Cong H, Zhao L, Wang H, Lin D. Application of 1H NMR-based metabonomics in the study of metabolic profiling of human hepatocellular carcinoma and liver cirrhosis. *Cancer Sci* 2009; **100**: 782-785 [PMID: 19469021 DOI: 10.1111/j.1349-7006.2009.01086.x]
34 **Wu H**, Xue R, Dong L, Liu T, Deng C, Zeng H, Shen X. Metabolomic profiling of human urine in hepatocellular carcinoma patients using gas chromatography/mass spectrometry. *Anal Chim Acta* 2009; **648**: 98-104 [PMID: 19616694 DOI: 10.1016/j.aca.2009.06.033]
35 **Soga T**, Sugimoto M, Honma M, Mori M, Igarashi K, Kashikura K, Ikeda S, Hirayama A, Yamamoto T, Yoshida H, Otsuka M, Tsuji S, Yatomi Y, Sakuragawa T, Watanabe H, Nihei K, Saito T, Kawata S, Suzuki H, Tomita M, Suematsu M. Serum metabolomics reveals γ-glutamyl dipeptides as biomarkers for discrimination among different forms of liver disease. *J Hepatol* 2011; **55**: 896-905 [PMID: 21334394 DOI: 10.1016/j.jhep.2011.01.031]
36 **Ressom HW**, Xiao JF, Tuli L, Varghese RS, Zhou B, Tsai TH, Ranjbar MR, Zhao Y, Wang J, Di Poto C, Cheema AK, Tadesse MG, Goldman R, Shetty K. Utilization of metabolomics to identify serum biomarkers for hepatocellular carcinoma in patients with liver cirrhosis. *Anal Chim Acta* 2012; **743**: 90-100 [PMID: 22882828 DOI: 10.1016/j.aca.2012.07.013]
37 **Xiao JF**, Varghese RS, Zhou B, Nezami Ranjbar MR, Zhao Y, Tsai TH, Di Poto C, Wang J, Goerlitz D, Luo Y, Cheema AK, Sarhan N, Soliman H, Tadesse MG, Ziada DH, Ressom HW. LC-MS based serum metabolomics for identification of hepatocellular carcinoma biomarkers in Egyptian cohort. *J Proteome Res* 2012; **11**: 5914-5923 [PMID: 23078175 DOI: 10.1021/pr300673x]
38 **Wang B**, Chen D, Chen Y, Hu Z, Cao M, Xie Q, Chen Y, Xu J, Zheng S, Li L. Metabonomic profiles discriminate hepatocellular carcinoma from liver cirrhosis by ultraperformance liquid chromatography-mass spectrometry. *J Proteome Res* 2012; **11**: 1217-1227 [PMID: 22200553 DOI: 10.1021/pr2009252]
39 **Zhou L**, Ding L, Yin P, Lu X, Wang X, Niu J, Gao P, Xu G. Serum metabolic profiling study of hepatocellular carcinoma infected with hepatitis B or hepatitis C virus by using liquid chromatography-mass spectrometry. *J Proteome Res* 2012; **11**: 5433-5442 [PMID: 22946841 DOI: 10.1021/pr300683a]
40 **Nahon P**, Amathieu R, Triba MN, Bouchemal N, Nault JC, Ziol M, Seror O, Dhonneur G, Trinchet JC, Beaugrand M, Le Moyec L. Identification of serum proton NMR metabolomic fingerprints associated with hepatocellular carcinoma in patients with alcoholic cirrhosis. *Clin Cancer Res* 2012; **18**: 6714-6722 [PMID: 23136190 DOI: 10.1158/1078-0432.CCR-12-1099]
41 **Yin P**, Wan D, Zhao C, Chen J, Zhao X, Wang W, Lu X, Yang S, Gu J, Xu G. A metabonomic study of hepatitis B-induced liver cirrhosis and hepatocellular carcinoma by using RP-LC and HILIC coupled with mass spectrometry. *Mol Biosyst* 2009; **5**: 868-876 [PMID: 19603122 DOI: 10.1039/b820224a]
42 **Li S**, Liu H, Jin Y, Lin S, Cai Z, Jiang Y. Metabolomics study of alcohol-induced liver injury and hepatocellular carcinoma xenografts in mice. *J Chromatogr B Analyt Technol Biomed Life Sci* 2011; **879**: 2369-2375 [PMID: 21763219 DOI: 10.1016/j.jchromb.2011.06.018]
43 **Budhu A**, Roessler S, Zhao X, Yu Z, Forgues M, Ji J, Karoly E, Qin LX, Ye QH, Jia HL, Fan J, Sun HC, Tang ZY, Wang XW. Integrated metabolite and gene expression profiles identify lipid biomarkers associated with progression of hepatocellular carcinoma and patient outcomes. *Gastroenterology* 2013; **144**: 1066-1075.e1 [PMID: 23376425 DOI: 10.1053/j.gastro.2013.01.054]
44 **Beyoğlu D**, Imbeaud S, Maurhofer O, Bioulac-Sage P, Zucman-Rossi J, Dufour JF, Idle JR. Tissue metabolomics of hepatocellular

carcinoma: tumor energy metabolism and the role of transcriptomic classification. *Hepatology* 2013; **58**: 229-238 [PMID: 23463346 DOI: 10.1002/hep.26350]

45 **Fitian AI**, Nelson DR, Liu C, Xu Y, Ararat M, Cabrera R. Integrated metabolomic profiling of hepatocellular carcinoma in hepatitis C cirrhosis through GC/MS and UPLC/MS-MS. *Liver Int* 2014; **34**: 1428-1444 [PMID: 24661807 DOI: 10.1111/liv.12541]

46 **Gao R**, Cheng J, Fan C, Shi X, Cao Y, Sun B, Ding H, Hu C, Dong F, Yan X. Serum Metabolomics to Identify the Liver Disease-Specific Biomarkers for the Progression of Hepatitis to Hepatocellular Carcinoma. *Sci Rep* 2015; **5**: 18175 [PMID: 26658617 DOI: 10.1038/srep18175]

47 **Meyer K**, Jia Y, Cao WQ, Kashireddy P, Rao MS. Expression of peroxisome proliferator-activated receptor alpha, and PPARalpha regulated genes in spontaneously developed hepatocellular carcinomas in fatty acyl-CoA oxidase null mice. *Int J Oncol* 2002; **21**: 1175-1180 [PMID: 12429965]

48 **Lalwani ND**, Reddy MK, Qureshi SA, Reddy JK. Development of hepatocellular carcinomas and increased peroxisomal fatty acid beta-oxidation in rats fed [4-chloro-6-(2,3-xylidino)-2-pyrimidinylthio] acetic acid (Wy-14,643) in the semipurified diet. *Carcinogenesis* 1981; **2**: 645-650 [PMID: 7273344 DOI: 10.1093/carcin/2.7.645]

49 **Reddy JK**, Hashimoto T. Peroxisomal beta-oxidation and peroxisome proliferator-activated receptor alpha: an adaptive metabolic system. *Annu Rev Nutr* 2001; **21**: 193-230 [PMID: 11375435 DOI: 10.1146/annurev.nutr.21.1.193]

50 **Christensen E**, Woldseth B, Hagve TA, Poll-The BT, Wanders RJ, Sprecher H, Stokke O, Christophersen BO. Peroxisomal beta-oxidation of polyunsaturated long chain fatty acids in human fibroblasts. The polyunsaturated and the saturated long chain fatty acids are retroconverted by the same acyl-CoA oxidase. *Scand J Clin Lab Invest Suppl* 1993; **215**: 61-74 [PMID: 8327852 DOI: 10.3109/00365519309090698]

51 **Ojala PJ**, Hirvonen TE, Hermansson M, Somerharju P, Parkkinen J. Acyl chain-dependent effect of lysophosphatidylcholine on human neutrophils. *J Leukoc Biol* 2007; **82**: 1501-1509 [PMID: 17884992 DOI: 10.1189/jlb.0507292]

52 **Furuya H**, Shimizu Y, Kawamori T. Sphingolipids in cancer. *Cancer Metastasis Rev* 2011; **30**: 567-576 [PMID: 22005951 DOI: 10.1007/s10555-011-9304-1]

53 **Bao M**, Chen Z, Xu Y, Zhao Y, Zha R, Huang S, Liu L, Chen T, Li J, Tu H, He X. Sphingosine kinase 1 promotes tumour cell migration and invasion via the S1P/EDG1 axis in hepatocellular carcinoma. *Liver Int* 2012; **32**: 331-338 [PMID: 22098666 DOI: 10.1111/j.1478-3231.2011.02666.x]

54 **Yang L**, Yue S, Yang L, Liu X, Han Z, Zhang Y, Li L. Sphingosine kinase/sphingosine 1-phosphate (S1P)/S1P receptor axis is involved in liver fibrosis-associated angiogenesis. *J Hepatol* 2013; **59**: 114-123 [PMID: 23466305 DOI: 10.1016/j.jhep.2013.02.021]

55 **El-Mir MY**, Badia MD, Luengo N, Monte MJ, Marin JJ. Increased levels of typically fetal bile acid species in patients with hepatocellular carcinoma. *Clin Sci* (Lond) 2001; **100**: 499-508 [PMID: 11294690 DOI: 10.1042/CS20000199]

56 **El-Houseini ME,** Amer MA, El-Din AS, El-Sherbiny M, Hussein TD, Mansour O. Evaluation of Serum Total Bile Acids in the Diagnosis of Hepatocellular Carcinoma. *Cancer Inst* 2000; **12**: 307-313

57 **Thompson J,** Zhang J, Vanden Heuvel J. Activation of farnesoid-X-receptor (FXR) by bioactive lipids. Available from: URL: http://indigobiosciences.com/wp-content/uploads/2014/03/fxrposterv2.pdf

58 **Fujino T**, Takeuchi A, Maruko-Ohtake A, Ohtake Y, Satoh J, Kobayashi T, Tanaka T, Ito H, Sakamaki R, Kashimura R, Ando K, Nishimaki-Mogami T, Ohkubo Y, Kitamura N, Sato R, Kikugawa K, Hayakawa M. Critical role of farnesoid X receptor for hepatocellular carcinoma cell proliferation. *J Biochem* 2012; **152**: 577-586 [PMID: 22969091 DOI: 10.1093/jb/mvs101]

59 **Kumagai A**, Fukushima J, Takikawa H, Fukuda T, Fukusato T. Enhanced expression of farnesoid X receptor in human hepatocellular carcinoma. *Hepatol Res* 2013; **43**: 959-969 [PMID: 23369163 DOI: 10.1111/hepr.12047]

60 **Marra M**, Sordelli IM, Lombardi A, Lamberti M, Tarantino L, Giudice A, Stiuso P, Abbruzzese A, Sperlongano R, Accardo M, Agresti M, Caraglia M, Sperlongano P. Molecular targets and oxidative stress biomarkers in hepatocellular carcinoma: an overview. *J Transl Med* 2011; **9**: 171 [PMID: 21985599 DOI: 10.1186/1479-5876-9-171]

61 **Suzuki Y**, Imai K, Takai K, Hanai T, Hayashi H, Naiki T, Nishigaki Y, Tomita E, Shimizu M, Moriwaki H. Hepatocellular carcinoma patients with increased oxidative stress levels are prone to recurrence after curative treatment: a prospective case series study using the d-ROM test. *J Cancer Res Clin Oncol* 2013; **139**: 845-852 [PMID: 23411687 DOI: 10.1007/s00432-013-1389-1]

62 **Kim JW**, Dang CV. Cancer's molecular sweet tooth and the Warburg effect. *Cancer Res* 2006; **66**: 8927-8930 [PMID: 16982728 DOI: 10.1158/0008-5472.CAN-06-1501]

63 **Luo J**. Cancer's sweet tooth for serine. *Breast Cancer Res* 2011; **13**: 317 [PMID: 22189202 DOI: 10.1186/bcr2932]

64 **Locasale JW**, Grassian AR, Melman T, Lyssiotis CA, Mattaini KR, Bass AJ, Heffron G, Metallo CM, Muranen T, Sharfi H, Sasaki AT, Anastasiou D, Mullarky E, Vokes NI, Sasaki M, Beroukhim R, Stephanopoulos G, Ligon AH, Meyerson M, Richardson AL, Chin L, Wagner G, Asara JM, Brugge JS, Cantley LC, Vander Heiden MG. Phosphoglycerate dehydrogenase diverts glycolytic flux and contributes to oncogenesis. *Nat Genet* 2011; **43**: 869-874 [PMID: 21804546 DOI: 10.1038/ng.890]

65 **Possemato R**, Marks KM, Shaul YD, Pacold ME, Kim D, Birsoy K, Sethumadhavan S, Woo HK, Jang HG, Jha AK, Chen WW, Barrett FG, Stransky N, Tsun ZY, Cowley GS, Barretina J, Kalaany NY, Hsu PP, Ottina K, Chan AM, Yuan B, Garraway LA, Root DE, Mino-Kenudson M, Brachtel EF, Driggers EM, Sabatini DM. Functional genomics reveal that the serine synthesis pathway is essential in breast cancer. *Nature* 2011; **476**: 346-350 [PMID: 21760589 DOI: 10.1038/nature10350]

66 **Jain M**, Nilsson R, Sharma S, Madhusudhan N, Kitami T, Souza AL, Kafri R, Kirschner MW, Clish CB, Mootha VK. Metabolite profiling identifies a key role for glycine in rapid cancer cell proliferation. *Science* 2012; **336**: 1040-1044 [PMID: 22628656 DOI: 10.1126/science.1218595]

67 **Kim Y**, Lin Q, Glazer PM, Yun Z. Hypoxic tumor microenvironment and cancer cell differentiation. *Curr Mol Med* 2009; **9**: 425-434 [PMID: 19519400 DOI: 10.2174/156652409788167113]

68 **Chaneton B**, Hillmann P, Zheng L, Martin AC, Maddocks OD, Chokkathukalam A, Coyle JE, Jankevics A, Holding FP, Vousden KH, Frezza C, O'Reilly M, Gottlieb E. Serine is a natural ligand and allosteric activator of pyruvate kinase M2. *Nature* 2012; **491**: 458-462 [PMID: 23064226 DOI: 10.1038/nature11540]

69 **Hannelien V**, Karel G, Jo VD, Sofie S. The role of CXC chemokines in the transition of chronic inflammation to esophageal and gastric cancer. *Biochim Biophys Acta* 2012; **1825**: 117-129

70 **Kong J**, Kong L, Kong J, Ke S, Gao J, Ding X, Zheng L, Sun H, Sun W. After insufficient radiofrequency ablation, tumor-associated endothelial cells exhibit enhanced angiogenesis and promote invasiveness of residual hepatocellular carcinoma. *J Transl Med* 2012; **10**: 230 [PMID: 23171368 DOI: 10.1186/1479-5876-10-230]

71 **Bechara C**, Chai H, Lin PH, Yao Q, Chen C. Growth related oncogene-alpha (GRO-alpha): roles in atherosclerosis, angiogenesis and other inflammatory conditions. *Med Sci Monit* 2007; **13**: RA87-RA90 [PMID: 17534244]

72 **Smith DF**, Galkina E, Ley K, Huo Y. GRO family chemokines are specialized for monocyte arrest from flow. *Am J Physiol Heart Circ Physiol* 2005; **289**: H1976-H1984 [PMID: 15937099 DOI: 10.1152/ajpheart.00153.2005]

73 **Zhao XL**, Sun T, Che N, Sun D, Zhao N, Dong XY, Gu Q, Yao Z, Sun BC. Promotion of hepatocellular carcinoma metastasis through matrix metalloproteinase activation by epithelial-mesenchymal transition regulator Twist1. *J Cell Mol Med* 2011; **15**: 691-700 [PMID: 20219012 DOI: 10.1111/j.1582-4934.2010.01052.x]

74 **Ebert MP**, Lamer S, Meuer J, Malfertheiner P, Reymond M,

Buschmann T, Röcken C, Seibert V. Identification of the thrombin light chain a as the single best mass for differentiation of gastric cancer patients from individuals with dyspepsia by proteome analysis. *J Proteome Res* 2005; **4**: 586-590 [PMID: 15822938 DOI: 10.1021/pr049771i]

75 **Szutowicz A**, Tomaszewicz M, Bielarczyk H. Disturbances of acetyl-CoA, energy and acetylcholine metabolism in some encephalopathies. *Acta Neurobiol Exp* (Wars) 1996; **56**: 323-339 [PMID: 8787193]

76 **Kreis R**, Farrow N, Ross BD. Localized 1H NMR spectroscopy in patients with chronic hepatic encephalopathy. Analysis of changes in cerebral glutamine, choline and inositols. *NMR Biomed* 1991; **4**: 109-116 [PMID: 1650239 DOI: 10.1002/nbm.1940040214]

77 **Bedossa P**, Carrat F. Liver biopsy: the best, not the gold standard. *J Hepatol* 2009; **50**: 1-3 [PMID: 19017551 DOI: 10.1016/j.jhep.2008.10.014]

P- Reviewer: Wei JF **S- Editor**: Qi Y **L- Editor**: A
E- Editor: Li D

World Journal of Hepatology

Submit a Manuscript: http://www.wjgnet.com/esps/
Help Desk: http://www.wjgnet.com/esps/helpdesk.aspx
DOI: 10.4254/wjh.v9.i1.18

World J Hepatol 2017 January 8; 9(1): 18-29
ISSN 1948-5182 (online)

REVIEW

PI3K/SHIP2/PTEN pathway in cell polarity and hepatitis C virus pathogenesis

Aline Awad, Ama Gassama-Diagne

Aline Awad, Ama Gassama-Diagne, Inserm Unité 1193, Hôpital Paul Brousse, 94800 Villejuif, France

Aline Awad, Ama Gassama-Diagne, Univ Paris-Sud, UMR-S 1193, Univsité Paris-Saclay, 94800 Villejuif, France

Author contributions: Awad A and Gassama-Diagne A discussed the ideas; Awad A wrote the manuscript; Gassama-Diagne A edited the manuscript.

Supported by Agence Nationale de Recherche sur le Sida et les hépatites (ANRS, France), Ligue contre le cancer, France.

Conflict-of-interest statement: Authors declare no conflict of interests for this article.

Manuscript source: Invited manuscript

Correspondence to: Ama Gassama-Diagne, MD, Inserm Unité 1193, Hôpital Paul Brousse, 12 Avenue Paul Vaillant Couturier, 94800 Villejuif, France. ama.gassama@inserm.fr
Telephone: +33-14-5596070
Fax: +33-14-5596090

Received: June 28, 2016
Peer-review started: June 30, 2016
First decision: August 10, 2016
Revised: September 10, 2016
Accepted: November 1, 2016
Article in press: November 2, 2016
Published online: January 8, 2017

Abstract

Hepatitis C virus (HCV) infects hepatocytes, polarized cells in the liver. Chronic HCV infection often leads to steatosis, fibrosis, cirrhosis and hepatocellular carcinoma, and it has been identified as the leading cause of liver transplantation worldwide. The HCV replication cycle is dependent on lipid metabolism and particularly an accumulation of lipid droplets in host cells. Phosphoinositides (PIs) are minor phospholipids enriched in different membranes and their levels are tightly regulated by specific PI kinases and phosphatases. PIs are implicated in a vast array of cellular responses that are central to morphogenesis, such as cytoskeletal changes, cytokinesis and the recruitment of downstream effectors to govern mechanisms involved in polarization and lumen formation. Important reviews of the literature identified phosphatidylinositol (PtdIns) 4-kinases, and their lipid products PtdIns(4)P, as critical regulators of the HCV life cycle. SH2-containing inositol polyphosphate 5-phosphatase (SHIP2), phosphoinositide 3-kinase (PI3K) and their lipid products PtdIns(3,4)P2 and PtdIns(3,4,5)P3, respectively, play an important role in the cell membrane and are key to the establishment of apicobasal polarity and lumen formation. In this review, we will focus on these new functions of PI3K and SHIP2, and their deregulation by HCV, causing a disruption of apicobasal polarity, actin organization and extracellular matrix assembly. Finally we will highlight the involvement of this pathway in the event of insulin resistance and nonalcoholic fatty liver disease related to HCV infection.

Key words: Hepatitis C virus; Phosphoinositide 3-kinase; SH2-containing inositol polyphosphate 5-phosphatase; Epithelial cell polarity; Phosphoinositides

Core tip: Chronic hepatitis C virus (HCV) infection leads to liver cirrhosis and cancer. HCV infection modulates the lipid metabolism. Phosphoinositides are minor phospholipids that are also modified by HCV infection. phosphatidylinositol (PtdIns)(3,4,5)P3 is mainly formed by phosphoinositide 3-kinase (PI3K), and

can be dephosphorylated by SH2-containing inositol polyphosphate 5-phosphatase (SHIP2) to generate PtdIns(3,4)P2. In this review, we will discuss the effects of SHIP2 and PI3K on the formation of cell polarity and how their expression and activation are modulated by HCV infection, leading to the disruption of cell polarity. This pathway is also discussed in the event of insulin resistance and nonalcoholic fatty liver disease related to HCV infection.

Awad A, Gassama-Diagne A. PI3K/SHIP2/PTEN pathway in cell polarity and hepatitis C virus pathogenesis. *World J Hepatol* 2017; 9(1): 18-29 Available from: URL: http://www.wjgnet.com/1948-5182/full/v9/i1/18.htm DOI: http://dx.doi.org/10.4254/wjh.v9.i1.18

INTRODUCTION

Chronic Hepatitis C virus (HCV) infection leads to cirrhosis that will develop complications such as liver failure and liver cancer[1]. The principal target of HCV is hepatocytes, which are highly polarized cells, their plasma membranes being separated by tight junctions into apical (canalicular) and basolateral (sinusoidal) domains[2,3]. After it enters the hepatocytes, the life cycle of HCV is very closely linked to cell lipid metabolism. The very low density lipoprotein (VLDL) pathway is required for the assembly and secretion of new viral particles[4,5]. However, the effect of lipid droplets (LD) on the replication of HCV is becoming increasingly clear[6]. HCV induces an accumulation and change to the cellular distribution of LDs, moving from a dispersed profile in the cytoplasm of non-infected cells to their perinuclear localization in infected cells. This relocation permits the interaction of LDs with viral proteins and genomes[7]. While much is known about the role of lipoproteins and LDs in the HCV life cycle, studies are only now emerging on the modulation of phosphoinositides (PI) by HCV infection[8].

PIs are phosphorylated derivatives of phosphatidylinositol (PtdIns). They are minor phospholipids (10%-20%) on the inner surface of the lipid bilayer and an important constituent of the cell membrane. The phosphorylation and dephosphorylation of PIs is achieved by various isoforms of PI kinases and PI phosphatases, distributed in a specific way in the cell, this result in the distribution of different PIs in cell compartments. These complex reactions are mediated by 19 kinases and 28 phosphatases that have been identified in mammals[9,10]. Figure 1 illustrates the phosphorylation and dephosphorylation cycles of different monophosphate, diphosphate and triphosphate PIs, as well as the most widely studied kinases and phosphatases. PIs are secondary messengers responsible for transmitting receptor signals to the effectors that induce a cellular response. PIs interact with these effectors *via* specific binding domains that are known to interact with the membrane, either by specific recognition of the membrane components or through attraction by its properties such as charge, structure, curvature and amphiphilicity[11]. As well as acting as precursors of secondary messengers, PIs are spatiotemporal regulators of several target proteins involved in vesicular trafficking [such as PtdIns(4)P and PtdIns(3)P] and cytoskeletal rearrangement [PtdIns (4,5)P2], by which they control cell polarity, migration, proliferation and differentiation [PtdIns(3,4)P2] and PtdIns(3,4,5)P3[12,13].

Given the importance of PI metabolism to cellular signaling and trafficking events, numerous intracellular pathogens modulate and exploit PIs in order to ensure their survival and efficient intracellular replication[14,15]. A considerable body of literature has addressed the modulation of PIs by HCV[8]. Changes to the localization of PtdIns(4)P and activation of PI4KⅢα following HCV infection have been identified as being key to membrane network formation and viral replication[1,16,17]. In this review we will focus on the roles of phosphoinositide 3-kinase (PI3K), SH2-containing inositol polyphosphate 5-phosphatase (SHIP2) and phosphatase and tensin homologue deleted on chromosome 10 (PTEN) and their lipid products in the establishment of plasma membrane polarity. We will also discuss how HCV infection modulates these polarity mechanisms to invade host cells and replicate. Finally, we will consider the involvement of the PI3K/PTEN/SHIP2 pathway in insulin resistance and nonalcoholic fatty liver disease (NAFLD) related to HCV infection.

HCV

HCV is an enveloped virus with linear, single-stranded RNA contained in a capsid protein called core. Following entry of the virus into a host cell and uncoating of the viral genome, the translation of viral RNA produces a polyprotein that will be degraded to form three structural proteins (core, E1 and E2), six non-structural proteins (NS2, NS3, NS4A, NS4B, NS5A and NS5B) and p7 protein. The structural and non-structural proteins will mate with viral RNA to form new viral particles. This viral assembly occurs near the endoplasmic reticulum, and then new viral particles are released from the cell through fusion with the cell membrane[18,19]. Chronic infection with HCV, especially in cases of cirrhosis or advanced fibrosis, remains the leading cause of hepatocellular carcinoma (HCC) worldwide through the modulation of different pathways such as inflammation, proliferation and differentiation, and DNA damage[20]. Effective treatments for HCV have recently been developed, and over 95% of patients can now be cured[21,22], but pathologies such as cancer induced by HCV infection remain a health problem for those already infected. Interactions between viral proteins and host cell mechanisms therefore remain central to understanding the pathogenesis of HCV.

POLARITY IN THE LIVER AND THE ENTRY OF HCV

The polarity of epithelial cells is a property that is ess-

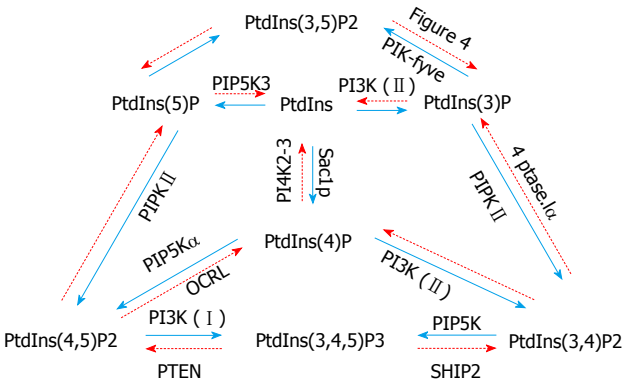

Figure 1 Phosphorylation and dephosphorylation cycles of different phosphoinositides. Monophosphate, diphosphate and triphosphate phosphoinositides are represented, as are the most widely studied kinases (in blue) and phosphatases (in red) that regulate their expression. PtdIns: Phosphatidylinositol; PI3K: Phosphoinositide 3-kinase; SHIP2: SH2-containing inositol polyphosphate 5-phosphatase; PTEN: Phosphatase and tensin homologue deleted on chromosome 10; OCRL: Inositol polyphosphate 5-phosphatase.

ential to maintaining the structure and function of the epithelium. A polarized epithelium provides an effective barrier against biological pathogens. It is characterized by an asymmetric formation of the plasma membrane, and the distribution of different intracellular organelles and cytoskeletons, including the proteins and lipids they contain. This asymmetry is created according to an apical-basal axis which reveals asymmetry of the cell from the basal pole in contact with the extracellular matrix (ECM) to the apical pole interfacing with the lumen of the tissue. The establishment of apical-basal polarity involves several steps, the first of them being contact between the cell with the ECM and also with adjacent cells by tight and adherens junctions[23] (Figure 2A). Numerous pathogens, including viruses and bacteria, are capable of modulating the regulators of cell polarity in order to infect and then replicate in host cells[14-24].

The principal target of HCV is hepatocytes, which are polarized cells in the liver. They communicate with the bloodstream *via* their basal surface which interfaces with sinusoidal endothelial cells, and they secrete bile from the apical surface, which faces and forms the bile canaliculi. The apical and basolateral domains of hepatocytes are separated by tight junctions that ensure integrity of the canaliculi and the secretory function of hepatocytes. The space between hepatocytes and sinusoidal endothelial cells is called the "space of Disse" containing hepatic stellate cells, which are mesenchymal cells responsible for much of the scarring that accompanies chronic liver injury[25] (Figure 2B). The polarization of hepatocytes is necessary to sustain the liver's architecture, and restrict infection by pathogens and the development of diseases. HCV disrupts this polarized architecture by modulating polarity proteins in order to ensure its entry and replication. In fact, HCV exploits tight junction proteins such as Claudin-1[26], occludin[27] and Interferon-induced transmembrane protein 1[28]. On the other hand, cell polarity and well maintained junctions significantly restrict HCV entry into Huh7 and HepG2 cells[29] by

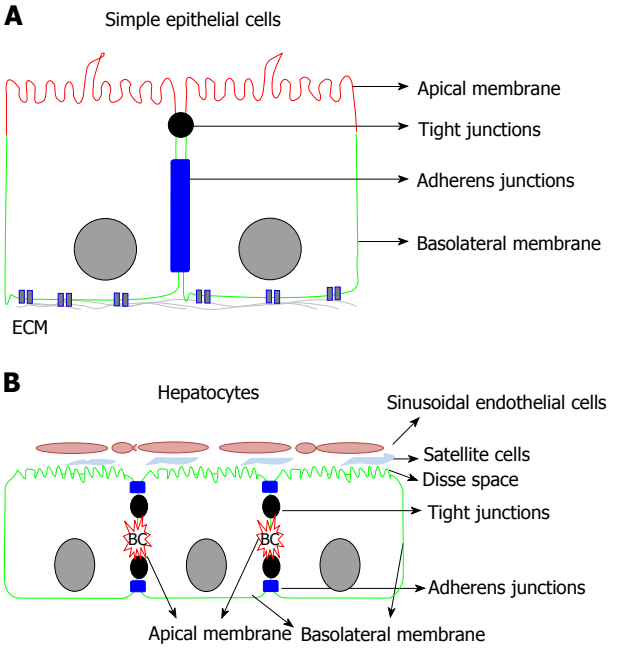

Figure 2 Comparison between simple epithelial cells polarity and hepatocytes polarity. A: The epithelial cell polarity presents a differentiation of the apical membrane (in red) to the light, and the basolateral membrane (in green) in contact with the extracellular matrix (ECM). Apical and basal membranes are separated with tight junctions (in black) and adherens junctions (in blue); B: The hepatocytes present a more complex polarity, with several apical membranes for the same cell forming bile ducts. The basolateral membrane is in contact with Disse space allowing the exchange with blood vessels.

reducing the expression of CD81 in the membrane and impairing the dynamics of scavenger receptor class B type Ⅰ (SR-B1)[30]. These findings highlight the important role of tight junctions and cell polarity in HCV entry[31,32], but pose the question as to whether HCV infection manipulates PIs in order to deregulate cell polarity, thus leading to pathogenesis. Indeed, the few studies that have focused on the link between HCV and epithelial apicobasal polarity strongly suggested that polarization restricts HCV entry into epithelial cells[33-35], so the role of PIs remains a challenging issue.

PI3K ACTIVITY, CELL POLARITY AND HCV INFECTION

PI3Ks phosphorylate the hydroxyl group 3-position of the inositol ring of PtdIns. The PI3K family of enzymes contains three different classes (Ⅰ, Ⅱ and Ⅲ), based on their substrate specificity and molecular structure[36]. PtdIns(3)P can be formed by PI3K-Ⅱ and PI3K-Ⅲ, and PtdIns(3,4)P2 is generated by the activity of PI3K-Ⅱ. The activity of PI3K-Ⅰ produces PtdIns(3,4,5)P3 which, once produced at the membrane, exercises its vital role of second messenger by recruiting different proteins containing a pleckstrin homology (PH) domain. The protein kinase Akt possesses a PH domain which was the first to be discovered and displays high affinity binding to phosphoinositides. The interaction between Akt and PtdIns(3,4,5)P3 induces a conformational change in

the Akt structure which permits its phosphorylation by phosphoinositide-dependent kinase 1 (PDPK1) at threonine 308, and the mammalian target of rapamycin complex 2 (mTORC2) at serine 473 (Figure 2). Activated Akt is responsible for triggering numerous cellular signaling pathways involved in proliferation, survival, apoptosis and autophagy[12-37]. PI3K and its lipid product PtdIns(3,4,5)P3 have been identified as key regulators of apicobasal polarity[38,39]. Watton and Downward showed that the adhesion of epithelial cells to the extracellular matrix provides protection from apoptosis *via* the activation of PI3K and Akt/PKB. They confirmed the localization of PI3K at the basolateral membrane producing PtdIns(3,4,5)P3[38]. Another study also revealed PI3K activation after interaction of the cell with the ECM and cell-cell contact. They showed that E-cadherin, which is responsible for cell-cell junctions, joins the p85 sub-unit of PI3K and activates PI3K/Akt to generate PtdIns(3,4,5)P3 during the early stages of cellular polarization[40]. Gassama-Diagne *et al*[39] studied the localization of PtdIns(3,4,5)P3 at the basolateral membrane in madin darby canine kidney (MDCK) polarized cells. This study confirmed that the formation of PtdIns(3,4,5)P3 at the basolateral membrane is essential to the initiation of basolateral polarization through the activation of Rac1. In fact, the experimental addition of exogenous PtdIns(3,4,5)P3 at the apical pole of polarized MDCK cells on transwell filters led in five minutes to the formation of PtdIns(3,4,5)P3 and basolateral protein-rich protrusions above the apical surface, from which apical proteins were excluded[39]. In MDCK 3D culture on matrigel, the formation of basolateral protein-rich protrusions was observed after three minutes of treatment with exogenous PtdIns(3,4,5)P3. The location and PI3K activity of these protrusions is important because the action of the PI3K inhibitor LY294002 inhibits the formation of protrusions, even when treating the cells with PtdIns(3,4,5)P3. By testing different ATP-competitive isoform-selective inhibitors of PI3K on the apicobasal polarity of MDCK grown in a 3D culture on Matrigel. Peng *et al*[41] recently showed that treatment with the p110δ inhibitors IC87114 and CAL-101 inverted the cell polarity of cysts displaying the apical marker Podocalyxin in contact with the ECM. The treatment of cells with other inhibitors such as PI-103, a multi-targeted inhibitor of p110α/β/δ/γ, and AS-605240 which targets p110γ, led to the formation of either multi-lumen or lumen-free cysts. Taken together, these data indicate that the P110δ isoform plays a role in establishing the apicobasal polarity axis. Next, the p110δ isoform was localized at the basolateral membrane of polarized cysts, and colocalized with the ECM receptor dystroglycan. The depletion of p110δ at the basolateral membrane disrupted laminin and type Ⅳ collagen assembly by down-regulating β1-integrin, which is a transmembrane protein with a specific role in ECM assembly and remodeling[42]. Overall, these findings revealed the role of epithelial p110δ in the orientation of cell polarity and lumen formation by regulating ECM assembly and interactions[41].

A growing body of evidence in the literature has revealed that PIs and their metabolic enzymes are essential to HCV replication at different stages of the cell cycle[16,43,44]. Some studies validated activation of the PI3K/Akt pathway following infection by HCV[45]. Epidermal growth factor receptor (EGFR), which activates the PI3K/Akt pathway, was recently shown to be a co-factor for HCV entry in a cell[46]. Moreover, Street *et al*[47] demonstrated an interaction between the viral protein NS5A and the p85 subunit of PI3K. This interaction is responsible for activating the p110 subunit of PI3K, which induces the formation of PtdIns(3,4,5)P3. The same study also showed that the NS5A protein induces the phosphorylation of Akt at tyrosine 308, thus causing anti-apoptotic activity. Other than its role in cell proliferation, transcription and migration, PI3K is also responsible for membrane expression of the SR-B1 receptor in HepG2 cells, promoting viral entry into the cells[48]. Furthermore, the NS4B protein induces lipogenesis in infected cells by activating the Akt pathway[49]. It has been shown that HCV core protein is expressed at the basal membrane of polarized cells, which leads to a deregulation of actin organization and affects focal contacts by increasing the expression of phosphorylated paxillin at the basal membrane[50]. The same study showed that the deregulation of actin is due to RhoA inhibition and Rac1 activation in cells expressing HCV core protein. These results also suggest that HCV core disrupts cell adhesion, inducing a reorganization of the actin cytoskeleton and a loss of cell polarity. Is PI3K involved in HCV core expression, thus inducing a disruption of cell adhesion? Many studies have revealed activation of the PI3K/Akt pathway and the formation of PtdIns(3,4,5)P3 following HCV infection[8,45,51,52]. This work focused on virus entry and replication and the epithelial to mesenchymal transition, but the effect of PI3K expression on the loss of cell polarity induced by HCV infection was not investigated. Nevertheless, the phenotype of cysts from MDCK cells expressing HCV core protein was of a multi-lumen type[50] which differed markedly from that of the inverted polarity cysts obtained from MDCK cells treated with the p100δ inhibitors IC87114 and CAL-101, but was similar to those from MDCK cells treated with the p110γ and p110β inhibitors AS-605240 and TGX115, respectively[41]. This observation reveals a potential role for p110γ and p110β in the loss of cell polarity induced by HCV infection. Interestingly, Peng *et al*[41]. studied an MDCK phenotype involving an over-expression of the PI3K p110 subunit. These cysts displayed a marked ECM assembly (laminin and type Ⅳ collagen) at the basal membrane and a loss of cell polarity, and they were flatter than control cells. This result allows us to advance the hypothesis that p110δ may be over-expressed in the context of HCV infection, leading to an accumulation of ECM which is responsible for cirrhosis. Taken together, these findings suggest a potential effect of PI3K and PtdIns(3,4,5)P3 on the deregulation of cell polarity induced by HCV infection.

SHIP2 ACTIVITY, CELL POLARITY AND HCV INFECTION

The level of PtdIns(3,4,5)P3 is maintained through its dephosphorylation by the phosphatases SHIP1/2 and PTEN to produce PtdIns(3,4)P2 and PtdIns(4,5)P2, respectively[53] (Figure 3). A recent study highlighted the role of PtdIns(3,4)P2 and SHIP2 as additional determinants of basolateral membrane formation[50]. In non-polarized cells, SHIP2 is localized in the perinuclear and cytoplasmic domains. After stimulation with serum, SHIP2 may be localized at focal contacts in the plasma membrane[53]. In 3D cultured MDCK cells, Awad *et al*[50] demonstrated a basolateral localization of SHIP2 and its lipid product PtdIns(3,4)P2. The enzymatic activity of SHIP2 gives rise to PtdIns(3,4)P2 and is essential for cell polarization. Indeed, SHIP2 inhibition by siRNA, and exogenous expression of the catalytic mutant of SHIP2 (D607A)[54,55] lead to a deregulation of cell polarity and the formation of multi-lumen cysts. Indeed, PtdIns(3,4)P2 is capable of binding Dlg1, the master regulator of basolateral polarity[56]. The inhibition of SHIP2 leads to a delocalization of the basolateral polarity proteins β-catenin, Scribble and Dlg1 from cell-cell contacts; moreover, their expression is markedly reduced. Overall, these data suggest that SHIP2 is required for the localization and expression of the basolateral complex proteins Dlg1 and Scribble in order to maintain cell morphogenesis[50]. Moreover, the Rho family of GTPases, and particularly RhoA and Rac1 which regulate the formation of stress fibers and lamelipodia, respectively[57], play a pivotal role in cell polarity[58]. It has been reported that SHIP2 increases the activation of RhoA in epithelial cells[50]. This activation is required for the polarization and migration of glioma cells[59]. Awad *et al*[50] confirmed that SHIP2 is an additional target for HCV infection. Their study examined the expression of SHIP2 and PtdIns(3,4)P2 in MDCK cells grown in a 3D culture on Matrigel, and in a 2D culture on transwell filters. MDCK cells expressing HCV core protein displayed a reduction of SHIP2 and PtdIns(3,4)P2 expression at the basal membrane. Interestingly, HCV core protein was localized specifically at the basal membrane in contact with the ECM. Together, these findings indicate that HCV core protein is able to subvert SHIP2 expression in order to disrupt cell membrane morphology[50]. In these cells, the down-regulation of SHIP2 and PtdIns(3,4)P2 leads to down-regulation of the expression of Dlg1 and Scribble at the basolateral membrane. These disturbances to the expression of polarity proteins lead accordingly a loss of apicobasal cell polarity and the formation of multi-lumen cysts. HCV core expression also displays a loss of RhoA activation, in the same way as SHIP2 depleted cells. Interestingly, an over-expression of SHIP2 cDNA in HCV core-expressing cells has been seen to restore single lumen formation, RhoA activation and cell polarity. Taken together, these data indicate that HCV core is able to subvert SHIP2 in order to disrupt cell polarity and infected polarized cells[50].

PTEN AND PTDINS(4,5)P2, CELL POLARITY AND HCV INFECTION

PTEN, the other phosphatase which antagonizes PI3K, is also implicated in cell polarity. Martin-Belmonte *et al*[60] identified PtdIns(4,5)P2 as a key regulator of the apical membrane. During the early stages of cyst formation, PtdIns(3,4,5)P3 and PtdIns(4,5)P2 are co-localized at the plasma membrane of non-polarized cells, while PtdIns(4,5)P2 becomes concentrated at the apical surface of polarized cells. The role of PIP5K in apical membrane trafficking, by which synthesizing PtdIns(4,5)P2, has recently been reported and confirmed the possible production of PtdIns(4,5)P2 at the apical membrane[61,62]. Meanwhile, PTEN regulates the apical recruitment of Par3, Par 6, Cdc42 and annexin 2 (Anx2), and is required for lumen development[63]. In addition, it has been shown that Par3 membrane targeting is dependent on the binding of its PDZ domain to PtdIns(4,5)P2, the product of PTEN[64,65]. The inhibition of PTEN by siRNA, or by a specific inhibitor bpV(pic), prevents the formation of a single central lumen in the cysts and causes a defective segregation of PtdIns(3,4,5)P3 and PtdIns(4,5)P2. This study also identified the fact that PTEN binds Anx2, which is responsible for the recruitment of Cdc42 and hence of apical aPKC, causing polarization of the apical membrane[60].

HCV replication is dependent on PtdIns(4,5)P2[66] the lipid product of PTEN. HCV infection leads to a down-regulation of PTEN, triggering an acceleration of lipid droplet formation and insulin resistance[67,68]. The down-regulation of PTEN causes a malformation of the apical domain in an MDCK 3D culture[60], suggesting that the multi-lumen phenotype in MCDK cells expressing HCV core protein may be caused not only by RhoA down-regulation[50] but also by modifying PTEN expression. It has been shown that the core protein of HCV genotype 3a Core decreases the expression of PTEN by blocking the translation of messenger RNA and causing an accumulation of lipid droplets in the cells. In addition, PTEN over-expression in these cells is capable of reducing the accumulation of lipid droplets. This study therefore suggests that this down-regulation of PTEN by HCV infection is a critical mechanism leading to steatosis and its progression toward fibrosis and hepatocellular carcinoma[67].

INSULIN RESISTANCE AND HCV INFECTION

Type Ⅱ diabetes, and more generally insulin resistance, is very common in the context of chronic HCV infection, as has been established by several recent epidemiological studies[69-71]. Other studies have also shown that HCV infection can cause insulin resistance by the phosphorylation of IRS-1 at a serine residue (Ser307) followed by a decreased phosphorylation of Akt Thr(308), Fox01 Ser(256) and GSK3β Ser(9), downstream players

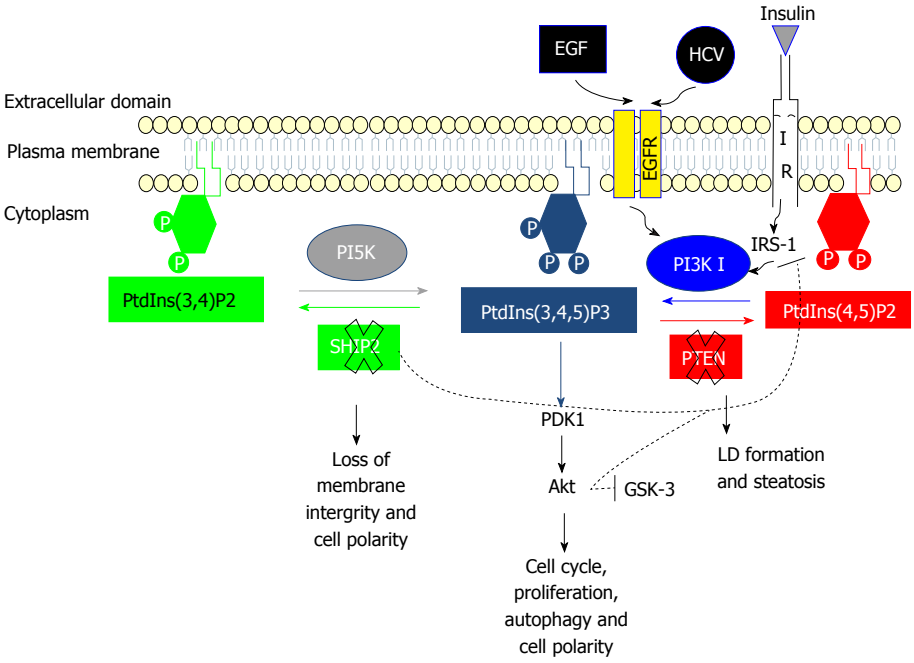

Figure 3 PI3K/Akt pathway and its activation by hepatitis C virus infection. When EGF binds to EGFR this will activate PI3K I. PI3K activation will increase the level of PtdIns(3,4,5)P3 to phosphorylate Akt and induce cell proliferation and cell polarity. Hepatitis C virus (HCV) is able to bind EGFR at its entry into a cell, thus increasing PI3K activation and the level of PtdIns(3,4,5)P3, the latter being sustained by the down-regulation of SHIP2 and PTEN. The down-regulation of SHIP2 by HCV induces a loss of membrane integrity and cell polarity, while the down regulation of PTEN induces lipid droplet (LD) formation and steatosis. PtdIns: Phosphatidylinositol; PI3K: Phosphoinositide 3-kinase; SHIP2: SH2-containing inositol polyphosphate 5-phosphatase; PTEN: Phosphatase and tensin homologue deleted on chromosome 10; EGFR: Epidermal growth factor receptor.

in the insulin signaling pathway[72,73]. These data raise the question whether insulin resistance is the cause of liver steatosis in patients with chronic HCV infection, or the consequence of viral molecular expression. Indeed, Shintani *et al*[74] showed that insulin resistance preceded the onset of steatosis in transgenic mice expressing HCV core protein, suggesting that insulin resistance was not a consequence of hepatic steatosis in these animals. Another study confirmed that the pathophysiology of fatty liver-associated chronic hepatitis C differed in patients infected with genotypes 1 and 3, showing that insulin resistance in genotype 1 patients is the cause rather than the consequence of hepatic steatosis and fibrosis, and suggesting that elevated circulating insulin levels are a risk factor for fibrosis through steatosis induced by insulin resistance. In genotype 3-infected patients, steatosis was related to HCV viral load[75]. These findings suggest that antiviral therapy in genotype 1-infected patients will not be sufficient. But does an improvement in metabolic syndrome increase the success rates of antiviral therapy? Walsh *et al*[76] confirmed that in patients with chronic HCV viral genotype 1, an increased expression of factors inhibiting interferon signaling could be a mechanism by which obesity reduces the biological response to IFN-α. In 2006, Tarantino *et al*[77] also confirmed that by improving metabolic syndrome, a lowering of the body mass index could play a key role in reducing the importance of metabolic co-factors and improving the foundations for a good antiviral response. For this reason, insulin sensitizers such as metformin are known to improve the response to HCV treatment and have been associated with a lower risk of developing HCC. Very recently, a clinical trial was initiated by the Ottawa Hospital Research Institute to evaluate the effects of metformin on liver fibrosis in HCV-HIV co-infected and HCV mono-infected patients suffering from insulin resistance. If metformin proves to be effective in reducing liver fibrosis in this patient population, it will represent a well-tolerated, easy-to-administer, inexpensive therapy that could protect against negative HCV outcomes. This study will also provide an opportunity to evaluate the impact of insulin resistance and hyperglycemia on viral clearance in HCV-infected patients treated with interferon-free regimens[78].

PI3K/SHIP2/PTEN PATHWAY AND INSULIN RESISTANCE

Akt activity is essential for the translocation and fusion of glucose transporter 4 (GLUT4) to the plasma membrane of cells in the skeletal muscle and adipose tissue. In turn, GLUT4 plays a crucial role in the absorption of glucose. Akt induced by insulin signaling is also critical to the regulation of gluconeogenesis and glycolysis in the liver. When binding insulin to its receptor, SHIP2 also binds to the cell membrane and negatively regulates insulin signaling. An over-expression of SHIP2 in adipocyte 3T3-L1 cells inhibits insulin signaling, and expression of the catalytic mutant SHIP2 enhances the activity of Akt induced by insulin and thus generates glucose uptake and glycogen synthesis[79]. In 2001, Clément *et al*[80] developed transgenic mice deficient in SHIP2.

They showed that adult mice with the heterozygous SHIP2 mutation increased their glucose tolerance and insulin sensitivity, which was also associated with an increase in recruitment of the glucose transporter GLUT4. Homozygous mice with a SHIP2 deficiency experienced severe neonatal hypoglycemia and died within three days. These results show that SHIP2 is a potent negative regulator of insulin signaling and insulin sensitivity *in vivo*. A second SHIP2 deficient mouse model was studied by Sleeman *et al*[81] in 2005. They found that SHIP2 deficient mice were viable, with normal glucose levels and normal tolerance to insulin. However, they were very resistant to putting on weight when fed a high-fat diet[81]. Although these two models had different phenotypes, the results suggest that SHIP2 is a key regulator of glucose, and its inhibition would be useful regarding efforts to improve diet-induced obesity. Furthermore, transgenic mice expressing catalytically-inactive SHIP2 have displayed altered lipid metabolism and insulin secretion[82]. In addition transgenic mice over-expressing SHIP2 WT are obese and suffer from hepatic insulin resistance[83]. These results show that the inhibition of SHIP2 may influence lipid metabolism and insulin signaling. For these reasons, the use of antisense oligonucleotides against SHIP2 in model diabetic rats produced a rapid improvement in insulin sensitivity[84]. Taken together, these *in vivo* studies suggest that an inhibition of SHIP2 expression may be effective in the treatment of type 2 diabetes. The relationship between SHIP2 and insulin resistance has also been studied in patients with type Ⅱ diabetes whose SHIP2 gene (*INPPL1*) had a deletion of the 3′ extremity. This mutation enhanced the expression of SHIP2 in the adipose tissue and skeletal muscles of diabetic patients, causing insulin resistance[85]. Overall, these findings suggest that SHIP2 is a key regulator of glucose homeostasis and could be targeted when treating diseases that affect insulin metabolism such as diabetes type Ⅱ. This central role of SHIP2 as a negative regulator of insulin signaling encouraged Sumie *et al*[86] to investigate changes to SHIP2 expression in HCC patients with HCV infection. They showed that the cumulative survival rate was significantly lower in the glucose intolerance group than that in the normal glucose tolerance group, and that the level of SHIP2 expression fell in a context of HCC when compared to that seen in non-tumor tissues. This study therefore indicated a prognostic role for glucose tolerance and SHIP2 expression in HCC patients with HCV infection.

PTEN is the second phosphoinositide phosphatase that negatively regulates insulin signaling[83-87]. Studies using 3T3-L1 adipocytes clearly demonstrated that PTEN over-expression inhibited the production of insulin-induced PtdIns(3,4)P2 and PtdIns(3,4,5)P3, the activation of Akt/PKB, the translocation of GLUT4 to the cell membrane and glucose uptake[88,89]. By contrast, the down-regulation of PTEN by small interfering RNAs enhanced Akt/PKB activation and glucose uptake in response to insulin[90]. Furthermore, an over-expression of catalytically-inactive or dominant-negative PTEN mutants also indicated that it is the lipid phosphatase activity of PTEN which is necessary to down-regulate Akt/PKB signaling and glucose uptake in response to insulin[89-91]. Finally, all these studies showed that the PI3K/Akt pathway offers a target to improve steatosis and insulin resistance during the development of NAFLD. Different treatments such as Silibinin and FAM3A (cytokine-like gene family) activate PI3K p110α/Akt signaling in order to ameliorate hepatic gluconeogenesis and lipogenesis[92,93]. Flanovol Quercetin is another treatment with favorable effects on the progression of NAFLD, acting *via* the PI3K/Akt pathway. Treatment with quercetin has been shown to reduce oxidative/nitrosative stress and inflammation, and genes related to lipid metabolism displayed a tendency to normalize in both *in vivo* and *in vitro* models[94].

PI3K/SHIP2/PTEN PATHWAY AND NAFLD

NAFLD is often associated with HCV infection. NAFLD is frequently described as encompassing a histological spectrum from nonalcoholic fatty liver to simple hepatic steatosis (SHS) plus a characteristic pattern of steatohepatitis [nonalcoholic steatohepatitis (NASH)]. HCV infection also gives rise to liver steatosis. So is the PI3K/SHIP2/PTEN pathway implicated in NAFLD in a context of HCV infection? In the liver, insulin controls lipid metabolism through its cell surface receptor and intracellular mediators such as PI3K and serine-threonine kinase Akt. It has been shown that insulin inhibits apoB100 secretion through the activation of PI3K. And insulin signaling *via* PI3K inhibited the maturation of VLDL lipoprotein particles by preventing lipidation of the VLDL precursor[95]. For this reason, a disruption of phospholipid metabolism is present in NAFLD. Indeed, a recent study demonstrated that plasma phospholipids differed between liver biopsies from NAFLD patients and healthy subjects. Phosphatidylinositol levels were higher in SHS and NASH patients compared with healthy controls[96]. Another study also identified the role of dietary phosphatidylinositol (and particularly phosphatidylcholine and phosphatidylserine) in preventing NAFLD in a rat model of metabolic syndrome[97]. Furthermore, in transgenic mice with hepatic steatosis and developing a tumor, alongside an abnormal accumulation of fatty acids, the study demonstrated activation of the Akt/mTOR pathway, and a reduction in the expression of tumor suppressor genes, including *Pten*. This confirmed that an accumulation of fatty acids may have a role in promoting *in vivo* hepatic tumorigenesis under constitutive activation of the PI3K pathway[98]. Another study confirmed that high unsaturated fatty acid levels significantly decreased PTEN mRNA expression in hepatic cells by means of a mechanism involving the sequential activation of mTOR and NFB, which were found to form a complex in cultured cells[99] which led to a significant alteration of PTEN expression. It is important to remember that inflammatory cytokines such as transforming growth factor β, tumor necrosis factor α, interleukin-6

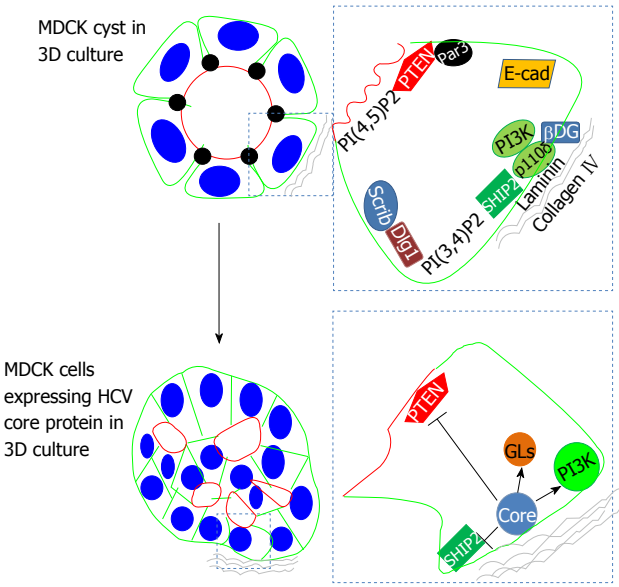

Figure 4 Effects of hepatitis C virus infection on cell polarity. In a 3D culture, MDCK form a cyst comprising a monolayer of cells around a lumen (the basolateral membrane is indicated in green, the apical membrane in red and the tight junctions in black). The right-hand column shows a zoom of a polarized cell. PI3K is activated by E-cadherin. The p110δ subunit is activated by ECM (Laminin and collagen Ⅳ). SHIP2 and PI(3,4)P2 at the basal membrane are responsible for the Dlg1/Scribble complex at the basolateral membrane. PTEN interacts with Par3 at the tight junctions and its lipid product PtdIns(4,5)P2 is localized at the apical membrane. The bottom column represents the multi-lumen phenotype of cysts expressing HCV core protein. The presence of this core protein at the basolateral membrane activates PI3K and inhibits SHIP2 and PTEN, leading to a loss of cell polarity and an accumulation of lipid droplets (LDs). HCV: Hepatitis C virus; PtdIns: Phosphatidylinositol; PI3K: Phosphoinositide 3-kinase; SHIP2: SH2-containing inositol polyphosphate 5-phosphatase; PTEN: Phosphatase and tensin homologue deleted on chromosome 10; MDCK: Madin darby canine kidney; DG: Dystroglycan.

and interleukin-1, which are produced in the course of NAFLD, also significantly alter PTEN expression, as has been shown in non-liver cells. These studies offer an interesting link between insulin resistance and steatosis, which may also explain (at least in part) the high risk of developing HCC associated with diabetes and obesity[100]. PTEN deregulation has also been demonstrated during *in vivo* studies. First, a study of heterozygous PTEN deletion was confirmed as inducing atypical adenomatous liver hyperplasia[101]. Subsequently, a genetic inhibition of PTEN expression, specifically in the liver of rodents, was shown to trigger liver steatosis, insulin hypersensitivity and HCC[102]. Because of the lack of PTEN activity, there may be an increase in fatty acid uptake by hepatocytes, and in fatty acid synthesis[103]. Hepatocyte-specific PTEN deficient mice display similar histological features to human NASH patients. These hepatocytes display enhanced lipid accumulation, inflammatory changes and hyperoxidation, and also develop into HCC[104]. Therefore, an impairment of PI3K/PTEN signaling could be involved in some NASH/HCC cases in humans. These results are very compatible with the down-regulation of PTEN in HCV infection, which leads to an acceleration of lipid droplet formation and insulin resistance[67,68]. Taken together, these studies have suggested a role for PTEN in regulating lipogenesis in liver cells; however, less information is available on the effects of another lipid phosphatase, SHIP2, on lipid and lipoprotein metabolism in the liver. A very recent study found a molecular link between SHIP2 expression and metabolic dyslipidemia using the over-expression or suppression of the *SHIP2* gene in HepG2 cells. SHIP2 over-expression led to higher lipid production and secretion *via* apoB100 secretion and de novo lipogenesis[105]. Another study confirmed that PBX-regulating protein 1 enhances *Ship2* transcription, leading to hepatic lipogenesis and steatohepatitis in mice. However, Prep1 hypomorphic heterozygous [Prep1 (i/+)] mice displayed lower SHIP2 levels, and significantly decreased serum triacylglycerol levels and the liver expression of fatty acid synthase[106]. We have discussed above the down-regulation of SHIP2 in HCV core-expressing cells, so is this down-regulation of SHIP2 the cause of lipid droplet accumulation in these cells? Overall, these findings confirm that SHIP2 is responsible for hepatic lipogenesis and secretion. To conclude, the PI3K/SHIP2/PTEN pathway, which is markedly deregulated in the context of HCV infection, activates Akt causing an over-expression of fatty acids, leading subsequently to liver steatosis, insulin hypersensitivity and HCC.

CONCLUSION

PI3K and SHIP2 have been widely studied for their roles in intracellular signaling and membrane trafficking. However, their membrane segregation and the effects of their enzymatic activity on the establishment of cell polarity are only now starting to be investigated. Recent studies have defined the manipulation of these PI enzymes and their lipid products by the hepatitis C virus, so that it can enter and replicate in epithelial host cells (Figure 4). The PI3K/PTEN/SHIP2 pathway is now better understood in the context of HCV infection, inasmuch as it induces changes to cell polarity and lipid metabolism which can generate several pathologies such as insulin resistance, liver steatosis, NAFLD and HCC.

ACKNOWLEDGMENTS

This work benefited from grant support for AGD from the French Agence Nationale de Recherches sur le Sida et les Hépatites Virales and the Association Ligue contre le cancer, France.

REFERENCES

1 **Paul D**, Madan V, Bartenschlager R. Hepatitis C virus RNA replication and assembly: living on the fat of the land. *Cell Host Microbe* 2014; **16**: 569-579 [PMID: 25525790 DOI: 10.1016/j.chom.2014.10.008]
2 **Wang L**, Boyer JL. The maintenance and generation of membrane polarity in hepatocytes. *Hepatology* 2004; **39**: 892-899 [PMID: 15057889]
3 **Treyer A**, Müsch A. Hepatocyte polarity. *Compr Physiol* 2013; **3**: 243-287 [PMID: 23720287 DOI: 10.1002/cphy.c120009]

4 **Lindenbach BD**. Virion assembly and release. *Curr Top Microbiol Immunol* 2013; **369**: 199-218 [PMID: 23463202 DOI: 10.1007/978-3-642-27340-7_8]
5 **Huang H**, Sun F, Owen DM, Li W, Chen Y, Gale M, Ye J. Hepatitis C virus production by human hepatocytes dependent on assembly and secretion of very low-density lipoproteins. *Proc Natl Acad Sci USA* 2007; **104**: 5848-5853 [PMID: 17376867]
6 **Salloum S**, Wang H, Ferguson C, Parton RG, Tai AW. Rab18 binds to hepatitis C virus NS5A and promotes interaction between sites of viral replication and lipid droplets. *PLoS Pathog* 2013; **9**: e1003513 [PMID: 23935497]
7 **Barba G**, Harper F, Harada T, Kohara M, Goulinet S, Matsuura Y, Eder G, Schaff Z, Chapman MJ, Miyamura T, Bréchot C. Hepatitis C virus core protein shows a cytoplasmic localization and associates to cellular lipid storage droplets. *Proc Natl Acad Sci USA* 1997; **94**: 1200-1205 [PMID: 9037030]
8 **Bishé B**, Syed G, Siddiqui A. Phosphoinositides in the hepatitis C virus life cycle. *Viruses* 2012; **4**: 2340-2358 [PMID: 23202467 DOI: 10.3390/v4102340]
9 **Gassama-Diagne A**, Payrastre B. Phosphoinositide signaling pathways: promising role as builders of epithelial cell polarity. *Int Rev Cell Mol Biol* 2009; **273**: 313-343 [PMID: 19215908 DOI: 10.1016/S1937-6448(08)01808-X]
10 **Balla T**. Phosphoinositides: tiny lipids with giant impact on cell regulation. *Physiol Rev* 2013; **93**: 1019-1137 [PMID: 23899561 DOI: 10.1152/physrev.00028.2012]
11 **Kutateladze TG**. Translation of the phosphoinositide code by PI effectors. *Nat Chem Biol* 2010; **6**: 507-513 [PMID: 20559318 DOI: 10.1038/nchembio.390]
12 **Cantley LC**. The phosphoinositide 3-kinase pathway. *Science* 2002; **296**: 1655-1657 [PMID: 12040186]
13 **Di Paolo G**, De Camilli P. Phosphoinositides in cell regulation and membrane dynamics. *Nature* 2006; **443**: 651-657 [PMID: 17035995]
14 **Pizarro-Cerdá J**, Cossart P. Subversion of phosphoinositide metabolism by intracellular bacterial pathogens. *Nat Cell Biol* 2004; **6**: 1026-1033 [PMID: 15516995]
15 **Altan-Bonnet N**, Balla T. Phosphatidylinositol 4-kinases: hostages harnessed to build panviral replication platforms. *Trends Biochem Sci* 2012; **37**: 293-302 [PMID: 22633842 DOI: 10.1016/j.tibs.2012.03.004]
16 **Hsu NY**, Ilnytska O, Belov G, Santiana M, Chen YH, Takvorian PM, Pau C, van der Schaar H, Kaushik-Basu N, Balla T, Cameron CE, Ehrenfeld E, van Kuppeveld FJ, Altan-Bonnet N. Viral reorganization of the secretory pathway generates distinct organelles for RNA replication. *Cell* 2010; **141**: 799-811 [PMID: 20510927 DOI: 10.1016/j.cell.2010.03.050]
17 **Lim YS**, Hwang SB. Hepatitis C virus NS5A protein interacts with phosphatidylinositol 4-kinase type IIIalpha and regulates viral propagation. *J Biol Chem* 2011; **286**: 11290-11298 [PMID: 21297162 DOI: 10.1074/jbc.M110.194472]
18 **Ariumi Y**, Kuroki M, Maki M, Ikeda M, Dansako H, Wakita T, Kato N. The ESCRT system is required for hepatitis C virus production. *PLoS One* 2011; **6**: e14517 [PMID: 21264300 DOI: 10.1371/journal.pone.0014517]
19 **Tamai K**, Shiina M, Tanaka N, Nakano T, Yamamoto A, Kondo Y, Kakazu E, Inoue J, Fukushima K, Sano K, Ueno Y, Shimosegawa T, Sugamura K. Regulation of hepatitis C virus secretion by the Hrs-dependent exosomal pathway. *Virology* 2012; **422**: 377-385 [PMID: 22138215 DOI: 10.1016/j.virol.2011.11.009]
20 **Shlomai A**, de Jong YP, Rice CM. Virus associated malignancies: the role of viral hepatitis in hepatocellular carcinoma. *Semin Cancer Biol* 2014; **26**: 78-88 [PMID: 24457013 DOI: 10.1016/j.semcancer.2014.01.004]
21 **Rice CM**, Saeed M. Hepatitis C: Treatment triumphs. *Nature* 2014; **510**: 43-44 [PMID: 24899301 DOI: 10.1038/510043a]
22 **Uhl P**, Fricker G, Haberkorn U, Mier W. Current status in the therapy of liver diseases. *Int J Mol Sci* 2014; **15**: 7500-7512 [PMID: 24786290 DOI: 10.3390/ijms15057500]
23 **Yu W**, Datta A, Leroy P, O'Brien LE, Mak G, Jou TS, Matlin KS, Mostov KE, Zegers MM. Beta1-integrin orients epithelial polarity via Rac1 and laminin. *Mol Biol Cell* 2005; **16**: 433-445 [PMID: 15574881]
24 **Wang Y,** Lu X. Cell Polarity: A Key Defence Mechanism Against Infection and Cancer Cell Invasion? *Springer* 2015; **2**: 167-186 [DOI: 10.1007/978-3-319-14466-5_7]
25 **Zong Y**, Stanger BZ. Molecular mechanisms of liver and bile duct development. *Wiley Interdiscip Rev Dev Biol* 2012; **1**: 643-655 [PMID: 23799566 DOI: 10.1002/wdev.47]
26 **Evans MJ**, von Hahn T, Tscherne DM, Syder AJ, Panis M, Wölk B, Hatziioannou T, McKeating JA, Bieniasz PD, Rice CM. Claudin-1 is a hepatitis C virus co-receptor required for a late step in entry. *Nature* 2007; **446**: 801-805 [PMID: 17325668]
27 **Ploss A**, Evans MJ, Gaysinskaya VA, Panis M, You H, de Jong YP, Rice CM. Human occludin is a hepatitis C virus entry factor required for infection of mouse cells. *Nature* 2009; **457**: 882-886 [PMID: 19182773 DOI: 10.1038/nature07684]
28 **Wilkins C**, Woodward J, Lau DT, Barnes A, Joyce M, McFarlane N, McKeating JA, Tyrrell DL, Gale M. IFITM1 is a tight junction protein that inhibits hepatitis C virus entry. *Hepatology* 2013; **57**: 461-469 [PMID: 22996292 DOI: 10.1002/hep.26066]
29 **Mee CJ**, Harris HJ, Farquhar MJ, Wilson G, Reynolds G, Davis C, van IJzendoorn SC, Balfe P, McKeating JA. Polarization restricts hepatitis C virus entry into HepG2 hepatoma cells. *J Virol* 2009; **83**: 6211-6221 [PMID: 19357163 DOI: 10.1128/JVI.00246-09]
30 **Harris HJ,** Clerte C, Farquhar MJ, Goodall M, Hu K, Rassam P, Dosset P, Wilson GK, Balfe P, Ijzendoorn SC, Milhiet PE and McKeating JA. Hepatoma polarization limits CD81 and hepatitis C virus dynamics. *Cell Microbiol* 2013; **15**: 430-445 [PMID: 23126643 DOI: 10.1111/cmi.12047]
31 **Snooks MJ**, Bhat P, Mackenzie J, Counihan NA, Vaughan N, Anderson DA. Vectorial entry and release of hepatitis A virus in polarized human hepatocytes. *J Virol* 2008; **82**: 8733-8742 [PMID: 18579610 DOI: 10.1128/JVI.00219-08]
32 **Benedicto I**, Molina-Jiménez F, Moreno-Otero R, López-Cabrera M, Majano PL. Interplay among cellular polarization, lipoprotein metabolism and hepatitis C virus entry. *World J Gastroenterol* 2011; **17**: 2683-2690 [PMID: 21734774 DOI: 10.3748/wjg.v17.i22.2683]
33 **Liu S**, Yang W, Shen L, Turner JR, Coyne CB, Wang T. Tight junction proteins claudin-1 and occludin control hepatitis C virus entry and are downregulated during infection to prevent superinfection. *J Virol* 2009; **83**: 2011-2014 [PMID: 19052094 DOI: 10.1128/JVI.01888-08]
34 **Benedicto I**, Molina-Jiménez F, Barreiro O, Maldonado-Rodríguez A, Prieto J, Moreno-Otero R, Aldabe R, López-Cabrera M, Majano PL. Hepatitis C virus envelope components alter localization of hepatocyte tight junction-associated proteins and promote occludin retention in the endoplasmic reticulum. *Hepatology* 2008; **48**: 1044-1053 [PMID: 18802961 DOI: 10.1002/hep.22465]
35 **Mee CJ**, Grove J, Harris HJ, Hu K, Balfe P, McKeating JA. Effect of cell polarization on hepatitis C virus entry. *J Virol* 2008; **82**: 461-470 [PMID: 17959672]
36 **Vanhaesebroeck B**, Stephens L, Hawkins P. PI3K signalling: the path to discovery and understanding. *Nat Rev Mol Cell Biol* 2012; **13**: 195-203 [PMID: 22358332 DOI: 10.1038/nrm3290]
37 **Manning BD**, Cantley LC. AKT/PKB signaling: navigating downstream. *Cell* 2007; **129**: 1261-1274 [PMID: 17604717]
38 **Watton SJ**, Downward J. Akt/PKB localisation and 3' phosphoinositide generation at sites of epithelial cell-matrix and cell-cell interaction. *Curr Biol* 1999; **9**: 433-436 [PMID: 10226029]
39 **Gassama-Diagne A**, Yu W, ter Beest M, Martin-Belmonte F, Kierbel A, Engel J, Mostov K. Phosphatidylinositol-3,4,5-trisphosphate regulates the formation of the basolateral plasma membrane in epithelial cells. *Nat Cell Biol* 2006; **8**: 963-970 [PMID: 16921364]
40 **Lampugnani MG**, Dejana E. Adherens junctions in endothelial cells regulate vessel maintenance and angiogenesis. *Thromb Res* 2007; **120** Suppl 2: S1-S6 [PMID: 18023702]
41 **Peng J**, Awad A, Sar S, Hamze Komaiha O, Moyano R, Rayal A, Samuel D, Shewan A, Vanhaesebroeck B, Mostov K, Gassama-Diagne A. Phosphoinositide 3-kinase p110δ promotes lumen

formation through the enhancement of apico-basal polarity and basal membrane organization. *Nat Commun* 2015; **6**: 5937 [PMID: 25583025 DOI: 10.1038/ncomms6937]

42 **Campbell ID**, Humphries MJ. Integrin structure, activation, and interactions. *Cold Spring Harb Perspect Biol* 2011; **3**: pii: a004994 [PMID: 21421922 DOI: 10.1101/cshperspect.a004994]

43 **Reiss S**, Rebhan I, Backes P, Romero-Brey I, Erfle H, Matula P, Kaderali L, Poenisch M, Blankenburg H, Hiet MS, Longerich T, Diehl S, Ramirez F, Balla T, Rohr K, Kaul A, Bühler S, Pepperkok R, Lengauer T, Albrecht M, Eils R, Schirmacher P, Lohmann V, Bartenschlager R. Recruitment and activation of a lipid kinase by hepatitis C virus NS5A is essential for integrity of the membranous replication compartment. *Cell Host Microbe* 2011; **9**: 32-45 [PMID: 21238945 DOI: 10.1016/j.chom.2010.12.002]

44 **Trotard M**, Lepère-Douard C, Régeard M, Piquet-Pellorce C, Lavillette D, Cosset FL, Gripon P, Le Seyec J. Kinases required in hepatitis C virus entry and replication highlighted by small interference RNA screening. *FASEB J* 2009; **23**: 3780-3789 [PMID: 19608626 DOI: 10.1096/fj.09-131920]

45 **He Y**, Nakao H, Tan SL, Polyak SJ, Neddermann P, Vijaysri S, Jacobs BL, Katze MG. Subversion of cell signaling pathways by hepatitis C virus nonstructural 5A protein via interaction with Grb2 and P85 phosphatidylinositol 3-kinase. *J Virol* 2002; **76**: 9207-9217 [PMID: 12186904]

46 **Lupberger J**, Zeisel MB, Xiao F, Thumann C, Fofana I, Zona L, Davis C, Mee CJ, Turek M, Gorke S, Royer C, Fischer B, Zahid MN, Lavillette D, Fresquet J, Cosset FL, Rothenberg SM, Pietschmann T, Patel AH, Pessaux P, Doffoël M, Raffelsberger W, Poch O, McKeating JA, Brino L, Baumert TF. EGFR and EphA2 are host factors for hepatitis C virus entry and possible targets for antiviral therapy. *Nat Med* 2011; **17**: 589-595 [PMID: 21516087 DOI: 10.1038/nm.2341]

47 **Street A**, Macdonald A, Crowder K, Harris M. The Hepatitis C virus NS5A protein activates a phosphoinositide 3-kinase-dependent survival signaling cascade. *J Biol Chem* 2004; **279**: 12232-12241 [PMID: 14709551]

48 **Shetty S**, Eckhardt ER, Post SR, van der Westhuyzen DR. Phosphatidylinositol-3-kinase regulates scavenger receptor class B type I subcellular localization and selective lipid uptake in hepatocytes. *Arterioscler Thromb Vasc Biol* 2006; **26**: 2125-2131 [PMID: 16794223]

49 **Park CY**, Jun HJ, Wakita T, Cheong JH, Hwang SB. Hepatitis C virus nonstructural 4B protein modulates sterol regulatory element-binding protein signaling via the AKT pathway. *J Biol Chem* 2009; **284**: 9237-9246 [PMID: 19204002 DOI: 10.1074/jbc.M808773200]

50 **Awad A**, Sar S, Barré R, Cariven C, Marin M, Salles JP, Erneux C, Samuel D, Gassama-Diagne A. SHIP2 regulates epithelial cell polarity through its lipid product, which binds to Dlg1, a pathway subverted by hepatitis C virus core protein. *Mol Biol Cell* 2013; **24**: 2171-2185 [PMID: 23699395 DOI: 10.1091/mbc.E12-08-0626]

51 **Maehama T**, Fukasawa M, Date T, Wakita T, Hanada K. A class II phosphoinositide 3-kinase plays an indispensable role in hepatitis C virus replication. *Biochem Biophys Res Commun* 2013; **440**: 150-156 [PMID: 24055031 DOI: 10.1016/j.bbrc.2013.09.048]

52 **Zhou Y**, Chen N, Liu X, Lin S, Luo W, Liu M. Kushenin induces the apoptosis of HCV-infected cells by blocking the PI3K-Akt-mTOR pathway via inhibiting NS5A. *Exp Cell Res* 2016; **345**: 108-114 [PMID: 27237092 DOI: 10.1016/j.yexcr.2016.05.002]

53 **Elong Edimo W**, Vanderwinden JM, Erneux C. SHIP2 signalling at the plasma membrane, in the nucleus and at focal contacts. *Adv Biol Regul* 2013; **53**: 28-37 [PMID: 23040614 DOI: 10.1016/j.jbior.2012.09.00]

54 **Pesesse X**, Dewaste V, De Smedt F, Laffargue M, Giuriato S, Moreau C, Payrastre B, Erneux C. The Src homology 2 domain containing inositol 5-phosphatase SHIP2 is recruited to the epidermal growth factor (EGF) receptor and dephosphorylates phosphatidylinositol 3,4,5-trisphosphate in EGF-stimulated COS-7 cells. *J Biol Chem* 2001; **276**: 28348-28355 [PMID: 11349134]

55 **Zhang J**, Liu Z, Rasschaert J, Blero D, Deneubourg L, Schurmans S, Erneux C, Pesesse X. SHIP2 controls PtdIns(3,4,5)P(3) levels and PKB activity in response to oxidative stress. *Cell Signal* 2007; **19**: 2194-2200 [PMID: 17643961]

56 **Bryant DM**, Mostov KE. From cells to organs: building polarized tissue. *Nat Rev Mol Cell Biol* 2008; **9**: 887-901 [PMID: 18946477 DOI: 10.1038/nrm2523]

57 **Burridge K**, Wennerberg K. Rho and Rac take center stage. *Cell* 2004; **116**: 167-179 [PMID: 14744429]

58 **Datta A**, Bryant DM, Mostov KE. Molecular regulation of lumen morphogenesis. *Curr Biol* 2011; **21**: R126-R136 [PMID: 21300279 DOI: 10.1016/j.cub.2010.12.003]

59 **Kato K**, Yazawa T, Taki K, Mori K, Wang S, Nishioka T, Hamaguchi T, Itoh T, Takenawa T, Kataoka C, Matsuura Y, Amano M, Murohara T, Kaibuchi K. The inositol 5-phosphatase SHIP2 is an effector of RhoA and is involved in cell polarity and migration. *Mol Biol Cell* 2012; **23**: 2593-2604 [PMID: 22593208 DOI: 10.1091/mbc.E11-11-0958]

60 **Martin-Belmonte F**, Gassama A, Datta A, Yu W, Rescher U, Gerke V, Mostov K. PTEN-mediated apical segregation of phosphoinositides controls epithelial morphogenesis through Cdc42. *Cell* 2007; **128**: 383-397 [PMID: 17254974 DOI: 10.1016/j.cell.2006.11.051]

61 **Rousso T**, Shewan AM, Mostov KE, Schejter ED, Shilo BZ. Apical targeting of the formin Diaphanous in Drosophila tubular epithelia. *Elife* 2013; **2**: e00666 [PMID: 23853710 DOI: 10.7554/eLife.00666]

62 **Szalinski CM**, Guerriero CJ, Ruiz WG, Docter BE, Rbaibi Y, Pastor-Soler NM, Apodaca G, Puthenveedu MA, Weisz OA. PIP5KIβ selectively modulates apical endocytosis in polarized renal epithelial cells. *PLoS One* 2013; **8**: e53790 [PMID: 23342003 DOI: 10.1371/journal.pone.0053790]

63 **Feng W**, Wu H, Chan LN, Zhang M. Par-3-mediated junctional localization of the lipid phosphatase PTEN is required for cell polarity establishment. *J Biol Chem* 2008; **283**: 23440-23449 [PMID: 18550519 DOI: 10.1074/jbc.M802482200]

64 **Wu H**, Feng W, Chen J, Chan LN, Huang S, Zhang M. PDZ domains of Par-3 as potential phosphoinositide signaling integrators. *Mol Cell* 2007; **28**: 886-898 [PMID: 18082612]

65 **Krahn MP**, Klopfenstein DR, Fischer N, Wodarz A. Membrane targeting of Bazooka/PAR-3 is mediated by direct binding to phosphoinositide lipids. *Curr Biol* 2010; **20**: 636-642 [PMID: 20303268 DOI: 10.1016/j.cub.2010.01.065]

66 **Cho NJ**, Lee C, Pang PS, Pham EA, Fram B, Nguyen K, Xiong A, Sklan EH, Elazar M, Koytak ES, Kersten C, Kanazawa KK, Frank CW, Glenn JS. Phosphatidylinositol 4,5-bisphosphate is an HCV NS5A ligand and mediates replication of the viral genome. *Gastroenterology* 2015; **148**: 616-625 [PMID: 25479136 DOI: 10.1053/j.gastro.2014.11.043]

67 **Clément S**, Peyrou M, Sanchez-Pareja A, Bourgoin L, Ramadori P, Suter D, Vinciguerra M, Guilloux K, Pascarella S, Rubbia-Brandt L, Negro F, Foti M. Down-regulation of phosphatase and tensin homolog by hepatitis C virus core 3a in hepatocytes triggers the formation of large lipid droplets. *Hepatology* 2011; **54**: 38-49 [PMID: 21465511 DOI: 10.1002/hep.24340]

68 **Peyrou M**, Clément S, Maier C, Bourgoin L, Branche E, Conzelmann S, Kaddai V, Foti M, Negro F. PTEN protein phosphatase activity regulates hepatitis C virus secretion through modulation of cholesterol metabolism. *J Hepatol* 2013; **59**: 420-426 [PMID: 23623999 DOI: 10.1016/j.jhep.2013.04.012]

69 **Caronia S**, Taylor K, Pagliaro L, Carr C, Palazzo U, Petrik J, O'Rahilly S, Shore S, Tom BD, Alexander GJ. Further evidence for an association between non-insulin-dependent diabetes mellitus and chronic hepatitis C virus infection. *Hepatology* 1999; **30**: 1059-1063 [PMID: 10498660 DOI: 10.1002/hep.510300416]

70 **Mason AL**, Lau JY, Hoang N, Qian K, Alexander GJ, Xu L, Guo L, Jacob S, Regenstein FG, Zimmerman R, Everhart JE, Wasserfall C, Maclaren NK, Perrillo RP. Association of diabetes mellitus and chronic hepatitis C virus infection. *Hepatology* 1999; **29**: 328-333 [PMID: 9918906 DOI: 10.1002/hep.510290235]

71 **Hui JM**, Sud A, Farrell GC, Bandara P, Byth K, Kench JG,

McCaughan GW, George J. Insulin resistance is associated with chronic hepatitis C virus infection and fibrosis progression [corrected]. *Gastroenterology* 2003; **125**: 1695-1704 [PMID: 14724822]

72 **Parvaiz F**, Manzoor S, Iqbal J, Sarkar-Dutta M, Imran M, Waris G. Hepatitis C virus NS5A promotes insulin resistance through IRS-1 serine phosphorylation and increased gluconeogenesis. *World J Gastroenterol* 2015; **21**: 12361-12369 [PMID: 26604643 DOI: 10.3748/wjg.v21.i43.12361]

73 **Kralj D**, Virović Jukić L, Stojsavljević S, Duvnjak M, Smolić M, Čurčić IB. Hepatitis C Virus, Insulin Resistance, and Steatosis. *J Clin Transl Hepatol* 2016; **4**: 66-75 [PMID: 27047774 DOI: 10.14218/JCTH.2015.00051]

74 **Shintani Y**, Fujie H, Miyoshi H, Tsutsumi T, Tsukamoto K, Kimura S, Moriya K, Koike K. Hepatitis C virus infection and diabetes: direct involvement of the virus in the development of insulin resistance. *Gastroenterology* 2004; **126**: 840-848 [PMID: 14988838]

75 **Fartoux L**, Poujol-Robert A, Guéchot J, Wendum D, Poupon R, Serfaty L. Insulin resistance is a cause of steatosis and fibrosis progression in chronic hepatitis C. *Gut* 2005; **54**: 1003-1008 [PMID: 15951550 DOI: 10.1136/gut.2004.050302]

76 **Walsh MJ**, Jonsson JR, Richardson MM, Lipka GM, Purdie DM, Clouston AD, Powell EE. Non-response to antiviral therapy is associated with obesity and increased hepatic expression of suppressor of cytokine signalling 3 (SOCS-3) in patients with chronic hepatitis C, viral genotype 1. *Gut* 2006; **55**: 529-535 [PMID: 16299039 DOI: 10.1136/gut.2005.069674]

77 **Tarantino G**, Conca P, Ariello M, Mastrolia M. Does a lower insulin resistance affect antiviral therapy response in patients suffering from HCV related chronic hepatitis? *Gut* 2006; **55**: 585 [PMID: 16531544]

78 **Doyle MA**, Singer J, Lee T, Muir M, Cooper C. Improving treatment and liver fibrosis outcomes with metformin in HCV-HIV co-infected and HCV mono-infected patients with insulin resistance: study protocol for a randomized controlled trial. *Trials* 2016; **17**: 331 [PMID: 27439433 DOI: 10.1186/s13063]

79 **Wada T**, Sasaoka T, Funaki M, Hori H, Murakami S, Ishiki M, Haruta T, Asano T, Ogawa W, Ishihara H, Kobayashi M. Overexpression of SH2-containing inositol phosphatase 2 results in negative regulation of insulin-induced metabolic actions in 3T3-L1 adipocytes via its 5'-phosphatase catalytic activity. *Mol Cell Biol* 2001; **21**: 1633-1646 [PMID: 11238900 DOI: 10.1128/MCB.21.5.1633-1646.2001]

80 **Clément S**, Krause U, Desmedt F, Tanti JF, Behrends J, Pesesse X, Sasaki T, Penninger J, Doherty M, Malaisse W, Dumont JE, Le Marchand-Brustel Y, Erneux C, Hue L, Schurmans S. The lipid phosphatase SHIP2 controls insulin sensitivity. *Nature* 2001; **409**: 92-97 [PMID: 11343120 DOI: 10.1038/35051094]

81 **Sleeman MW**, Wortley KE, Lai KM, Gowen LC, Kintner J, Kline WO, Garcia K, Stitt TN, Yancopoulos GD, Wiegand SJ. Absence of the lipid phosphatase SHIP2 confers resistance to dietary obesity. *Nat Med* 2005; **2**: 199-205 [PMID: 15654325 DOI: 10.1038/nm1178]

82 **Garofalo NA**, Teixeira Neto FJ, Pereira CD, Pignaton W, Vicente F, Alvaides RK. Cardiorespiratory and neuroendocrine changes induced by methadone in conscious and in isoflurane anaesthetised dogs. *Vet J* 2012; **194**: 398-404 [PMID: 22750283 DOI: 10.1016/cellsig.2012.06.012]

83 **Kagawa S**, Soeda Y, Ishihara H, Oya T, Sasahara M, Yaguchi S, Oshita R, Wada T, Tsuneki H, Sasaoka T. Impact of transgenic overexpression of SH2-containing inositol 5'-phosphatase 2 on glucose metabolism and insulin signaling in mice. *Endocrinology* 2008; **149**: 642-650 [PMID: 18039790 DOI: 10.1210/en.2007-0820]

84 **Buettner R**, Ottinger I, Gerhardt-Salbert C, Wrede CE, Schölmerich J, Bollheimer LC. Antisense oligonucleotides against the lipid phosphatase SHIP2 improve muscle insulin sensitivity in a dietary rat model of the metabolic syndrome. *Am J Physiol Endocrinol Metab* 2007; **292**: E1871-E1878 [PMID: 17327370 DOI: 10.1152/ajpendo.00263.2006]

85 **Marion E**, Kaisaki PJ, Pouillon V, Gueydan C, Levy JC, Bodson A, Krzentowski G, Daubresse JC, Mockel J, Behrends J, Servais G, Szpirer C, Kruys V, Gauguier D, Schurmans S. The gene INPPL1, encoding the lipid phosphatase SHIP2, is a candidate for type 2 diabetes in rat and man. *Diabetes* 2002; **51**: 2012-2017 [PMID: 12086927]

86 **Sumie S**, Kawaguchi T, Komuta M, Kuromatsu R, Itano S, Okuda K, Taniguchi E, Ando E, Takata A, Fukushima N, Koga H, Torimura T, Kojiro M, Sata M. Significance of glucose intolerance and SHIP2 expression in hepatocellular carcinoma patients with HCV infection. *Oncol Rep* 2007; **18**: 545-552 [PMID: 17671700]

87 **Vinciguerra M**, Foti M. PTEN and SHIP2 phosphoinositide phosphatases as negative regulators of insulin signalling. *Arch Physiol Biochem* 2006; **112**: 89-104 [PMID: 16931451 DOI: 10.1080/13813450600711359]

88 **Nakashima N**, Sharma PM, Imamura T, Bookstein R, Olefsky JM. The tumor suppressor PTEN negatively regulates insulin signaling in 3T3-L1 adipocytes. *J Biol Chem* 2000; **275**: 12889-12895 [PMID: 10777587]

89 **Ono H**, Katagiri H, Funaki M, Anai M, Inukai K, Fukushima Y, Sakoda H, Ogihara T, Onishi Y, Fujishiro M, Kikuchi M, Oka Y, Asano T. Regulation of phosphoinositide metabolism, Akt phosphorylation, and glucose transport by PTEN (phosphatase and tensin homolog deleted on chromosome 10) in 3T3-L1 adipocytes. *Mol Endocrinol* 2001; **15**: 1411-1422 [PMID: 11463863 DOI: 10.1210/mend.15.8.0684]

90 **Tang X**, Powelka AM, Soriano NA, Czech MP, Guilherme A. PTEN, but not SHIP2, suppresses insulin signaling through the phosphatidylinositol 3-kinase/Akt pathway in 3T3-L1 adipocytes. *J Biol Chem* 2005; **280**: 22523-22529 [PMID: 15824124 DOI: 10.1074/jbc.M501849200]

91 **Wu X**, Senechal K, Neshat MS, Whang YE, Sawyers CL. The PTEN/MMAC1 tumor suppressor phosphatase functions as a negative regulator of the phosphoinositide 3-kinase/Akt pathway. *Proc Natl Acad Sci USA* 1998; **95**: 15587-15591 [PMID: 9861013]

92 **Zhang Y**, Hai J, Cao M, Zhang Y, Pei S, Wang J, Zhang Q. Silibinin ameliorates steatosis and insulin resistance during non-alcoholic fatty liver disease development partly through targeting IRS-1/PI3K/Akt pathway. *Int Immunopharmacol* 2013; **17**: 714-720 [PMID: 24036369 DOI: 10.1016/j.intimp.2013.08.019]

93 **Wang C**, Chi Y, Li J, Miao Y, Li S, Su W, Jia S, Chen Z, Du S, Zhang X, Zhou Y, Wu W, Zhu M, Wang Z, Yang H, Xu G, Wang S, Yang J, Guan Y. FAM3A activates PI3K p110α/Akt signaling to ameliorate hepatic gluconeogenesis and lipogenesis. *Hepatology* 2014; **59**: 1779-1790 [PMID: 24806753 DOI: 10.1002/hep.26945]

94 **Pisonero-Vaquero S**, Martínez-Ferreras Á, García-Mediavilla MV, Martínez-Flórez S, Fernández A, Benet M, Olcoz JL, Jover R, González-Gallego J, Sánchez-Campos S. Quercetin ameliorates dysregulation of lipid metabolism genes via the PI3K/AKT pathway in a diet-induced mouse model of nonalcoholic fatty liver disease. *Mol Nutr Food Res* 2015; **59**: 879-893 [PMID: 25712622 DOI: 10.1002/mnfr.201400913]

95 **Berk PD**, Verna EC. Nonalcoholic Fatty Liver Disease: Lipids and Insulin Resistance. *Clin Liver Dis* 2016; **20**: 245-262 [PMID: 27063267 DOI: 10.1016/j.cld.2015.10.007]

96 **Ma DW**, Arendt BM, Hillyer LM, Fung SK, McGilvray I, Guindi M, Allard JP. Plasma phospholipids and fatty acid composition differ between liver biopsy-proven nonalcoholic fatty liver disease and healthy subjects. *Nutr Diabetes* 2016; **6**: e220 [PMID: 27428872 DOI: 10.1038/nutd.2016.27]

97 **Shirouchi B**, Nagao K, Inoue N, Furuya K, Koga S, Matsumoto H, Yanagita T. Dietary phosphatidylinositol prevents the development of nonalcoholic fatty liver disease in Zucker (fa/fa) rats. *J Agric Food Chem* 2008; **56**: 2375-2379 [PMID: 18324772 DOI: 10.1021/jf703578d]

98 **Kudo Y**, Tanaka Y, Tateishi K, Yamamoto K, Yamamoto S, Mohri D, Isomura Y, Seto M, Nakagawa H, Asaoka Y, Tada M, Ohta M, Ijichi H, Hirata Y, Otsuka M, Ikenoue T, Maeda S, Shiina S, Yoshida H, Nakajima O, Kanai F, Omata M, Koike K. Altered composition of fatty acids exacerbates hepatotumorigenesis

during activation of the phosphatidylinositol 3-kinase pathway. *J Hepatol* 2011; **55**: 1400-1408 [PMID: 21703185 DOI: 10.1016/j.jhep.2011.03.025]

99 **Vinciguerra M**, Veyrat-Durebex C, Moukil MA, Rubbia-Brandt L, Rohner-Jeanrenaud F, Foti M. PTEN down-regulation by unsaturated fatty acids triggers hepatic steatosis via an NF-kappaBp65/mTOR-dependent mechanism. *Gastroenterology* 2008; **134**: 268-280 [PMID: 18166358 DOI: 10.1053/j.gastro.2007.10.010]

100 **Peyrou M**, Bourgoin L, Foti M. PTEN in non-alcoholic fatty liver disease/non-alcoholic steatohepatitis and cancer. *Dig Dis* 2010; **28**: 236-246 [PMID: 20460918 DOI: 10.1159/000282095]

101 **Suzuki A**, de la Pompa JL, Stambolic V, Elia AJ, Sasaki T, del Barco Barrantes I, Ho A, Wakeham A, Itie A, Khoo W, Fukumoto M, Mak TW. High cancer susceptibility and embryonic lethality associated with mutation of the PTEN tumor suppressor gene in mice. *Curr Biol* 1998; **8**: 1169-1178 [PMID: 9799734]

102 **Stiles B**, Wang Y, Stahl A, Bassilian S, Lee WP, Kim YJ, Sherwin R, Devaskar S, Lesche R, Magnuson MA, Wu H. Liver-specific deletion of negative regulator Pten results in fatty liver and insulin hypersensitivity [corrected]. *Proc Natl Acad Sci USA* 2004; **101**: 2082-2087 [PMID: 14769918 DOI: 10.1073/pnas.0308617100]

103 **Matsuda S**, Kobayashi M, Kitagishi Y. Roles for PI3K/AKT/PTEN Pathway in Cell Signaling of Nonalcoholic Fatty Liver Disease. *ISRN Endocrinol* 2013; **2013**: 472432 [PMID: 23431468 DOI: 10.1155/2013/472432]

104 **Sato W**, Horie Y, Watanabe S, Suzuki A. [Tumor suppressor gene PTEN and non-alcoholic steatohepatitis (NASH)]. *Nihon Rinsho* 2005; **63**: 1475-1483 [PMID: 16101243]

105 **Gorgani-Firuzjaee S**, Khatami S, Adeli K, Meshkani R. SH2 domain-containing inositol 5-phosphatase (SHIP2) regulates de-novo lipogenesis and secretion of apoB100 containing lipoproteins in HepG2 cells. *Biochem Biophys Res Commun* 2015; **464**: 1028-1033 [PMID: 26188518 DOI: 10.1016/j.bbrc.2015.07.059]

106 **Gorgani-Firuzjaee S**, Adeli K, Meshkani R. Inhibition of SH2-domain-containing inositol 5-phosphatase (SHIP2) ameliorates palmitate induced-apoptosis through regulating Akt/FOXO1 pathway and ROS production in HepG2 cells. *Biochem Biophys Res Commun* 2015; **464**: 441-446 [PMID: 26123392 DOI: 10.1016/j.bbrc.2015.06.134]

P- Reviewer: Tarantino G **S- Editor**: Qi Y **L- Editor**: A
E- Editor: Li D

World Journal of Hepatology

Submit a Manuscript: http://www.wjgnet.com/esps/
Help Desk: http://www.wjgnet.com/esps/helpdesk.aspx
DOI: 10.4254/wjh.v9.i1.30

World J Hepatol 2017 January 8; 9(1): 30-37
ISSN 1948-5182 (online)

MINIREVIEWS

Drug-induced liver injury: Towards early prediction and risk stratification

Emanuel Raschi, Fabrizio De Ponti

Emanuel Raschi, Fabrizio De Ponti, Department of Medical and Surgical Sciences, University of Bologna, 40126 Bologna, Italy

Author contributions: Both authors provided comments to the first draft and approved the final version of the manuscript.

Conflict-of-interest statement: The authors declare no conflicts of interest regarding this manuscript.

Manuscript source: Invited manuscript

Correspondence to: Fabrizio De Ponti, MD, PhD, Department of Medical and Surgical Sciences, University of Bologna, Via Irnerio, 48, 40126 Bologna, Italy. fabrizio.deponti@unibo.it
Telephone: +39-051-2091805
Fax: +39-051-2091780

Received: August 2, 2016
Peer-review started: August 3, 2016
First decision: September 12, 2016
Revised: September 29, 2016
Accepted: November 27, 2016
Article in press: November 29, 2016
Published online: January 8, 2017

Abstract

Drug-induced liver injury (DILI) is a hot topic for clinicians, academia, drug companies and regulators, as shown by the steadily increasing number of publications and agents listed as causing liver damage (http://livertox.nih.gov/). As it was the case in the past decade with drug-induced QT prolongation/arrhythmia, there is an urgent unmet clinical need to develop tools for risk assessment and stratification in clinical practice and, in parallel, to improve prediction of pre-clinical models to support regulatory steps and facilitate early detection of liver-specific adverse drug events. Although drug discontinuation and therapy reconciliation still remain the mainstay in patient management to minimize occurrence of DILI, especially acute liver failure events, different multidisciplinary attempts have been proposed in 2016 to predict and assess drug-related risk in individual patients; these promising, albeit preliminary, results strongly support the need to pursue this innovative pathway.

Key words: Hepatotoxicity; Predictivity; Risk assessment; Safety

Core tip: The interest in drug-induced liver injury (DILI) is growing, especially in 2015-2016, with pioneering studies addressing DILI annotation, *i.e.*, risk stratification of drugs capable of causing liver damage. The latest experiences from worldwide consortia provided promising data, although there is still room for improvement before reaching an algorithm capable of discriminating hepatotoxic from non-hepatotoxic compounds, or at least of classifying high, intermediate and low risk drugs within the same therapeutic class. We should take advantage of integration of real-world data (*i.e.*, registries, healthcare databases, spontaneous reporting systems, literature) with cheminformatics to provide a comprehensive DILI risk score.

Raschi E, De Ponti F. Drug-induced liver injury: Towards early prediction and risk stratification. *World J Hepatol* 2017; 9(1): 30-37 Available from: URL: http://www.wjgnet.com/1948-5182/

full/v9/i1/30.htm DOI: http://dx.doi.org/10.4254/wjh.v9.i1.30

INTRODUCTION

The year 2015 witnessed an outstanding scientific production of studies dealing with drug-induced liver injury (DILI) and the list of drugs capable of causing liver dysfunction needs constant update, thus making DILI an emerging safety issue requiring attention by academia, regulators, drug companies and clinicians, both in specialty and general practice[1,2].

A search in MEDLINE using the strategy "DILI or drug-induced liver injury or drug-induced liver damage or herb-induced liver injury or herb-induced liver damage or hepatotoxicity" yielded 2196 publications in 2015 (performed on June 7th, 2016) (Figure 1), with more than 2000 studies per year published in the past 4 years. The proportion among the different types of studies has not substantially changed over time, with pre-clinical investigations representing the majority of publications (more than 60% of total studies in 2015). This body of evidence has generated concern within the scientific community, especially among clinicians, who are not fully aware that a number of drugs are likely to affect liver function and must be therefore considered among the differential diagnoses in patients presenting with elevated transaminases.

DILI has tremendous impact on medical prescribing attitudes: The latest data confirmed that hepatotoxicity was the most commonly reported adverse drug reaction leading to drug withdrawal worldwide (81 cases; 18%)[3]. Several global registries (in United States, Latin America, Europe and China) have continued to update case series and implement completeness and accuracy of data[4]. It is interesting to note that antinfectives/antimicrobials are the most frequently implicated drugs in DILI reports across all data registries and population-based studies, with herbal and dietary supplements being an emerging concern especially in United States[5-7].

While population-based studies are useful to estimate DILI incidence (despite suffering the inability to account for genetic backgrounds), prospective registries across various DILI consortia allow careful case adjudication. It is worth mentioning that registries consistently enrolled sicker patients as compared to epidemiological studies, with 70% of the patients jaundiced at presentation and half of them requiring hospitalization, thus the proportion of non-"true" DILI cases is probably negligible. This selection bias, probably related to the fact that DILI patients are mainly recruited in hospital units, is useful to appreciate phenotypes of liver damage (hepatocellular, cholestatic and mixed) and investigate specific features or drug signatures: Female sex, hepatocellular type of damage and high bilirubin levels emerged as risk factors for fulminant liver failure and death[8], with higher mortality risk in patients with preexisting liver disease[9].

In this minireview, we highlight advances in DILI research, focusing on recent studies that, in our opinion, provide key contribution towards an unmet clinical need: Risk stratification of drugs capable of causing liver damage, also known as DILI annotation.

SUSPECTING AND DIAGNOSING DILI: A CURRENT DILEMMA

The contribution of drugs in DILI occurrence

Different drugs have been convincingly documented to cause liver injury in numerous case reports and case series[10]. Paracetamol has been consistently reported as a leading cause of acute liver failure, whereas chlorpromazine, halothane, sulpiride and amoxicillin-clavulanate such as found to be the most common drugs leading to hepatotoxicity in all prospective studies[11]. Apart from antibiotics, the list of top 10 drugs implicated in DILI cases (in terms of frequency) comprises statins (only rarely severe liver injury was likely to be associated with statins), antitumor necrosis factor antagonists (with infliximab being the most common implicated agent, with autoimmune features), and herbal and dietary supplements (with weight loss and bodybuilding products being the most frequent causes of serious hepatotoxicity)[12].

A risk of DILI greater than 100 per 100000 users was found for chlorpromazine and sulpiride. Drugs with an intermediate risk were amoxicillin-clavulanic acid and emerged with a risk of 10 per 100000 users[13]. All other drugs were found to be less than 10 per 100000 users.

Unfortunately, in most of the cases, DILI is unpredictable because of its idiosyncratic nature; in fact, only rarely have the precise underlying mechanisms been identified (*e.g.,* mitochondrial injury, reactive metabolites, biliary transport inhibition, and immune responses). Paracetamol is a well-known example of drug causing dose-dependent DILI.

Obtaining evidence-based data to support DILI diagnosis

DILI is a diagnosis of exclusion, thus strengthening the importance of anamnesis and clinical experience. Apart from ruling out competing causes (*e.g.,* viral infections), it is crucial in the clinician's mind to have information on the notoriety, *i.e.,* whether the drug is known or has the potential to cause hepatotoxicity. However, these evidence-based data are not always easily accessible[11].

The first aid is represented by the product information or summary of the product characteristics (in United States and Europe, respectively), which however is variable in terms of details and may also substantially differ in the labeling of liver risk[14]. The key information to be checked is the existence of contraindications in patients with pre-existing liver diseases and the presence of specific warnings on the risk of liver damage, with relevant precautions in appropriate monitoring and management. It must also be kept in mind that the wording of these documents follows rules that are not always patient- and physician-friendly. Other sources of information are therefore highly needed.

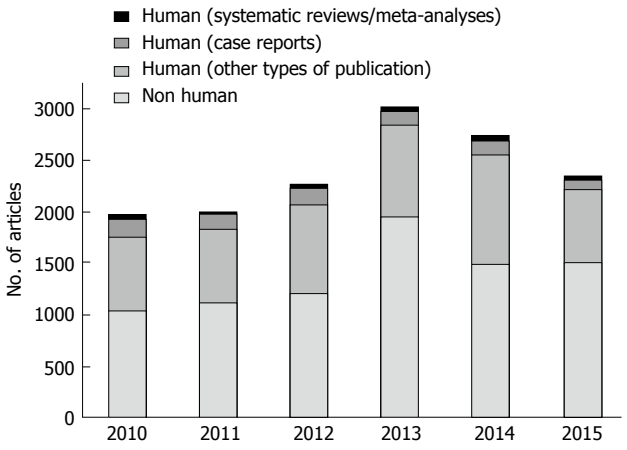

Figure 1 Trend in publication of articles on drug-induced liver injury, classified in terms of types of evidence. The search was performed in MEDLINE on June 7th, 2016, through automatic filters and keywords.

Ascertainment of the literature is the second step, which is a more challenging and time-consuming task. While some drugs have been convincingly documented to cause liver injury and clinical signatures have been demonstrated (*e.g.,* isoniazid, amoxicillin-clavulanic acid), for some agents only a few case reports are available and, most importantly, only in a minority critical clinical data are provided to ascertain the causative role of drugs[15].

The third source of data is represented by LiverTox® (http://livertox.nih.gov/), a public website set up to provide up-to-date, accurate, and easily accessible information on the diagnosis, causes, frequency and patterns of liver injury attributable to both prescription and nonprescription medications. Although LiverTox® is based on a thorough literature analysis, the quality of the published reports and the causality of the suspected liver injury reported are not provided.

Specific algorithms, such as the Roussel Uclaf Causality Assessment Method scale, have been proposed and validated to assess causality, although it should be recognized that these scores are particularly useful for regulatory and research purposes, *i.e.,* to verify a posteriori the likelihood of the association rather than to support a prospective diagnosis[16]. During the preapproval development process, Hy's Law (*i.e.,* ALT/AST > 3 ULN in combination with total bilirubin > 2 ULN in the absence of cholestatic injury - alkaline phosphatase < 2 ULN) is an essential part of the stopping rules to prevent hepatotoxicity, although it was never specifically validated in a clinical trial. Different research group have recently attempted to optimize the definition of Hy's Law and develop models for predicting acute liver failure in DILI, in combination with other biomarkers such as total bilirubin and platelet count[8,17]. However, whether such revised definitions can become part of clinical practice is yet to be determined.

Risk stratification of DILI in clinical practice: A dream or a reality?

Current expectations regard the development and implementation of risk stratification tools to assign a certain liver risk to a given drug. In other words, clinical research is trying to establish the so-called DILI annotation, a global score reflecting the frequency, causal role and severity of DILI for each drug[18]. This scenario recalls what occurred in the past decade with drug-induced QT prolongation and Torsade de Pointes (DITdP), which has been a largely debated regulatory issue for the past 20 years with still suboptimal tools for risk stratification in clinical practice[19]. With this experience in mind, we should immediately understand the importance of coordinating and harmonizing the various ongoing projects and the need to set up a global response to efficiently assess drug-related hazards. A parallel between DILI and DITdP is presented in Table 1.

Identification of baseline risk is the first step towards final risk stratification. DILI has a multifactorial nature with both environment- drug- and patient-related risk factors that may coexist and increase the likelihood of DILI occurrence.

Apart from age and sex, genetics plays a role, at least for some drugs. A recent genome-wide association study involving 620 European cases of DILI and 10588 population controls, the DRB1*16:01-DQB1*05:02 haplotype was identified as a risk factor for flupirtine-induced liver damage[20]. Although the inclusion of genetic tests in causality assessment may improve consistency and precision of DILI diagnosis as well as appropriateness of drug administration, there is only initial positive experience in clinical application of N-acetyltransferase 2 genotyping to determine the appropriate dose of isoniazid[21].

A current area of research deals with the identification of biomarkers, keeping in mind the aim of detecting patient's susceptibility to DILI prior to and during drug exposure, predicting the course of DILI once it occurs and differentiate DILI from other causes of liver injury. Among others, miR-122 expression was demonstrated to be a liver specific biomarker of paracetamol hepatotoxicity; high levels of High Mobility Group Box-1 with circulating colony stimulating factor-1 were correlated to poor prognosis and outcome in patients with established acute liver injury following paracetamol overdose; likewise, the prognostic utility of Keratin-18 has been proposed; notably, up-regulation of Kidney Injury Molecule-1, a marker of renal proximal tubular epithelia, could be a determinant of mortality in patients with paracetamol overdose and secondary kidney damage; finally, Glutamate Dehydrogenase might indicate hepatocellular necrosis, although lacking specificity in discriminating benign transaminases elevation from severe DILI occurrence. All these biomarkers, however, still require formal qualification before being considered for routine clinical use[22].

Among drug-related features, oral medications with high lipophilicity (*i.e.,* logP $\geqslant$ 3) administered at daily doses of $\geqslant$ 100 mg (known as the concept of the "Rule-of-2") have been associated with higher risk of DILI[23]. Bile salt export pump and multidrug resistance-associated protein 4 inhibitions have been also identified

Table 1 Similarities and differences between drug-induced torsade de pointes and drug-induced liver injury

	DITdP	DILI
Endpoint/biomarker	Surrogate, but well defined biomarker of risk (QT prolongation with specific thresholds)	Surrogate, but well defined biomarker of risk (transaminase elevation with specific thresholds)
Key mechanism	Largely described (dose-dependent hERG K^+ channel inhibition)	Only partially understood (different hypotheses)
Dose-response relationship	Dose dependent (with only a few exceptions)	Idiosyncratic, although dose-dependence exists
Regulatory impact	Pre-clinical and clinical guidelines (pre-marketing)	Clinical guideline (pre-marketing)
Clinical impact	Significant (a leading cause of drug withdrawal worldwide)	Significant (a leading cause of drug withdrawal worldwide)
Predictivity of pre-clinical assays	Reasonably good (new models under investigation)	Sub-optimal (especially for *in vivo* models)
Predictivity of clinical studies	Good (thorough QT study), albeit imperfect	Good (Hy's law), albeit imperfect
Role of genetics	Important (long QT syndrome)	Partially defined (only for some drugs)
Awareness (clinicians, regulators, drug developers, researchers)	Significant at all levels	Significant at some levels (drug developers, researchers)
Risk assessment tools (clinical)	Drug- and patient-related risk factors are well recognized (www.crediblemeds.org); CDSSs are under implementation	Drug- and patient-related risk factors are only partially recognized (www.livertox.nih.gov)
Causality assessment tools (clinical)	Not present, but the majority of TdP cases are drug induced (the so-called designated medical event); phenotype standardized	Specific, but challenging (several differential diagnoses)
Therapy	Magnesium sulphate, electrical cardioversion or isoproterenol (isoprenaline) or transvenous pacing (refractory TdP cases); removal or correction of precipitants, including drugs	No specific treatment other than drug discontinuation; liver transplantation may be required in acute liver failure cases

For details on DITdP[50-53]. CDSSs: Clinical decision support systems; DILI: Drug-induced liver injury; DITdP: Drug-induced torsade de pointes.

as important determinants of cholestatic DILI risk in humans[24,25]. However, the contents and the extent of information of these transporters in the summaries of the product characteristics may vary considerably between United States and Europe, especially for novel drugs[26].

Therefore, the recent literature attempted to annotate DILI risk through different approaches, all of which rely on the assessment of already available data. Among the various experiences, risk categories were created based on the information extracted from drug compendium, such as Physicians Desk Reference, and case reports (alone or integrated with literature and drug labeling)[18,27-32]. However, the validity of these published annotations is still a matter of debate because all methods present limitations and a gold standard to define DILI risk is lacking[33]. This is an unresolved concern, common to all drug-related safety issues.

Very recently, two different approaches stimulate interest in annotating DILI risk. Chen *et al*[34] combined the rule-of-two with the capacity to produce reactive metabolites and implemented a model to assess the risk of DILI onset and severity. Both dose-based and Cmax based-scores were calculated. Initial validation of this score indicated that half (19/38) of DILI cases with a dose-based DILI score $\geqslant$ 7 were associated with severe clinical outcome (*e.g.,* hepatic failure or death), while none of the cases with a DILI score < 3 were linked to severe liver injury. Statistical analysis revealed that a DILI score $\geqslant$ 7 and < 3 was significantly associated with higher or lower risk for severe hepatic outcome.

Conversely, Björnsson *et al*[35] classified drugs listed in LiverTox® website. Specifically, drugs were categorized based on the number of case reports (Category A $\geqslant$ 50 published reports, B = 12-50, C = 4-12, and D = 1-3) and another category, T, was added for agents leading to hepatotoxicity mainly in higher-than-therapeutic doses. In this study, fewer drugs than expected emerged with a documented hepatotoxicity. Among 671 drugs available for analysis, 353 (53%) had published convincing case reports of hepatotoxicity. Thus, overall, 47% of the drugs listed in LiverTox actually do not have evidence of hepatotoxicity. However, the main limitation of this analysis is that new drugs approved within the last five years were not included. Therefore, old drugs with consolidated clinical use are likely to result in higher risk. In fact, drugs in categories A and B were more likely than those in C and D to have been marketed for a long time, and both were more likely to have at least one fatal case of liver injury and reported cases of positive rechallenge. While there is little doubt that the majority drugs in category A and B are hepatotoxic, it is still unclear whether agents listed in C and D are really liver offenders.

A CRITICAL ANALYSIS OF THE DILI RISK SCORE: THE CASE OF DIRECT-ACTING ORAL ANTICOAGULANTS

Liver safety of direct-acting oral anticoagulants (DOACs) was highly debated in 2014-2015, when several publications highlighted possible occurrence of liver damage (including acute liver failure) during DOAC administration[36-39]. The majority of data are derived from case reports/series, which emphasized the relatively rapid time-to-onset and the concomitant reporting of drug that are implicated in liver damage or have the potential to result in drug interactions[39]. In particular, the time-to-onset from published case reports suggests

Table 2 Chemical and pharmacological properties of direct-acting anticoagulants likely to be associated with drug-induced liver injury risk in humans

	Dabigatran etexilate	Rivaroxaban	Apixaban	Edoxaban
Max daily dose (indication)[1]	220 (DVT prophylaxis) - 300 (NVAF)	5 (post ACS[2]) - 10 (DVT prophylaxis) - 20 (NVAF) - 30 (treatment of DVT/PE)	5 (DVT prophylaxis) - 20 (acute treatment of DVT/PE)	60 (NVAF and DVT)
Bioavailability[1]	6.50%	80%-100%	50%	62%
Protein binding	35%	> 90%	87%	55%
Cmax (ng/mL)	697 (at steady state after 400 mg/3 die)[54]	450 (multiple dose 30 mg/die)[55]	469 (single 20 mg dose)[56]	424 (90 mg daily at day 10)[57]
Lipophilicity (LogP)[5]	5.17	1.74	2.22	1.61
Biotransformation[1]	Conjugation forming 4 pharmacologically active acylglucuronides	Oxidative degradation of the morpholinone moiety and hydrolysis of the amide bonds	O-demethylation and hydroxylation at the 3-oxopiperidinyl moiety	Hydrolysis (mediated by carboxylesterase 1), conjugation or oxidation by CYP3A4/5 (< 10%)
Hepatic metabolism[1]	Only the prodrug is a substrate of P-gp; no induction/inhibition of principal isoenzymes of cytochrome P450	CYP3A4, CYP2J2 and CYP-independent mechanisms. Substrate of P-gp and BCRP	CYP3A4/5. Substrate of P-gp and BCRP	Substrate of P-gp
Structural alerts associated with RM formation	NO (aniline motif)[58,59]	NO (chlorothiophene and bis-anilide motifs)[42,58]	NO (para-methoxyaniline and bis-anilide motifs)[41,58]	ND (no published data in the literature)
Dose-based DILI Risk Score[3]	2.68	1.29	1.29	1.45[4]
Cmax-based DILI Risk Score[3]	2.98	1.87	2.02	1.82[4]

[1]From official European Summary of Product Characteristics; [2]Only in EU; [3]Calculated based on formulas reported by Chen *et al*[34]; [4]Calculated based on formulas reported by Chen *et al*[34] and assuming no RM formation; [5]Data obtained from Drug Bank (www.drugbank.ca; source: ALOGPS). ACS: Acute coronary syndrome; BCRP: Breast cancer resistance protein; DVT: Deep vein thrombosis; NVAF: Non valvular atrial fibrillation; ND: Not determined; RM: Reactive metabolites; DITdP: Drug-induced torsade de pointes.

that early evaluation of hepatic enzymes (*i.e.*, within the first month) may be considered at least in patients under complex treatment regimen with comorbidities; subsequently, liver function can be monitored on a yearly basis[40]. This is especially the case of rivaroxaban, for which a probable but unquantified association is likely to exist. Notably, rivaroxaban is the only DOAC reported in the list provided by Björnsson *et al*[35] and classified in category B.

Therefore, we applied the score developed by Chen *et al*[34] to DOACs and found intriguing data (Table 2). Based on these results, different issues emerge: (1) no DOAC appears to be associated with risk of severe liver damage (they all received a score well below the threshold of 7); (2) the highest score emerged for dabigatran; (3) the risk does not appear to be strongly influenced by dose or Cmax (there is only a small increase in Cmax-based score), or chemical motifs; (4) DOACs pose a lower risk as compared to warfarin (the dose-based risk score is 4.67, according to Chen *et al*[34]).

However, among DOACs, it is difficult to discriminate the agent with the highest risk, keeping in mind that post-marketing data have reported rivaroxaban to be most likely associated with DILI[40]. Therefore, these data suggested that current performance of this risk stratification tool is still suboptimal. In fact, this algorithm is based on pharmacokinetics characteristics and chemical features. Based on published data, apixaban, rivaroxaban and dabigatran contain structural moieties that suggest some alerts (para-methoxyaniline and bis-anilide motifs in apixaban; chlorothiophene and bis-anilide motifs in rivaroxaban; bis-anilide motifs in dabigatran), which, however, do not seem to undergo metabolism and/or generate reactive metabolites[41,42]. In the case of rivaroxaban, the pendant chlorothiophene motif is also essential for pharmacology and cannot be replaced. The aniline structural moiety is also present in the oral direct thrombin inhibitor dabigatran, which, however is not subject to oxidative metabolism by CYP enzymes in humans[43]. In summary, only partially may these peculiarities explain the risk observed in humans for rivaroxaban. This is also emphasized by the case of ximelagatran, which does not possess structural moieties implicated in liver toxicity (dose-based risk score = 2.55; Cmax-based risk score = 1.90, according to Chen *et al*[34]), thus suggesting that additional mechanisms are likely to be implicated in DILI occurrence in humans.

Therefore, our hypothesis is that there should be additional aspects that may modify the likelihood of DILI occurrence in DOAC users. Apart from host-related factors (which are not modifiable), we propose that: (1) concomitant drug with hepatotoxic and/or interacting potential may cause a subclinical liver damage that can results in symptomatic injury in susceptible patients (a concept similar to the repolarization reserve postulated for DITdP[44]); and (2) the underlying disease for which the DOAC is prescribed may contribute in increasing the likelihood of DILI with unknown mechanisms. In fact, the

majority of published case reports occurred in surgical patients with venous thromboembolism rather than with atrial fibrillation.

This calls for monitoring of liver safety when making treatment changes (addition of drugs with recognized hepatotoxicity potential, especially for long-term use) considering the different therapeutic indications of DOACs, where their role is still incompletely defined (*e.g.,* heparin-induced thrombocytopenia, cancer, triple therapy, coronary diseases, heart failure)[45]. In the meantime, chemists, pharmacologists and clinicians should join efforts to understand drug signature subtending the mechanistic basis of DILI and establish causality.

CONCLUSION AND PERSPECTIVE

Early detection, prediction and accurate risk stratification represent an urgent need for clinicians, basic scientists, regulators and drug companies. As compared to DITdP, predictivity of pre-clinical assays for DILI is still suboptimal. The role of animal studies remains questionable, mainly because of the incomplete understanding of the mechanisms underlying DILI, as well as marked species differences in response to, and in the metabolism of, xenobiotics.

As a result, there is currently no universally accepted animal model. It seems unlikely that a single *in vitro* system will be able to mimic the complex interactions in the human liver. Three-dimensional multicellular systems together with toxicogenomics-based methodologies and next-generation sequencing technologies are promising tools to develop predictive models in the near future[46]. In particular, pluripotent stem cells, which include embryonic and induced pluripotent stem cells, are being investigated to replace human primary hepatocytes (the current gold standard for preclinical toxicological screening), because they provide a stable source of hepatocytes and can be exploited for multiple applications, including early preclinical hepatotoxicity screening[47].

Risk stratification in humans is even more challenging, especially for herbals/food supplements as well as biotechnological products, because of their unpredictable kinetics and sometimes variable content.

Case reports are of course of great importance for timely detection of safety signals, although they cannot be formally used *per se* for a reliable risk assessment and stratification, but should be integrated with other data sources such as clinical trials, cohort and case-control analyses.

The importance of this global approach in the overall assessment of drug-related toxicities is recommended by the recent Pharmacovigilance legislation, which calls for integrated risk/benefit assessment based on an integrated view of all pieces of evidence[48]. This was the case of pancreatitis with incretin-based drugs: While the signal emerged from case reports, the actual existence and the magnitude of a true association was later investigated through multiple data sources, including a recent systematic review with meta-analysis of both clinical trials and observational studies, which suggested that the incidence of pancreatitis in users of incretin-based therapy is low and that the drugs do not increase the risk of pancreatitis[49-59].

In conclusion, existing consortia should pursue a joint effort along this innovative pathway aiming to develop algorithms capable not only of discriminating hepatotoxic from non-hepatotoxic compounds, but also to differentiate the risk among agents belonging to the same therapeutic class. In particular, in the era of big data, it is important to integrate real-world information (*i.e.,* registries, healthcare databases, spontaneous reporting systems, literature) with cheminformatics in order to provide a comprehensive DILI risk score and fulfill clinicians' and patients' expectations about "primum non nocere".

REFERENCES

1 **Sarges P**, Steinberg JM, Lewis JH. Drug-Induced Liver Injury: Highlights from a Review of the 2015 Literature. *Drug Saf* 2016; **39**: 801-821 [PMID: 27142208 DOI: 10.1007/s40264-016-0427-8]

2 **Lewis JH**. The Art and Science of Diagnosing and Managing Drug-induced Liver Injury in 2015 and Beyond. *Clin Gastroenterol Hepatol* 2015; **13**: 2173-2189.e8 [PMID: 26116527 DOI: 10.1016/j.cgh.2015.06.017]

3 **Onakpoya IJ**, Heneghan CJ, Aronson JK. Post-marketing withdrawal of 462 medicinal products because of adverse drug reactions: a systematic review of the world literature. *BMC Med* 2016; **14**: 10 [PMID: 26843061 DOI: 10.1186/s12916-016-0553-2]

4 **Andrade RJ**, Ortega-Alonso A, Lucena MI. "Drug-Induced Liver Injury Clinical Consortia: a global research response for a worldwide health challenge". *Expert Opin Drug Metab Toxicol* 2016; **12**: 589-593 [PMID: 26820043 DOI: 10.1517/17425255.2016.1141896]

5 **García-Cortés M**, Robles-Díaz M, Ortega-Alonso A, Medina-Caliz I, Andrade RJ. Hepatotoxicity by Dietary Supplements: A Tabular Listing and Clinical Characteristics. *Int J Mol Sci* 2016; **17**: 537 [PMID: 27070596 DOI: 10.3390/ijms17040537]

6 **Avigan MI**, Mozersky RP, Seeff LB. Scientific and Regulatory Perspectives in Herbal and Dietary Supplement Associated Hepatotoxicity in the United States. *Int J Mol Sci* 2016; **17**: 331 [PMID: 26950122 DOI: 10.3390/ijms17030331]

7 **Navarro VJ**, Barnhart H, Bonkovsky HL, Davern T, Fontana RJ, Grant L, Reddy KR, Seeff LB, Serrano J, Sherker AH, Stolz A, Talwalkar J, Vega M, Vuppalanchi R. Liver injury from herbals and dietary supplements in the U.S. Drug-Induced Liver Injury Network. *Hepatology* 2014; **60**: 1399-1408 [PMID: 25043597 DOI: 10.1002/hep.27317]

8 **Robles-Diaz M**, Lucena MI, Kaplowitz N, Stephens C, Medina-Cáliz I, González-Jimenez A, Ulzurrun E, Gonzalez AF, Fernandez MC, Romero-Gómez M, Jimenez-Perez M, Bruguera M, Prieto M, Bessone F, Hernandez N, Arrese M, Andrade RJ. Use of Hy's law and a new composite algorithm to predict acute liver failure in patients with drug-induced liver injury. *Gastroenterology* 2014; **147**: 109-118.e5 [PMID: 24704526 DOI: 10.1053/j.gastro.2014.03.050]

9 **Chalasani N**, Bonkovsky HL, Fontana R, Lee W, Stolz A, Talwalkar J, Reddy KR, Watkins PB, Navarro V, Barnhart H, Gu J, Serrano J. Features and Outcomes of 899 Patients With Drug-Induced Liver Injury: The DILIN Prospective Study. *Gastroenterology* 2015; **148**: 1340-1352.e7 [PMID: 25754159 DOI: 10.1053/j.gastro.2015.03.006]

10 **Raschi E**, Poluzzi E, Koci A, Caraceni P, De Ponti F. Assessing liver injury associated with antimycotics: Concise literature review and clues from data mining of the FAERS database. *World J Hepatol* 2014; **6**: 601-612 [PMID: 25232453 DOI: 10.4254/wjh.

v6.i8.60]
11 **Björnsson ES**. Hepatotoxicity by Drugs: The Most Common Implicated Agents. *Int J Mol Sci* 2016; **17**: 224 [PMID: 26861310 DOI: 10.3390/ijms17020224]
12 **Björnsson ES**. Drug-induced liver injury: an overview over the most critical compounds. *Arch Toxicol* 2015; **89**: 327-334 [PMID: 25618544 DOI: 10.1007/s00204-015-1456-2]
13 **de Abajo FJ**, Montero D, Madurga M, García Rodríguez LA. Acute and clinically relevant drug-induced liver injury: a population based case-control study. *Br J Clin Pharmacol* 2004; **58**: 71-80 [PMID: 15206996 DOI: 10.1111/j.1365-2125.2004.02133.x]
14 **Bjornsson ES**, Jacobsen EI, Einarsdottir R, Chalasani N. Discrepancies in liver disease labeling in the package inserts of commonly prescribed medications. *Gastroenterology* 2015; **148**: 269-273 [PMID: 25527971 DOI: 10.1053/j.gastro.2014.12.007]
15 **Agarwal VK**, McHutchison JG, Hoofnagle JH. Important elements for the diagnosis of drug-induced liver injury. *Clin Gastroenterol Hepatol* 2010; **8**: 463-470 [PMID: 20170750 DOI: 10.1016/j.cgh.2010.02.008]
16 **Danan G**, Teschke R. RUCAM in Drug and Herb Induced Liver Injury: The Update. *Int J Mol Sci* 2015; **17**: pii: E14 [PMID: 26712744 DOI: 10.3390/ijms17010014]
17 **Lo Re V**, Haynes K, Forde KA, Goldberg DS, Lewis JD, Carbonari DM, Leidl KB, Reddy KR, Nezamzadeh MS, Roy J, Sha D, Marks AR, De Boer J, Schneider JL, Strom BL, Corley DA. Risk of Acute Liver Failure in Patients With Drug-Induced Liver Injury: Evaluation of Hy's Law and a New Prognostic Model. *Clin Gastroenterol Hepatol* 2015; **13**: 2360-2368 [PMID: 26122767 DOI: 10.1016/j.cgh.2015.06.020]
18 **Chen M**, Vijay V, Shi Q, Liu Z, Fang H, Tong W. FDA-approved drug labeling for the study of drug-induced liver injury. *Drug Discov Today* 2011; **16**: 697-703 [PMID: 21624500 DOI: 10.1016/j.drudis.2011.05.007]
19 **Stockbridge N**, Morganroth J, Shah RR, Garnett C. Dealing with global safety issues: was the response to QT-liability of non-cardiac drugs well coordinated? *Drug Saf* 2013; **36**: 167-182 [PMID: 23417505 DOI: 10.1007/s40264-013-0016-z]
20 **Nicoletti P**, Werk AN, Sawle A, Shen Y, Urban TJ, Coulthard SA, Bjornsson ES, Cascorbi I, Floratos A, Stammschulte T, Gundert-Remy U, Nelson MR, Aithal GP, Daly AK. HLA-DRB1*16:01-DQB1*05: 02 is a novel genetic risk factor for flupirtine-induced liver injury. *Pharmacogenet Genomics* 2016; **26**: 218-224 [PMID: 26959717 DOI: 10.1097/FPC.0000000000000209]
21 **Aithal GP**. Pharmacogenetic testing in idiosyncratic drug-induced liver injury: current role in clinical practice. *Liver Int* 2015; **35**: 1801-1808 [PMID: 25809692 DOI: 10.1111/liv.12836]
22 **Clarke JI**, Dear JW, Antoine DJ. Recent advances in biomarkers and therapeutic interventions for hepatic drug safety - false dawn or new horizon? *Expert Opin Drug Saf* 2016; **15**: 625-634 [PMID: 26923482 DOI: 10.1517/14740338.2016.1160057]
23 **Chen M**, Borlak J, Tong W. High lipophilicity and high daily dose of oral medications are associated with significant risk for drug-induced liver injury. *Hepatology* 2013; **58**: 388-396 [PMID: 23258593 DOI: 10.1002/hep.26208]
24 **Aleo MD**, Luo Y, Swiss R, Bonin PD, Potter DM, Will Y. Human drug-induced liver injury severity is highly associated with dual inhibition of liver mitochondrial function and bile salt export pump. *Hepatology* 2014; **60**: 1015-1022 [PMID: 24799086 DOI: 10.1002/hep.27206]
25 **Köck K**, Ferslew BC, Netterberg I, Yang K, Urban TJ, Swaan PW, Stewart PW, Brouwer KL. Risk factors for development of cholestatic drug-induced liver injury: inhibition of hepatic basolateral bile acid transporters multidrug resistance-associated proteins 3 and 4. *Drug Metab Dispos* 2014; **42**: 665-674 [PMID: 24154606 DOI: 10.1124/dmd.113.054304]
26 **König J**, Müller F, Fromm MF. Transporters and drug-drug interactions: important determinants of drug disposition and effects. *Pharmacol Rev* 2013; **65**: 944-966 [PMID: 23686349 DOI: 10.1124/pr.113.007518]
27 **Xu JJ**, Henstock PV, Dunn MC, Smith AR, Chabot JR, de Graaf D. Cellular imaging predictions of clinical drug-induced liver injury. *Toxicol Sci* 2008; **105**: 97-105 [PMID: 18524759 DOI: 10.1093/toxsci/kfn109]
28 **Suzuki A**, Andrade RJ, Bjornsson E, Lucena MI, Lee WM, Yuen NA, Hunt CM, Freston JW. Drugs associated with hepatotoxicity and their reporting frequency of liver adverse events in VigiBase: unified list based on international collaborative work. *Drug Saf* 2010; **33**: 503-522 [PMID: 20486732 DOI: 10.2165/11535340-000000000-00000]
29 **Greene N**, Fisk L, Naven RT, Note RR, Patel ML, Pelletier DJ. Developing structure-activity relationships for the prediction of hepatotoxicity. *Chem Res Toxicol* 2010; **23**: 1215-1222 [PMID: 20553011 DOI: 10.1021/tx1000865]
30 **Sakatis MZ**, Reese MJ, Harrell AW, Taylor MA, Baines IA, Chen L, Bloomer JC, Yang EY, Ellens HM, Ambroso JL, Lovatt CA, Ayrton AD, Clarke SE. Preclinical strategy to reduce clinical hepatotoxicity using in vitro bioactivation data for & gt; 200 compounds. *Chem Res Toxicol* 2012; **25**: 2067-2082 [PMID: 22931300 DOI: 10.1021/tx300075j]
31 **Zhu X**, Kruhlak NL. Construction and analysis of a human hepatotoxicity database suitable for QSAR modeling using post-market safety data. *Toxicology* 2014; **321**: 62-72 [PMID: 24721472 DOI: 10.1016/j.tox.2014.03.009]
32 **Chen M**, Suzuki A, Thakkar S, Yu K, Hu C, Tong W. DILIrank: the largest reference drug list ranked by the risk for developing drug-induced liver injury in humans. *Drug Discov Today* 2016; **21**: 648-653 [PMID: 26948801 DOI: 10.1016/j.drudis.2016.02.015]
33 **Chen M**, Bisgin H, Tong L, Hong H, Fang H, Borlak J, Tong W. Toward predictive models for drug-induced liver injury in humans: are we there yet? *Biomark Med* 2014; **8**: 201-213 [PMID: 24521015 DOI: 10.2217/bmm.13.146]
34 **Chen M**, Borlak J, Tong W. A Model to predict severity of drug-induced liver injury in humans. *Hepatology* 2016; **64**: 931-940 [PMID: 27302180 DOI: 10.1002/hep.28678]
35 **Björnsson ES**, Hoofnagle JH. Categorization of drugs implicated in causing liver injury: Critical assessment based on published case reports. *Hepatology* 2016; **63**: 590-603 [PMID: 26517184 DOI: 10.1002/hep.28323]
36 **Russmann S**, Niedrig DF, Budmiger M, Schmidt C, Stieger B, Hürlimann S, Kullak-Ublick GA. Rivaroxaban postmarketing risk of liver injury. *J Hepatol* 2014; **61**: 293-300 [PMID: 24681117 DOI: 10.1016/j.jhep.2014.03.026]
37 **Liakoni E**, Rätz Bravo AE, Krähenbühl S. Hepatotoxicity of New Oral Anticoagulants (NOACs). *Drug Saf* 2015; **38**: 711-720 [PMID: 26138527 DOI: 10.1007/s40264-015-0317-5]
38 **Raschi E**, De Ponti F. Drug- and herb-induced liver injury: Progress, current challenges and emerging signals of post-marketing risk. *World J Hepatol* 2015; **7**: 1761-1771 [PMID: 26167249 DOI: 10.4254/wjh.v7.i13.1761]
39 **Raschi E**, Poluzzi E, Koci A, Salvo F, Pariente A, Biselli M, Moretti U, Moore N, De Ponti F. Liver injury with novel oral anticoagulants: assessing post-marketing reports in the US Food and Drug Administration adverse event reporting system. *Br J Clin Pharmacol* 2015; **80**: 285-293 [PMID: 25689417 DOI: 10.1111/bcp.12611]
40 **Raschi E**, Bianchin M, Ageno W, De Ponti R, De Ponti F. Adverse events associated with the use of direct-acting oral anticoagulants in clinical practice: beyond bleeding complications. *Pol Arch Med Wewn* 2016; **126**: 552-561 [PMID: 27578223 DOI: 10.20452/pamw.3529]
41 **Zhang D**, He K, Raghavan N, Wang L, Mitroka J, Maxwell BD, Knabb RM, Frost C, Schuster A, Hao F, Gu Z, Humphreys WG, Grossman SJ. Comparative metabolism of 14C-labeled apixaban in mice, rats, rabbits, dogs, and humans. *Drug Metab Dispos* 2009; **37**: 1738-1748 [PMID: 19420130 DOI: 10.1124/dmd.108.025981]
42 **Weinz C**, Schwarz T, Kubitza D, Mueck W, Lang D. Metabolism and excretion of rivaroxaban, an oral, direct factor Xa inhibitor, in rats, dogs, and humans. *Drug Metab Dispos* 2009; **37**: 1056-1064 [PMID: 19196845 DOI: 10.1124/dmd.108.025569]
43 **Stangier J**. Clinical pharmacokinetics and pharmacodynamics

of the oral direct thrombin inhibitor dabigatran etexilate. *Clin Pharmacokinet* 2008; **47**: 285-295 [PMID: 18399711 DOI: 10.2165/00003088-200847050-00001]

44 **Roden DM**. Taking the "idio" out of "idiosyncratic": predicting torsades de pointes. *Pacing Clin Electrophysiol* 1998; **21**: 1029-1034 [PMID: 9604234 DOI: 10.1111/j.1540-8159.1998.tb00148.x]

45 **Chan NC**, Eikelboom JW, Weitz JI. Evolving Treatments for Arterial and Venous Thrombosis: Role of the Direct Oral Anticoagulants. *Circ Res* 2016; **118**: 1409-1424 [PMID: 27126650 DOI: 10.1161/CIRCRESAHA.116.306925]

46 **Jiang J**, Wolters JE, van Breda SG, Kleinjans JC, de Kok TM. Development of novel tools for the in vitro investigation of drug-induced liver injury. *Expert Opin Drug Metab Toxicol* 2015; **11**: 1523-1537 [PMID: 26155718 DOI: 10.1517/17425255.2015.1065814]

47 **Gómez-Lechón MJ**, Tolosa L. Human hepatocytes derived from pluripotent stem cells: a promising cell model for drug hepatotoxicity screening. *Arch Toxicol* 2016; **90**: 2049-2061 [PMID: 27325232 DOI: 10.1007/s00204-016-1756-1]

48 **Raschi E**, De Ponti F. Drug Utilization Research and Pharmacovigilance. In: Elseviers M, Wettermark B, Almarsdóttir AB, Andersen M, Benko R, Bennie M, Eriksson I, Godman B, Krska J, Poluzzi E, Taxis K, Vlahović-Palčevski V, Vander Stichele R. Drug Utilization Research: Methods and Applications. Chichester UK: John Wiley & Sons, 2016: 399-407

49 **Li L**, Shen J, Bala MM, Busse JW, Ebrahim S, Vandvik PO, Rios LP, Malaga G, Wong E, Sohani Z, Guyatt GH, Sun X. Incretin treatment and risk of pancreatitis in patients with type 2 diabetes mellitus: systematic review and meta-analysis of randomised and non-randomised studies. *BMJ* 2014; **348**: g2366 [PMID: 24736555 DOI: 10.1136/bmj.g2366]

50 **Drew BJ**, Ackerman MJ, Funk M, Gibler WB, Kligfield P, Menon V, Philippides GJ, Roden DM, Zareba W. Prevention of torsade de pointes in hospital settings: a scientific statement from the American Heart Association and the American College of Cardiology Foundation. *Circulation* 2010; **121**: 1047-1060 [PMID: 20142454 DOI: 10.1161/CIRCULATIONAHA.109.192704]

51 **Behr ER**, January C, Schulze-Bahr E, Grace AA, Kääb S, Fiszman M, Gathers S, Buckman S, Youssef A, Pirmohamed M, Roden D. The International Serious Adverse Events Consortium (iSAEC) phenotype standardization project for drug-induced torsades de pointes. *Eur Heart J* 2013; **34**: 1958-1963 [PMID: 22752616 DOI: 10.1093/eurheartj/ehs172]

52 **Thomas SH**, Behr ER. Pharmacological treatment of acquired QT prolongation and torsades de pointes. *Br J Clin Pharmacol* 2016; **81**: 420-427 [PMID: 26183037 DOI: 10.1111/bcp.12726]

53 **Schwartz PJ**, Woosley RL. Predicting the Unpredictable: Drug-Induced QT Prolongation and Torsades de Pointes. *J Am Coll Cardiol* 2016; **67**: 1639-1650 [PMID: 27150690 DOI: 10.1016/j.jacc.2015.12.063]

54 **Stangier J**, Rathgen K, Stähle H, Gansser D, Roth W. The pharmacokinetics, pharmacodynamics and tolerability of dabigatran etexilate, a new oral direct thrombin inhibitor, in healthy male subjects. *Br J Clin Pharmacol* 2007; **64**: 292-303 [PMID: 17506785 DOI: 10.1111/j.1365-2125.2007.02899.x]

55 **Kubitza D**, Becka M, Wensing G, Voith B, Zuehlsdorf M. Safety, pharmacodynamics, and pharmacokinetics of BAY 59-7939--an oral, direct Factor Xa inhibitor--after multiple dosing in healthy male subjects. *Eur J Clin Pharmacol* 2005; **61**: 873-880 [PMID: 16328318 DOI: 10.1007/s00228-005-0043-5]

56 **Raghavan N**, Frost CE, Yu Z, He K, Zhang H, Humphreys WG, Pinto D, Chen S, Bonacorsi S, Wong PC, Zhang D. Apixaban metabolism and pharmacokinetics after oral administration to humans. *Drug Metab Dispos* 2009; **37**: 74-81 [PMID: 18832478 DOI: 10.1124/dmd.108.023143]

57 **Ogata K**, Mendell-Harary J, Tachibana M, Masumoto H, Oguma T, Kojima M, Kunitada S. Clinical safety, tolerability, pharmacokinetics, and pharmacodynamics of the novel factor Xa inhibitor edoxaban in healthy volunteers. *J Clin Pharmacol* 2010; **50**: 743-753 [PMID: 20081065 DOI: 10.1177/0091270009351883]

58 **Kalgutkar AS**, Dalvie D. Predicting toxicities of reactive metabolite-positive drug candidates. *Annu Rev Pharmacol Toxicol* 2015; **55**: 35-54 [PMID: 25292426 DOI: 10.1146/annurev-pharmtox-010814-124720]

59 **Liu R**, Yu X, Wallqvist A. Data-driven identification of structural alerts for mitigating the risk of drug-induced human liver injuries. *J Cheminform* 2015; **7**: 4 [PMID: 25717346 DOI: 10.1186/s13321-015-0053-y]

P- Reviewer: Cao GW, He ST, Morales-Gonzalez JA, Oda S
S- Editor: Qiu S **L- Editor**: A **E- Editor**: Li D

World Journal of Hepatology

Submit a Manuscript: http://www.wjgnet.com/esps/
Help Desk: http://www.wjgnet.com/esps/helpdesk.aspx
DOI: 10.4254/wjh.v9.i1.38

World J Hepatol 2017 January 8; 9(1): 38-47
ISSN 1948-5182 (online)

ORIGINAL ARTICLE

Basic Study

Ultrasound shear wave elastography and liver fibrosis: A Prospective Multicenter Study

Joyce Anyona Sande, Suleman Verjee, Sudhir Vinayak, Farin Amersi, Munir Ghesani

Joyce Anyona Sande, Sudhir Vinayak, Department of Radiology, Aga Khan University Hospital, Nairobi 30270-00100, Kenya

Suleman Verjee, Department of Statistical, Versante International LLC, Oakland, CA 94606, United States

Farin Amersi, Department of Surgery, Cedars-Sinai Medical Center, Los Angeles, CA 90048, United States

Munir Ghesani, Department of Radiology, NYU Langone Medical Center, New York, NY 10016, United States

Author contributions: Sande JA performed the research; Sande JA and Verjee S designed the research and analyzed the data; Sande JA, Verjee S, Vinayak S, Amersi F and Ghesani M contributed equally to this work; Vinayak S contributed new reagents/analytic tools; all the authors wrote the paper.

Institutional review board statement: Aga Khan University Faculty of Health Sciences Research and Ethics Committee reviewed the proposal and related documentation submitted and approved the study based on core scientific and ethical standards which were fully instituted in the protocol.

Informed consent statement: Informed voluntary consent was acquired from all the study participants.

Conflict-of-interest statement: All authors declare no conflicting interests (including but not limited to commercial, personal, political, intellectual or religious interests).

Data sharing statement: Technical appendix, statistical code and data set available from the corresponding author at sande.joyce@gmail.com. Presented data are anonymised and risk of identification is nil.

Manuscript source: Unsolicited manuscript

Correspondence to: Joyce Anyona Sande, MBCHB, Department of Radiology, Aga Khan University Hospital, Stadium Road, Nairobi 30270-00100, Kenya. sande.joyce@gmail.com
Telephone: +254-20-87706015

Received: April 5, 2016
Peer-review started: April 6, 2016
First decision: May 17, 2016
Revised: June 24, 2016
Accepted: August 6, 2016
Article in press: August 8, 2016
Published online: January 8, 2017

Abstract

AIM

To assess the accuracy of shear wave elastography (SWE) alone and in combination with aminotransferase platelet ratio index (APRI) score in the staging of liver fibrosis.

METHODS

A multicenter prospective study was conducted to assess the accuracy of SWE (medians) and APRI to predict biopsy results. The analysis focused on distinguishing the different stages of liver disease, namely, F0 from F1-4, F0-1 from F2-4, F0-2 from F3-4 and F0-3 from F4; F0-F1 from F2-F4 being of primary interest. The area under the receiver operating characteristic (AUROC) curve was computed using logistic regression model. The role of age, gender and steatosis was also assessed.

RESULTS

SWE alone accurately distinguished F0-1 from F2-4 with a high probability. The AUROC using SWE alone was 0.91 compared to 0.78 for using the APRI score alone.

The APRI score, when used in conjunction with SWE, did not make a significant contribution to the AUROC. SWE and steatosis were the only significant predictors that differentiated F0-1 from F2-4 with an AUROC of 0.944.

CONCLUSION

Our study validates the use of SWE in the diagnosis and staging of liver fibrosis. Furthermore, the probability of a correct diagnosis is significantly enhanced with the addition of steatosis as a prognostic factor.

Key words: Shear wave elastography; Aminotransferase platelet ration; Liver fibrosis; Liver biopsy

Core tip: The gold standard in the diagnosis and staging of liver fibrosis is an invasive liver biopsy. The accuracy of non-invasive tools such as ultrasound shear wave elastography either alone or in combination with the use of the aspartate transaminase platelet ratio index score compared to histology to guide management of liver fibrosis is not known. We addressed this question in a multicenter trial in patients with chronic progressive liver disease in a low to middle income country.

Sande JA, Verjee S, Vinayak S, Amersi F, Ghesani M. Ultrasound shear wave elastography and liver fibrosis: A Prospective Multicenter Study. *World J Hepatol* 2017; 9(1): 38-47 Available from: URL: http://www.wjgnet.com/1948-5182/full/v9/i1/38.htm DOI: http://dx.doi.org/10.4254/wjh.v9.i1.38

INTRODUCTION

Liver fibrosis is a progressive condition that if diagnosed early and staged accurately, allows early clinical intervention that may arrest or slow down progression to end stage decompensated cirrhosis. The spectrum of chronic liver disease and fibrosis that leads to end stage decompensated cirrhosis, is an important cause of morbidity and mortality in the world[1]. Early diagnosis, accurate staging and re-evaluation of liver fibrosis is aimed at avoiding the progression from normal to minimal to significant fibrosis and timely management of patients with advanced disease.

There are several chronic progressive liver diseases that lead to liver fibrosis. Non-alcoholic fatty liver disease (NAFLD) is one of the most common. NAFLD is closely associated with obesity and insulin resistance. Pathological changes in the biochemical profile of the liver that lead to liver fibrosis also occur due to chronic metabolic conditions such as diabetes and degenerative conditions like atherosclerosis[2,3]. Other common causes of liver fibrosis include infections such as chronic viral hepatitis and human immunodeficiency virus. Drugs and other toxins also play an important role. This list is not exhaustive but this paper focuses on the last four causes. Liver fibrosis is characterized by excessive accumulation of extracellular matrix due to the release of inflammatory mediators and free radicals to cause oxidative stress and liver fibrogenesis. During this process hepatic stellate cells activation occurs. Platelet derived growth factor, tumor necrosis factor α, transforming growth factor β or reactive oxygen species play a role in the progression to liver fibrosis. Several phenotypic alterations occur with the end result being irreversible[4].

The current gold standard in the diagnosis and staging of liver fibrosis is liver biopsy. Liver biopsy and more recently ultrasound guided liver biopsy only evaluates 1/50000 of the liver parenchyma. It is invasive, has a complication rate (albeit small,) and is subject to intra and inter-observer variability[5]. Because of the imperfect nature of liver biopsies, over the last several years there has been a growing trend to validate non-invasive tools to diagnose and stage liver fibrosis. Alkaline aminotransferase platelet ratio index (APRI) is a laboratory marker that has been shown to have some value but is inferior to liver biopsy. Ultrasound and magnetic resonance have been used for elasticity imaging. Magnetic resonance elastography, even though promising, has some disadvantages. Aside from the significant cost of the study, it cannot be performed in a liver with iron overload because of signal-to-noise limitations; has longer examination times compared to ultrasound elastography, and is subject to respiratory artifact[6]. Ultrasound elastography has been validated and has been shown in many studies to have similar sensitivity and specificity to liver biopsies[5,7].

Ultrasound elastography measures the liver stiffness/elasticity by assessing at least 100 times the proportion of the liver that a biopsy does. Transient elastography (TE) has been validated in multiple studies[8] but shear wave elastography (SWE) may be preferred because unlike transient elastography, which consists of a vibrator producing shear waves, the latter can perform a conventional ultrasound at the same time. The technique is integrated into an ultrasound system. The principle behind the interpretation of shear wave elastography is that shear waves produced by a focused ultrasound beam are directly related to the stiffness of the liver from where they are generated[5,7,8]. SWE is also reportedly more accurate than TE in assessing significant fibrosis ($\geqslant$ F2)[8,9]. The use of shear wave elastography in the diagnosis and staging of liver fibrosis has been increasing. Being a non-invasive technique proves advantageous because repeat measurements can be obtained in patients with chronic progressive liver diseases. However, this non-invasive procedure does have some pitfalls. It is subject to intra- and inter-observer variability, validated cut-offs have mainly only been demonstrated in hepatitis C; Acute hepatitis can have false positives. In patients with a high body mass index, erroneous values may be obtained. A very practical pitfall is confounding factors such as edema, inflammation, cholestasis and congestion. All these

must be put in context and a multidisciplinary clinical approach used in the interpretation of the results[5,7,8,10].

A limitation of prior studies is the lack of integration of the accuracy and limitations of elastography. No prior study has combined elastography with the use of APRI and histology to guide management of liver fibrosis. This study addresses the gaps and makes practical inferences that focus on accurate early diagnosis and staging. The focus in our study is "interpretation within a clinical context". This multi-institutional study performed in Kenya aims to capture and highlight factors based on the disease burden in this region. Ultrasound elastography has only recently been made available in East Africa. The findings, therefore, could be of wider benefit because of the high burden of other etiologies of liver disease such as hepatitis B in the region. Most studies thus far have been carried out in the West with the disease burden focused on hepatitis C. In addition, the literature largely reports data from middle-high economic areas whereas adherence to clinical guidelines may not be as feasible in poor/resource challenged facilities.

MATERIALS AND METHODS

Objectives

The primary objective was to analyze the accuracy of shear wave elastography in comparison to liver biopsy in differentiating the various stages of liver fibrosis. The secondary objective was to evaluate whether the addition of the APRI score to SWE would improve the accuracy of this differentiation. With these, illustrate the role of the shear wave elastography, APRI score, and biopsy solely and or in combination in the diagnostic algorithm of accurate quantification of liver fibrosis. We also sought to assess the role of other covariates, namely, age, gender and steatosis, and their influence on the relative importance of SWE and the APRI score in predicting the extent of liver fibrosis.

Design

Three hospitals were included in this prospective study: Aga Khan University (AKU) Hospital, Kenyatta Teaching and Referral Hospital and St Mary's Mission Hospital. Approval was obtained from the relevant Scientific and Ethics committees. All consecutive patients referred for an ultrasound guided liver biopsy at all three institutions were subject to recruitment based on the inclusion and exclusion criteria as well as informed written consent. The study included patients above eighteen years of age with chronic progressive diffuse liver disease. Patients were excluded from the study if they did not have any of the three diagnostic tests, *i.e.*, liver biopsy, APRI score or SWE.

Consecutive patients were recruited by the principle investigator in three ways: (1) referral for an ultrasound guided liver biopsy at the AKU Radiology Department; (2) referral from St Mary's Hospital with biopsy performed by the AKU Radiology department and pathological analysis performed at AKU department; and (3) referral for a liver biopsy request to be analyzed at the Pathology department of Kenyatta National Hospital.

At recruitment, a study file was opened for each patient by the principle investigator at the AKU. Routine liver function tests, platelet counts, and demographic information related to confounding factors of chronic liver disease, including information on alcohol use, Human Immunodeficiency Virus status, viral load and CD4 levels, hepatitis B and C status was collected. Men who had been drinking more than 30 g of alcohol per day and women who had been drinking more than 20 g of alcohol per day were considered current drinkers. Patients who had stopped drinking completely for more than six months before the biopsy were considered ex-drinkers[11].

At the AKU routine ultrasound of the liver was performed to qualitatively record presence (grade 0-3) or absence of steatosis using established criteria published by Lupşor-Platon *et al*[12]. Any other diffuse or focal lesions were documented followed by SWE. At AKU elastography measurements were taken from the right lobe[13] of the liver with the patients holding their breath. Measurements were considered successful using validated criteria established by Castéra *et al*[14]: "(1) 10 valid shots; (2) a ratio of valid shots to the total number of shots of 60% or higher; and (3) variability of measurements less than 30% of the median value of liver stiffness measurements". Philips iU22 ultrasound machine with its C5-1 curvilinear transducer was used. The units for SWE readouts (liver stiffness) were kilopascals (kPa). Four sonologists each with more than 5 years' experience in routine liver scanning and validated ultrasound elastography experience from uniform training performed each exam independently. The median stiffness (used to grade the fibrosis), average stiffness and standard deviation of measurements generated by the software were recorded and interpreted by the four sonologists independently[7,10]. Each patient had one liver biopsy specimen taken from the right lobe[13] after the ultrasound elastography which was graded histologically for fibrosis based on the Metavir classification system[15,16]. This was done by two experienced histopathologists at the AKU and KNH Pathology departments. Each specimen was evaluated by the two histopathologists from each respective pathology department. Discrepancies were resolved by consensus between the two. The histopathologists from the two sites were full-time faculty, certified by the Kenya Medical Practitioners and Dentists Board, practicing in University Hospitals each with greater than ten years' experience in liver biopsy assessment for fibrosis. In each patient the time interval between ultrasound, elastography and histology was not more than one month. The pathologists and sonologists were blinded to clinical data and elastography or histology grade.

Interpretation of liver fibrosis by shear wave elastography in kPa divided the entity into no fibrosis (F0), mild fibrosis (F1), severe fibrosis (F2), significant fibrosis (F3)

Table 1 Summary illustrating sample size calculation above

AUROC	Total (*n*)	% Positive	# Positive	# Negative	SE	Confidence interval	
						Lower	Upper
0.8	110	30	33	77	0.050	0.701	0.899
0.8	130	30	39	91	0.046	0.709	0.891

AUROC: Area under the receiver operating characteristic.

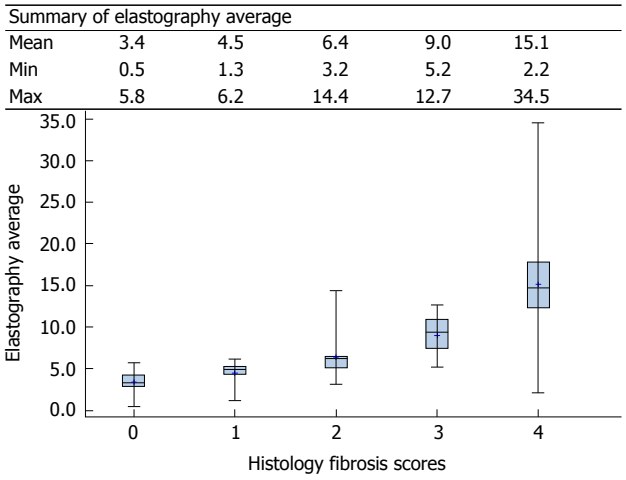

Figure 1 Elastography average *vs* histology fibrosis score (Box Plot).

and cirrhosis (F4). Automatic median value generated by the ultrasound software was used to establish the elastography grade as follows < 4.6 = F0, 4.6-5.6 = F1, 5.7-7.0 = F2, 7.1-12.0 = F3 and > 12 = F4[10,17-19]. APRI score was calculated using a formula proposed by original study of Wai *et al*[20]: APRI = [(AST level/ULN)/platelet counts (10^9/L)] × 100. A score of < 0.5 was graded as F0, 0.5-1.5 as F1-3 and > 1.5 as F4. The corresponding histology grade was assessed[21,22].

Sample size estimates

The sample size was determined with the aim to keep the standard error of the AUROC at 0.05. This set the difference between the upper and lower 95%CI limits to 0.20 (± 2 standard errors). From previous publications the range for the AUROC for significant fibrosis, as determined from non-invasive tests, is approximately 0.69 to 0.89; for cirrhosis the range is from 0.81 to 0.98. Assuming the AUROC to be approximately 0.8[20] the sample size of 110 patients would yield a standard error of 0.05 (Table 1).

Shear wave elastography has been shown to have a lower operator error technique than transient elastography (3%-16%)[23-25]. As a precautionary measure we raised the sample size from 110 to 130.

Statistical analysis

The statistical review of the study was performed by a biomedical statistician. Logistic regression models with backward elimination, using SAS version 9.3, were utilized to assess the significance of SWE median, the APRI score and the covariates age (categorized as below and above the median), gender and steatosis. Besides the *P*-values, the analysis provided the ORs and their respective 95%CI limits. The sensitivity and the specificity were computed based on the variables included in the model. This in turn enabled the ROCs and the AUROC to be determined. Summary statistics and correlation coefficients, where appropriate, were computed.

RESULTS

Demographics and baseline characteristics

One hundred and twenty-eight patients were recruited for the study. AKU, KNH and St. Mary's contributed 54 (42.2%), 53 (41.4%) and 21 (16.4%) patients, respectively. The most prevalent viral infection was hepatitis B that was noted in 30 (23.4%) patients. This was followed by human immunodeficiency virus (HIV) with 18 (14.1%) and hepatitis C with 13 (10.2%) patients (Appendix 1); fifteen patients had 2 or more infections. Sixty-three (49.2%) of the patients had a steatosis score of 0 and 61 (47.7%) of the patients had a histology fibrosis score of 0. Eighty-one (63.3%) patients fell in the histology fibrosis score subgroup F0-1; the remaining 47 (36.7%) fell in the F2-F4 subgroup. Fifty percent of the patients had an elastography score of F0 and 59 (46%) of the patients the APRI score of F0 (Appendix 2). The elastography median scores were the lowest among HIV subjects followed by those with hepatitis B and then a hepatitis C infection. The highest scores were from those with multiple viral infections. The APRI scores also follow the pattern described above for the elastography median scores (Appendix 3). There appears to be a good correlation between the elastography median scores and the histology fibrosis scores (Appendix 4). The elastography and APRI fibrosis score are statistically significantly correlated with the histology fibrosis scores (Appendix 5) (Figure 1 and Table 2).

Logistics regression results

Table 3 summarizes some of the key results that stemmed from the analysis of the SWE median and APRI score data using logistic regression. Both variables show a high degree of statistical significance in their individual ability to distinguish between the lower stages of fibrosis compared to the higher stages. This is true across all possible partitions of the Metavir fibrosis scores. However, the AUROCs for SWE medians are much higher than

Table 2 Summary of liver disease scores by histology fibrosis score (discrete variables) *n* (%)

	Histology fibrosis scores					Total	χ^2
	0 (*n* = 61)	1 (*n* = 20)	2 (*n* = 20)	3 (*n* = 10)	4 (*n* = 17)	(*n* = 128)	*P* value
Elastography fibrosis score							
F0	51 (83.6)	7 (35.0)	5 (25.0)	0 (0.0)	1 (5.9)	64 (50.0)	< 0.0001
F1	10 (16.4)	10 (50.0)	2 (10.0)	2 (20.0)	1 (5.9)	25 (19.5)	
F2	0 (0.0)	3 (15.0)	9 (45.0)	1 (10.0)	0 (0.0)	13 (10.2)	
F3	0 (0.0)	0 (0.0)	3 (15.0)	7 (70.0)	1 (5.9)	11 (8.6)	
F4	0 (0.0)	0 (0.0)	1 (5.0)	0 (0.0)	14 (82.4)	15 (11.7)	
APRI fibrosis score							
0	45 (73.8)	6 (30.0)	6 (30.0)	1 (10.0)	1 (5.9)	59 (46.1)	< 0.0001
1 to 3	14 (23.0)	13 (65.0)	9 (45.0)	9 (90.0)	8 (47.1)	53 (41.4)	
4	2 (3.3)	1 (5.0)	5 (25.0)	0 (0.0)	8 (47.1)	16 (12.5)	
Steatosis							
Grade 0	48 (78.7)	8 (40.0)	2 (10.0)	1 (10.0)	4 (23.5)	63 (49.2)	< 0.0001
Grade 1	6 (9.8)	8 (40.0)	5 (25.0)	1 (10.0)	1 (5.9)	21 (16.4)	
Grade 2	6 (9.8)	2 (10.0)	7 (35.0)	4 (40.0)	0 (0.0)	19 (14.8)	
Grade 3	1 (1.6)	2 (10.0)	6 (30.0)	4 (40.0)	12 (70.6)	25 (19.5)	

APRI: Aminotransferase platelet ratio index.

Table 3 Shear wave elastography median and aminotransferase platelet ratio index score to differentiate between metavir subgroups

		F0-3 *vs* F4	F0-2 *vs* F3-4	F0-1 *vs* F2-4	F0 *vs* F1-4
SWE median	*P* value	< 0.0001	< 0.0001	< 0.0001	< 0.0001
	OR	1.708	1.789	2.983	2.683
	95%CI	1.379, 2.115	1.432, 2.236	1.839, 4.838	1.789, 4.025
	AUROC	0.926	0.929	0.908	0.879
APRI score	*P* value	0.0202	0.039	0.0005	0.0008
	OR	1.511	1.404	3.482	4.651
	95%CI	1.067, 2.141	1.018, 1.938	1.727, 7.018	1.895, 11.416
	AUROC	0.812	0.784	0.780	0.803
SWE and APRI[1]	AUROC	0.927	0.931	0.920	0.890
	APRI influence	0.001	0.002	0.012	0.011

[1]SWE median and APRI score. OR: Odds ratio; SWE: Shear wave elastography; APRI: Aminotransferase platelet ratio index; AUROC: Area under the receiver operating characteristic.

those for APRI score.

The SWE median differentiates the Metavir fibrosis subgroups F0-1 and F2-4 with an AUROC of 0.908 compared to 0.780 for the APRI score. These results imply that the SWE on its own is a better predictor of the differentiating the subgroups than the APRI score. When we utilize both variables simultaneously, the increase in the AUROC attributed to the APRI score is less than 1.2% higher than that predicted by SWE median. This amounts to about 13% of the 9% not predicted correctly by the SWE median. The results for other partitions of the histology fibrosis scores mimic those described above with the AUROC for SWE median being around 0.9 and that of the APRI score being about 0.8.

Additional logistic regression models incorporated several other variables in the analysis to evaluate their impact on the AUROC. The variables considered, in addition to the SWE median and the APRI score were the covariates age (categorized as below and above the median), gender and steatosis score. The results of the logistic regression analysis (Table 4) with all of the aforementioned variables in the model showed that SWE and the steatosis score were the only two variables that made significant contributions to the predictive power of the model.

Using the backward elimination method, all of the variables that were not making a significant contribution at the 0.1 level were dropped from the model. The results of these analysis (Table 5) show that for the primary objective of differentiating between F0-1 and F2-4 is accomplished quite well with an AUROC of 0.944; the two variables that made a significant contribution were SWE and steatosis. The steatosis score adds significantly to the prediction model that tries to identify the fibrosis group that a patient belongs to (Table 5); this is true in every case except for the F0-3 *vs* F4 partition. The APRI score on the other hand makes a significant contribution to only the partition F0-2 *vs* F3-4. Given that the APRI score appears in only one partition as an important predictor, an additional analysis was performed by dropping the APRI score from the model. This resulted in adding a few additional observations to the data set used for analysis since missing APRI scores had contributed to a slightly reduced sample size. In addition, the steatosis score was added to the F0-3 *vs* F4 model in order to have a unique set of predictors across

Table 4 Prediction of histology fibrosis score (Grouping: F0-1 *vs* F2-4) using elastography median, aminotransferase platelet ratio index score, age category[1], sex and steatosis maximum likelihood and odds ratio estimates

Variable		DF	Coefficient estimate	Standard error	Wald χ^2	Pr > χ^2	OR estimate	Lower 95%CI limit for OR	Upper 95%CI limit for OR
Intercept		1	-6.6482	1.3510	24.2158	< 0.0001			
Age category	LE median	1	0.0971	0.3219	0.0910	0.7629	1.214	0.344	4.288
APRI score		1	0.1946	0.3873	0.2526	0.6153	1.215	0.569	2.595
Elastography median		1	0.9041	0.2513	12.9464	0.0003	2.470	1.509	4.042
Sex	Female	1	0.3330	0.3551	0.8797	0.3483	1.947	0.484	7.830
Steatosis		1	1.1317	0.3462	10.6843	0.0011	3.101	1.573	6.112

[1]Age category (years): *n* = 128. Mean (SD) 46 (16.99). Median 42; Minimum 18; Maximum 108. OR: Odds ratio; APRI: Aminotransferase platelet ratio index.

Table 5 Significance of predictive values associated with key pre-identified variables

	F0-3 *vs* F4	F0-2 *vs* F3-4	F0-1 *vs* F2-4	F0 *vs* F1-4
SWE median	< 0.0001	< 0.0001	0.0003	0.0002
APRI score	NS[1]	0.0404	NS	NS
Age	NS	NS	NS	NS
Gender	NS	NS	NS	NS
Steatosis	NS	0.0263	0.0002	0.0007
AUROC	0.926	0.962	0.944	0.902

[1]NS: Not significant at the 0.1 level. SWE: Shear wave elastography; APRI: Aminotransferase platelet ratio index; AUROC: Area under the receiver operating characteristic.

all partitions. These results are presented in Table 6. The fact that the results from Tables 5 and 6 are very similar implies that the missing data points did not influence the outcome in any meaningful way.

The F0-2 *vs* F3-4 data shows that the AUROC obtained with the use of the SWE median and the steatosis score is 0.954 (Table 6). By adding the APRI score (Table 5) the AUROC increase of 0.008 or 0.8%. This represents a decrease of about 13% (0.008 of 0.046) in the error rate. On the other hand, adding steatosis to the model after including the SWE median and the APRI score, the AUROC increase from 0.931 (Table 3) to 0.962 (Table 5), an increase of 0.031 or 3.1%. This represents a decrease of about 44.9% (0.031 of 0.069) in the error rate.

DISCUSSION

Summary of findings

The infection with the highest prevalence was hepatitis B. There were also patients with HIV, hepatitis C and the co-infections in this cohort. While the prevalence of hepatitis B, C and HIV in Sub-Saharan Africa has not been conclusively established[26], it has been postulated that hepatitis B is relatively more prevalent than hepatitis C as compared to the western world where hepatitis C is more prevalent[27]. Most studies on liver fibrosis quantification have been carried out in the western world therefore it is important to have the same studies carried out in Sub-Saharan Africa where the epidemiology of the viral infections is likely to be different. The elastography median scores were the lowest among HIV subjects

Table 6 Elastography median and steatosis

Variable	Pr > χ^2	OR estimate	Lower 95%CI limit for OR	Upper 95%CI limit for OR
F0-3 *vs* F4				
Intercept	< 0.0001			
Elastography median	< 0.0001	1.681	1.347	2.099
Steatosis	0.6529	1.187	0.563	2.502
AUROC = 0.936				
F0-2 *vs* F3-4				
Intercept	< 0.0001			
Elastography median	< 0.0001	1.684	1.353	2.097
Steatosis	0.0568	1.846	0.982	3.467
AUROC = 0.954				
F0-1 *vs* F2-4				
Intercept	< 0.0001			
Elastography median	0.0003	2.397	1.500	3.828
Steatosis	0.0002	3.135	1.703	5.772
AUROC = 0.944				
F0 *vs* F1-4				
Intercept	< 0.0001			
Elastography median	0.0002	2.221	1.463	3.370
Steatosis	0.0007	2.496	1.473	4.230
AUROC = 0.902				

OR: Odds ratio; AUROC: Area under the receiver operating characteristic.

followed by those with hepatitis B infection; the next highest score was for patients with a hepatitis C infection. The lowest score was from those with multiple infections. The APRI scores also follow the pattern described above for the elastography scores. This pattern corresponds with what has previously been described. Hepatitis C most likely has higher levels of quantified liver fibrosis because of the three viruses it has the most indolent and chronic clinical course. The mortality from these infections is correlated to chronic liver disease and not due to progression of the virus due to the success of antiretroviral therapy[27,28].

Analysis categorized fibrosis as, F0 *vs* F1-4, F0-1 *vs* F2-4, F0-2 *vs* F3-4, F0-3 *vs* F4. The results focus on F0-1 *vs* F2-4 which is of most clinical significance (no and non-significant fibrosis *vs* significant fibrosis that demands intervention). There is a good correlation between the elastography median scores and the histology fibrosis scores. The OR of 3.0 implies that the elastography median scores are 3 times more likely to correctly identify a fibrosis score of F2-4 compared to F0-1. The upper and lower limits for the OR with 95%CI do not cross 1 which

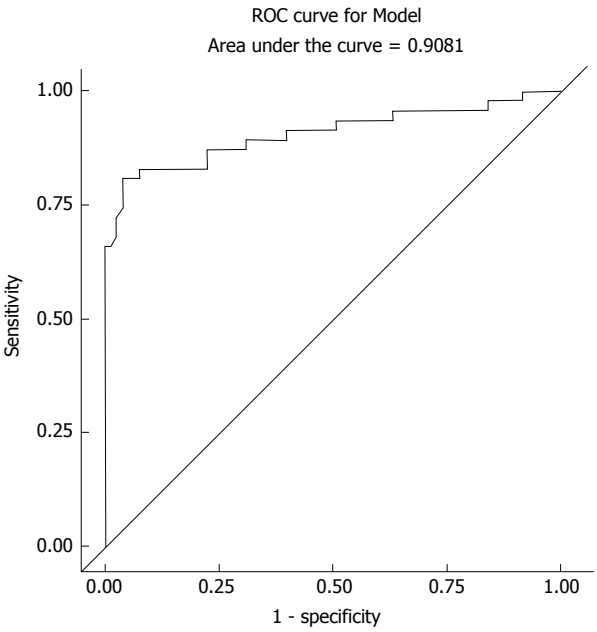

Figure 2 Prediction of histology fibrosis score (Grouping: F0-F1 *vs* F2-F4) using elastography median. ROC: Receiver operating characteristic.

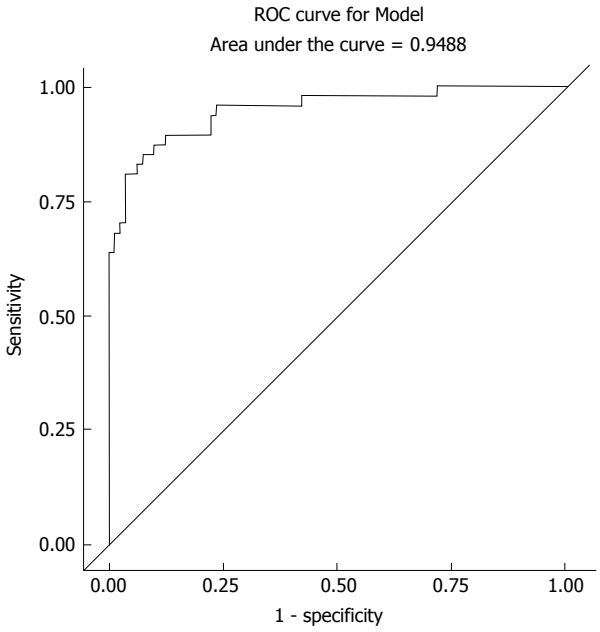

Figure 3 Prediction of histology fibrosis score (Grouping: F0-1 *vs* F2-4) using elastography median, aminotransferase platelet ratio index score, age categor, sex and steatosis.

strengthens this result. However, the limits are wide 1.8-5. This may be due to the small sample size and because close to 50% of the sample at F0. If F0 were to be eliminated from the analysis this may reduce the limits with a questionable effect on clinical significance. The accuracy of the elastography median depends on the sensitivity and specificity. This is clear from the raw data used to generate the ROC curve. An elastography median of approximately 3.8 is the point at which you get the best sensitivity matched with specificity. The ROC curve for model, which depicts sensitivity and specificity, illustrates how for a very high sensitivity, specificity is low and as sensitivity reduces; one arrives at a point where specificity is acceptable clinically. That is, one can identify disease with a high sensitivity and be correct (specifically know that you are also picking the non-diseased). The AUROC for the elastography median was 0.91. The elastography and APRI fibrosis score are statistically significantly correlated with the histology fibrosis scores. However, APRI score in itself or when combined with elastography median score does not significantly increase the accuracy of elastography in the differentiation of non-significant *vs* significant fibrosis. APRI had an AUROC of 0.78. APRI and elastography median had an AUROC of 0.92. Therefore APRI does not have a statistically significant effect on the prediction of F0-1 from F2-4 when added to elastography. And when used alone it is significantly less accurate than elastography. However in patients with chronic progressive liver fibrosis who need repeated analysis to categorize and monitor the progress of liver fibrosis APRI does have a clinically significant role in the management algorithm of liver fibrosis.

Previous studies vary on the accuracy of elastography. The sensitivity, specificity and diagnostic accuracy of shear wave elastography in the determination of liver stiffness compared with biopsy results is comparable to[8-10]. The accuracy of elastography mirrors those depicted by these studies albeit a slightly higher accuracy in this study. This may be due to the difference in grouping of the fibrosis scores for analysis. Also, if the F0 of this study are removed from the analyses this may lead to more similar figures since the F0 constitute approximately 50%. The diagnostic accuracy of shear wave elastography and APRI score in the determination of liver stiffness has not been reported before[8-10].

Ordinal regression and backward elimination was used to analyze significance of HIV, hepatitis B, alcohol use, steatosis, age and gender. It showed that steatosis has a significant OR and *P*-value in the analysis for fibrosis. Ferraioli *et al*[10] showed that steatosis does not affect the performance of elastography. The challenge as stated in this paper is the confounding effect of various pathologies in the diagnosis and staging of liver fibrosis. This is particularly relevant in the generation and given the wide use of reference ranges for all modalities used in the diagnosis and staging of liver fibrosis. It is for this reason that to date several studies have used variable reference ranges for F0-F4[8,10,17-19]. Our results highlight the potential effect of the presence of steatosis (EF-S_1_10_3_Logistic_All Variables_F0-F1VsF2-F4 document) on the diagnosis and characterization of liver fibrosis. Of note from this result is the increase in the AUROC from 0.91 (Figure 2) to 0.95 (Figure 3) in the logistic regression backward elimination analysis that is attributable to the elastography median and steatosis each with a significant *P*-value and OR (Table 4). This is an area that needs further study, especially since steatosis was measured subjectively in this study. The data on HIV and alcohol use as variables were not adequately

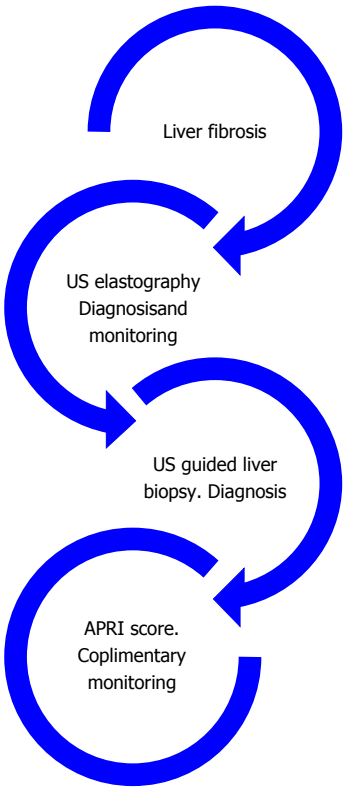

Figure 4 Link between diagnostic tests used in the evaluation of liver fibrosis. US: Ultrasound; APRI: Aminotransferase platelet ratio index.

powered to add to this analysis.

Strengths

This study is timely because of the growing use of elastography in the developed world. In the developing world the use of this diagnostic tool needs to grow *via* an evidence based approach that is tailored to the local disease burden. Most research in the west has focused on hepatitis C and alcohol or nonalcoholic steatosis. The wider disease burden covered in this study is thus a more homogenous representation of chronic liver fibrosis pathology. The complimentary use of APRI score is especially relevant in resource limited setups.

Theoretical and practical implications of these findings

This study brought to light theoretical implication of the need to standardize the diagnosis and accurate staging and follow-up of liver fibrosis. Figure 4 depicts the link between all tests used in the evaluation of liver fibrosis (Figure 4).

The use of all tests should be complimentary and histology has its place but the noninvasive tests may be more logical in the beginning and for progressive monitoring. Inference from the results generates a flowchart below describing a management algorithm (Figure 5).

Inference from the results: Consider the following flowchart at diagnosis

Practical unique and reported challenges exist. Care needs to be taken in interpretation and training for elastography. Technical and interpretation skill for elastography specifically when choosing the ten values to include in the report; this includes excluding/ignoring far outliers, though these outliers may represent focal areas of different fibrotic stages! Use of the median to give a final conclusion of the ten chosen readings is appropriate especially in the setting of variable readings. But, care must be exercised. There should be a low threshold to recommend a biopsy (still the gold standard) to confirm the findings especially if the mean elastography reading is in keeping with a diagnosis of no fibrosis yet the standard deviation is high in the presence of individual readings of cirrhosis[5]. The challenge of the heterogeneously fibrotic liver or presence of lesions, *e.g.,* metastasis causing heterogeneity of the liver rendering fibrosis assessment questionable in terms of using just the median to conclude on the level of fibrosis especially when there is a big difference in the individual stiffness values must be remembered. These issues red flag the danger of not allowing room to vary an impression and advise further evaluation with an United States guided liver biopsy to correlate[5]. Indeed, one must also bear in mind that the suggestion to further evaluate with a liver biopsy is inherently flawed because of the attend pitfalls of the tool. Chronic progressive liver fibrosis needs accurate early diagnosis and interval monitoring. Elastography is a validated tool. APRI can be used as a complimentary tool though its effect is not of statistical significance but clinical significance. Biopsy remains the gold standard. We propose a flow chart at diagnosis. Further, the probability of a correct diagnosis is significantly enhanced with the addition of steatosis as a prognostic factor (Figure 5).

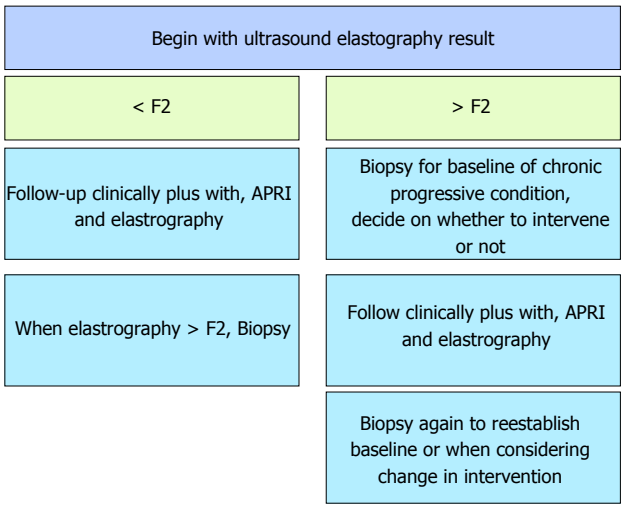

Figure 5 Flow chart depicting use of diagnostic tests in liver fibrosis. Begin with US SWE result. US: Ultrasound; SWE: Shear wave elastography; APRI: Aminotransferase platelet ratio index.

Limitations and problems encountered in the method

The number of ultrasound guided liver biopsies for the assessment of liver fibrosis has continued to reduce because of the increasing use of elastography which is noninvasive and without the side effects associated with

liver biopsy. This diagnostic trend is reinforced by the continued validation of elastography[5,7,10,12]. Therefore during this study the recruitment rate was low. As such participants were recruited from three different sites to meet the sample size requirement to adequately power the results. The ultrasound and elastography where all performed at the same site (AKU). Biopsy results were analyzed by pathologists at two of the three sites (AKU and KNH). This may have potentially led to variable histological inter-observer variability. To counter this each sample was read by each pathologist at each respective site and discrepant values were resolved by consensus. However, major and minor discrepancy analyses of histology for inter-observer discrepancies were not assessed.

There are limitations associated with elastography, including the confounding effects of inflammatory activity, and to a lesser extent, steatosis[13], on liver stiffness evaluation. There is also reduced accuracy observed in lower fibrosis stages (F0-F2). Furthermore, the incidences of failed and unreliable scans have been reported to be approximately 3% to 16% in transient elastography but less in shear wave elastography (figures not reported yet)[22]. The sample size was inflated by 5% to cater for this. A typical liver biopsy covers 1/10000th of the liver while elastography covers a larger area. Matching the two sites covered by the two exams may not have been 100%.

The information sort in the data collection form to analyze the secondary objectives was sensitive in nature including queries about alcohol use and HIV status. This precluded complete disclosure from participants and led to inadequate data on related parameters. This led to a reduction in the power of inferences regarding the role of alcohol and HIV.

Suggestions for improvement and further work

This has been an East African experience: Unique challenges and similar differences to those published. More comprehensive analysis needs to be done to further reveal the extent of confounding factors affecting the use of elastography in the diagnosis and staging of liver fibrosis. The role of steatosis needs further objective assessment. Further work needs to be done to describe the in cooperation of magnetic resonance elastography in the diagnostic algorithm of liver fibrosis.

Our study validates the use of ultrasound shear wave elastography in the diagnosis and staging of fibrosis within the context of liver disease in a LMIC.

ACKNOWLEDGMENTS

We would like to thank the Aga Khan United States Research funding body and research support team for funding this study and their non-wavering technical support. Many thanks to the Aga Khan Research team for support and to all patients and staff that were involved in this endeavor.

COMMENTS

Background

Chronic progressive liver diseases cause liver fibrosis whose end result is decompensated liver failure. Liver fibrosis that results from these diseases can be reversed if diagnosed early. The current gold standard in the diagnosis of liver fibrosis is a liver biopsy preferably ultrasound guided, which is an invasive procedure with limitations and risks. Recent research have validated the use of shear wave ultrasound based liver elastography which is a non-invasive imaging based tool that has a sensitivity and specificity that almost parallels histological diagnosis from a liver biopsy. The staging of liver fibrosis at diagnosis uses a Metavir scoring system that has been adapted by elastography. Aminotransferase to platelet ratio index is a liver function test that has some usefulness in the diagnosis of liver fibrosis. The combined use of histology, elastography and aminotransferase to platelet ratio index has not been elucidated.

Research frontiers

Previous studies have shown that ultrasound based elastography can substitute liver biopsy in the accurate diagnosis of liver fibrosis.

Innovations and breakthroughs

This is the first study to evaluate the combined role of ultrasound based elastography, histology and aminotransferase to platelet ratio index in a low to middle income country for the management of progressive liver fibrosis.

Applications

The use of the three tests should be complimentary and histology has its place but the noninvasive tests may be more logical in the beginning and for progressive monitoring. More comprehensive analysis needs to be done to further reveal the extent of confounding factors affecting the use of elastography in the diagnosis and staging of liver fibrosis. Further work needs to be done to describe the in cooperation of magnetic resonance elastography in the diagnostic algorithm of liver fibrosis.

Terminology

Elastography is radiological based software that can diagnose and quantify the degree of liver fibrosis. It is either ultrasound or magnetic resonance based. Ultrasound bases elastography uses sound have to assess for and quantify liver stiffness that is directly related to liver fibrosis. Aminotransferase to platelet ratio is a laboratory parameter derived from part of the routine liver function tests and platelet count.

Peer-review

The authors have validated the use of ultrasound shear wave elastography in the diagnosis and staging of fibrosis within the context of liver disease in a low to middle income country. Practical management algorithms that in cooperate the use of ultrasound based elastography, histology and aminotransferase to platelet ratio index have been demonstrated. More comprehensive analysis needs to be done to further reveal the extent of confounding factors affecting the use of ultrasound or magnetic resonance based elastography.

REFERENCES

1 **Bataller R**, Brenner DA. Liver fibrosis. *J Clin Invest* 2005; **115**: 209-218 [PMID: 15690074 DOI: 10.1172/JCI24282]

2 **Fan Y**, Fang X, Tajima A, Geng X, Ranganathan S, Dong H, Trucco M, Sperling MA. Evolution of hepatic steatosis to fibrosis and adenoma formation in liver-specific growth hormone receptor knockout mice. *Front Endocrinol* (Lausanne) 2014; **5**: 218 [PMID: 25566190 DOI: 10.3389/fendo.2014.00218]

3 **Kochan K**, Marzec KM, Chruszcz-Lipska K, Jasztal A, Maslak E, Musiolik H, Chłopicki S, Baranska M. Pathological changes in the biochemical profile of the liver in atherosclerosis and diabetes assessed by Raman spectroscopy. *Analyst* 2013; **138**: 3885-3890 [PMID: 23515303 DOI: 10.1039/C3AN00216K]

4 **Dong D**, Yin L, Qi Y, Xu L, Peng J. Protective Effect of the Total Saponins from Rosa laevigata Michx Fruit against Carbon

Tetrachloride-Induced Liver Fibrosis in Rats. *Nutrients* 2015; **7**: 4829-4850 [PMID: 26083117 DOI: 10.3390/nu7064829]

5 **Ferraioli G**, Tinelli C, Dal Bello B, Zicchetti M, Lissandrin R, Filice G, Filice C, Above E, Barbarini G, Brunetti E, Calderon W, Di Gregorio M, Gulminetti R, Lanzarini P, Ludovisi S, Maiocchi L, Malfitano A, Michelone G, Minoli L, Mondelli M, Novati S, Patruno SF, Perretti A, Poma G, Sacchi P, Zanaboni D, Zaramella M. Performance of liver stiffness measurements by transient elastography in chronic hepatitis. *World J Gastroenterol* 2013; **19**: 49-56 [PMID: 23326162 DOI: 10.3748/wjg.v19.i1.49]

6 **Lee JE**, Lee JM, Lee KB, Yoon JH, Shin CI, Han JK, Choi BI. Noninvasive assessment of hepatic fibrosis in patients with chronic hepatitis B viral infection using magnetic resonance elastography. *Korean J Radiol* 2014; **15**: 210-217 [PMID: 24643284 DOI: 10.3348/kjr.2014.15.2.210]

7 **Ferraioli G**, Parekh P, Levitov AB, Filice C. Shear wave elastography for evaluation of liver fibrosis. *J Ultrasound Med* 2014; **33**: 197-203 [PMID: 24449721 DOI: 10.7863/ultra.33.2.197]

8 **Frulio N**, Trillaud H. Ultrasound elastography in liver. *Diagn Interv Imaging* 2013; **94**: 515-534 [PMID: 23623211 DOI: 10.1016/j.diii.2013.02.005]

9 **Ferraioli G**, Tinelli C, Dal Bello B, Zicchetti M, Filice G, Filice C. Accuracy of real-time shear wave elastography for assessing liver fibrosis in chronic hepatitis C: a pilot study. *Hepatology* 2012; **56**: 2125-2133 [PMID: 22767302 DOI: 10.1002/hep.25936]

10 **Ferraioli G**, Tinelli C, Lissandrin R, Zicchetti M, Dal Bello B, Filice G, Filice C. Point shear wave elastography method for assessing liver stiffness. *World J Gastroenterol* 2014; **20**: 4787-4796 [PMID: 24782633 DOI: 10.3748/wjg.v20.i16.4787]

11 **Matteoni CA**, Younossi ZM, Gramlich T, Boparai N, Liu YC, McCullough AJ. Nonalcoholic fatty liver disease: a spectrum of clinical and pathological severity. *Gastroenterology* 1999; **116**: 1413-1419 [PMID: 10348825 DOI: 10.1016/S0016-5085(99)70506-8]

12 **Lupşor-Platon M**, Stefănescu H, Mureşan D, Florea M, Szász ME, Maniu A, Badea R. Noninvasive assessment of liver steatosis using ultrasound methods. *Med Ultrason* 2014; **16**: 236-245 [PMID: 25110765]

13 **Beland MD**, Brown SF, Machan JT, Taliano RJ, Promrat K, Cronan JJ. A pilot study estimating liver fibrosis with ultrasound shear-wave elastography: does the cause of liver disease or location of measurement affect performance? *AJR Am J Roentgenol* 2014; **203**: W267-W273 [PMID: 25148183 DOI: 10.2214/AJR.13.11718]

14 **Castéra L**, Vergniol J, Foucher J, Le Bail B, Chanteloup E, Haaser M, Darriet M, Couzigou P, De Lédinghen V. Prospective comparison of transient elastography, Fibrotest, APRI, and liver biopsy for the assessment of fibrosis in chronic hepatitis C. *Gastroenterology* 2005; **128**: 343-350 [PMID: 15685546 DOI: 10.1053/j.gastro.2004.11.018]

15 **Fung J,** Lai CL, Seto WK, Yuen MF. The use of transient elastography in the management of chronic hepatitis B. *Hepatol Int* 2011; **5**: 868-875 [PMID: 21695588 DOI: 10.1007/s12072-011-9288-5]

16 **Kim BK**, Kim HS, Park JY, Kim do Y, Ahn SH, Chon CY, Park YN, Han KH, Kim SU. Prospective validation of ELF test in comparison with Fibroscan and FibroTest to predict liver fibrosis in Asian subjects with chronic hepatitis B. *PLoS One* 2012; **7**: e41964 [PMID: 22848675 DOI: 10.1371/journal.pone.0035825]

17 **Suh CH,** Kim SY, Kim KW, Lim YS, Lee SJ, Lee MG, Lee J, Lee SG, Yu E. Determination of Normal Hepatic Elasticity by Using Real-time Shear-wave Elastography. *Radiology* 2014; **271**: 895-900 [PMID: 24555633 DOI: 10.1148/radiol.14131251]

18 **Suh C**, Kim SY, Kim KW. Estimation of reference values for liver elasticity in biopsy-proven normal liver using Supersonic Shear Wave imaging: measurement reliability and effect of steatosis. *Euro Soc Radiol* 2013 [DOI: 10.1594/ecr2013/B-0091.1-16]

19 **Sporea I**, Bota S, Gradinaru-Taşcău O, Sirli R, Popescu A, Jurchiş A. Which are the cut-off values of 2D-Shear Wave Elastography (2D-SWE) liver stiffness measurements predicting different stages of liver fibrosis, considering Transient Elastography (TE) as the reference method? *Eur J Radiol* 2014; **83**: e118-e122 [PMID: 24380640 DOI: 10.1016/j.ejrad.2013.12.011]

20 **Wai CT**, Greenson JK, Fontana RJ, Kalbfleisch JD, Marrero JA, Conjeevaram HS, Lok AS. A simple noninvasive index can predict both significant fibrosis and cirrhosis in patients with chronic hepatitis C. *Hepatology* 2003; **38**: 518-526 [PMID: 12883497 DOI: 10.1053/jhep.2003.50346]

21 **Castera L,** Forns X, Alberti A. Non-invasive evaluation of liver fibrosis using transient elastography. *J Hepatol* 2008; **48**: 835-847 [PMID: 18334275 DOI: 10.1016/j.jhep.2008.02.008]

22 **Jang HW**, Kim SU, Park JY, Ahn SH, Han KH, Chon CY, Park YN, Choi EH, Kim do Y. How many valid measurements are necessary to assess liver fibrosis using FibroScan® in patients with chronic viral hepatitis? An analysis of subjects with at least 10 valid measurements. *Yonsei Med J* 2012; **53**: 337-345 [PMID: 22318821 DOI: 10.3349/ymj.2012.53.2.337]

23 **Baranova A**, Lal P, Birerdinc A, Younossi ZM. Non-invasive markers for hepatic fibrosis. *BMC Gastroenterol* 2011; **11**: 91 [PMID: 21849046 DOI: 10.1186/1471-230X-11-91]

24 **Poynard T**, Munteanu M, Luckina E, Perazzo H, Ngo Y, Royer L, Fedchuk L, Sattonnet F, Pais R, Lebray P, Rudler M, Thabut D, Ratziu V. Liver fibrosis evaluation using real-time shear wave elastography: applicability and diagnostic performance using methods without a gold standard. *J Hepatol* 2013; **58**: 928-935 [PMID: 23321316 DOI: 10.1016/j.jhep.2012.12.021]

25 **Osaki A**, Kubota T, Suda T, Igarashi M, Nagasaki K, Tsuchiya A, Yano M, Tamura Y, Takamura M, Kawai H, Yamagiwa S, Kikuchi T, Nomoto M, Aoyagi Y. Shear wave velocity is a useful marker for managing nonalcoholic steatohepatitis. *World J Gastroenterol* 2010; **16**: 2918-2925 [PMID: 20556839 DOI: 10.3748/wjg.v16.i23.2918]

26 **Apata IW,** Averhoff F, Pitman J, Bjork A, Yu J, Amin NA, Dhingra N, Kolwaite A, Marfin A. Progress toward prevention of transfusion-transmitted hepatitis B and hepatitis C infection--sub-Saharan Africa, 2000-2011. *MMWR Morb Mortal Wkly Rep* 2014; **63**: 613-619 [PMID: 25055184]

27 **Clausen LN**, Lundbo LF, Benfield T. Hepatitis C virus infection in the human immunodeficiency virus infected patient. *World J Gastroenterol* 2014; **20**: 12132-12143 [PMID: 25232248 DOI: 10.3748/wjg.v20.i34.12132]

28 **Rosenthal E**, Roussillon C, Salmon-Céron D, Georget A, Hénard S, Huleux T, Gueit I, Mortier E, Costagliola D, Morlat P, Chêne G, Cacoub P. Liver-related deaths in HIV-infected patients between 1995 and 2010 in France: the Mortavic 2010 study in collaboration with the Agence Nationale de Recherche sur le SIDA (ANRS) EN 20 Mortalité 2010 survey. *HIV Med* 2015; **16**: 230-239 [PMID: 25522874 DOI: 10.1111/hiv.12204]

P- Reviewer: Jiang ZG, Peng JY, Yuan YF **S- Editor**: Qi Y
L- Editor: A **E- Editor**: Li D

World Journal of Hepatology

Submit a Manuscript: http://www.wjgnet.com/esps/
Help Desk: http://www.wjgnet.com/esps/helpdesk.aspx
DOI: 10.4254/wjh.v9.i1.48

World J Hepatol 2017 January 8; 9(1): 48-56
ISSN 1948-5182 (online)

ORIGINAL ARTICLE

Retrospective Study

Efficacy and safety of tenofovir in chronic hepatitis B: Australian real world experience

Grace C Lovett, Tin Nguyen, David M Iser, Jacinta A Holmes, Robert Chen, Barbara Demediuk, Gideon Shaw, Sally J Bell, Paul V Desmond, Alexander J Thompson

Grace C Lovett, Tin Nguyen, David M Iser, Jacinta A Holmes, Robert Chen, Barbara Demediuk, Gideon Shaw, Sally J Bell, Paul V Desmond, Alexander J Thompson, Department of Gastroenterology, St Vincent's Hospital Melbourne, Fitzroy 3065, Australia

Grace C Lovett, Tin Nguyen, David M Iser, Jacinta A Holmes, Robert Chen, Barbara Demediuk, Gideon Shaw, Sally J Bell, Paul V Desmond, Alexander J Thompson, Faculty of Medicine, University of Melbourne, Parkville 3010, Australia

Author contributions: Lovett GC data collection, data analysis and manuscript composition; Nguyen T, Iser DM, Chen R, Demediuk B, Shaw G and Bell SJ data collection; Holmes JA data collection and manuscript reviewing; Desmond PV planned study, supervised data collection and analysis and revised manuscript; Thompson AJ planned study, supervised data collection and analysis and revised manuscript.

Institutional review board statement: This study was reviewed and approved by the St Vincent's Hospital Melbourne Review Board.

Informed consent statement: Informed consent was not required for this study as only a retrospective audit was undertaken. The confidentiality of participant records has been maintained at all times, with patient information remaining deidentified.

Conflict-of-interest statement: Thompson AJ is an advisor/consultant to Gilead Sciences; has received research funding and acted as a speaker for Gilead Sciences; NHMRC fellowship Translational studies into viral hepatitis.

Data sharing statement: No data were created so no data are available.

Manuscript source: Unsolicited manuscript

Correspondence to: Alexander J Thompson, MBBS, FRACP, PhD, Department of Gastroenterology, St Vincent's Hospital Melbourne, Level 4 Daly Wing, 35 Victoria Parade, Fitzroy 3065, Victoria, Australia. alexander.thompson@svha.org.au
Telephone: +61-3-92883581

Received: May 8, 2016
Peer-review started: May 10, 2016
First decision: June 18, 2016
Revised: July 29, 2016
Accepted: September 21, 2016
Article in press: September 22, 2016
Published online: January 8, 2017

Abstract

AIM

To evaluate the long-term treatment outcomes of tenofovir therapy in patients in a real world Australian tertiary care setting.

METHODS

We performed a retrospective analysis of treatment outcomes among treatment-naïve and treatment-experienced patients receiving a minimum 3 mo tenofovir therapy through St Vincent's Hospital Melbourne, Australia. We included patients receiving tenofovir [tenofovir disoproxil fumarate (TDF)] monotherapy, as well as patients treated with TDF in combination with a second antiviral agent. Patients were excluded if they demonstrated human immune-deficiency virus/hepatitis C virus/hepatitis delta virus coinfection or were less than 18 years of age. We considered virological and biochemical

response, as well as safety outcomes. Virological response was determined by measurement of hepatitis B virus (HBV) DNA using sensitive assays; biochemical response was determined *via* serum liver function tests; histological response was determined from liver biopsy and fibroscan; safety analysis focused on glomerular renal function and bone mineral density. The primary efficacy endpoint was complete virological suppression over time, defined by HBV DNA < 20 IU/mL. Secondary efficacy endpoints included rates of biochemical response, and HB e antigen (HBeAg)/HB surface antigen loss and seroconversion over time.

RESULTS

Ninety-two patients were identified who fulfilled the enrolment criteria. Median follow-up was 26 mo (range 3-114). Mean age was 46 (24-78) years, 64 (70%) were male and 77 (84%) were of Asian origin. 55 (60%) patients were treatment-naïve and 62 patients (67%) were HBeAg-negative. Complete virological suppression was achieved by 45/65 (71%) patients at 12 mo, 37/46 (80%) at 24 mo and 25/28 (89%) at 36 mo. Partial virological response (HBV DNA 20-2000 IU/mL) was achieved by 89/92 (96.7%) of patients. Multivariate analysis showed a significant relationship between virological suppression at end of follow-up and baseline HBV DNA level (OR = 0.897, 95%CI: 0.833-0.967, P = 0.0046) and HBeAg positive status (OR = 0.373, 95%CI: 0.183-0.762, P = 0.0069). There was no difference in response comparing treatment-naïve and treatment-experienced patients. Three episodes of virological breakthrough occurred in the setting of non-compliance. Tenofovir therapy was well tolerated.

CONCLUSION

Tenofovir is an efficacious, safe and well-tolerated treatment in an Australian real-world tertiary care setting. Our data are similar to the reported experience from registration trials.

Key words: Tenofovir; Hepatitis B virus; Australia; Real-life; Virological suppression; Chronic hepatitis B

Core tip: Clinical trials have demonstrated that tenofovir is a safe and efficacious treatment for patients with chronic hepatitis B, with high rates of sustained virological suppression. There are limited data evaluating the safety and efficacy of tenofovir in real-world settings. The aim of this study was to evaluate the long-term treatment outcomes of tenofovir therapy in patients in an Australian tertiary care setting. We performed a retrospective analysis of treatment outcomes among treatment-naïve and treatment-experienced patients.

Lovett GC, Nguyen T, Iser DM, Holmes JA, Chen R, Demediuk B, Shaw G, Bell SJ, Desmond PV, Thompson AJ. Efficacy and safety of tenofovir in chronic hepatitis B: Australian real world experience. *World J Hepatol* 2017; 9(1): 48-56 Available from: URL: http://www.wjgnet.com/1948-5182/full/v9/i1/48.htm DOI: http://dx.doi.org/10.4254/wjh.v9.i1.48

INTRODUCTION

Chronic hepatitis B (CHB) affects 240-400 million people around the world[1]. It is estimated that 218000 people in Australia live with CHB, a population prevalence of approximately 1%[2]. CHB is associated with the long-term complications of cirrhosis, liver failure and hepatocellular carcinoma (HCC), in 15%-40% of patients. CHB is one of the most common causes of HCC, the most rapidly rising cause of cancer deaths in Australia[3-5].

The goal of treatment for CHB is to improve survival by preventing disease progression to cirrhosis, liver failure and HCC[6]. This can be achieved by long-term suppression of hepatitis B virus (HBV) DNA levels[7-10]. In long-term follow-up, sustained virological suppression has been associated with histological improvement and regression of cirrhosis, as well as reduced risk of hepatic decompensation and HCC[6,11-14]. Surrogate endpoints used in clinical trials include rates of biochemical [serum alanine aminotransferase (ALT) < upper limit of normal (ULN)], virological (undetectable HBV DNA level), serological [HB e antigen (HBeAg)/HB surface antigen (HBsAg) loss ± seroconversion] and histological (improvements in necro-inflammatory grade and fibrosis stage) response[13]. Current therapies approved for CHB include peginterferon-alpha, lamivudine (LMV), adefovir (ADV), telbivudine, entecavir (ETV) and tenofovir (TDF).

Tenofovir is a nucleotide analogue (NA) recommended as first-line treatment for CHB. Tenofovir was first developed as an antiviral for the treatment of human immune-deficiency virus (HIV). The safety and efficacy of TDF for the treatment of chronic HBV infection was confirmed in two phase-Ⅲ clinical trials, enrolling patients with HBeAg-positive and HBeAg-negative CHB respectively. Rates of virological suppression were 76% and 93% at week 48 in HBeAg-positive and HBeAg-negative patients respectively[13], and > 98% overall at week 240[15]. Among HBeAg-positive patients, rates of HBeAg seroconversion were 21% and 40%, and rates of HBsAg seroconversion were 3% and 7%, at weeks 48 and 240, respectively[15]. Genotypic resistance to TDF has not been described. TDF is effective for the treatment of both treatment-naïve and treatment-experienced patients. TDF has a reported good safety profile. Reversible renal toxicity has been reported in < 2% of patients in registration/post-registration studies[16]. Decreased bone mineral density has been reported in HIV-infected patients treated with TDF, but the effect in HBV-mono-infected patients remains unclear[17,18].

There are limited data that describe the safety and efficacy of TDF in the "real world". The few studies that have been published describe populations in Europe and North America[19-21]. There have been no reports

of the experience with TDF in Australia. Such data are important. Australia is a multi-cultural country, and the CHB population is unique for the diversity of HBV genotypes, reflecting immigration patterns from Southern Europe, South-East Asia and Sub-Saharan Africa[2]. The rates of TDF response and resistance in Australia are unknown.

The aim of this study was to evaluate the efficacy and safety of long term TDF therapy in an Australian single-centre real-world cohort of CHB patients.

MATERIALS AND METHODS

Data collection

Data were collected retrospectively from a comprehensive clinical database of CHB patients receiving TDF through liver clinics at St Vincent's Hospital Melbourne (Australia) between 7 March 2006 and 18 February 2014.

Selection criteria

All patients receiving TDF 300 mg daily therapy for HBV mono-infection through St Vincent's Hospital Melbourne were considered for analysis. Inclusion criteria included age > 18 years and treatment duration > 3 mo. Patients could be treatment-naïve or treatment-experienced. We included patients receiving TDF monotherapy, as well as patients treated with TDF in combination with a second antiviral agent. Patients were excluded in the setting of HIV, hepatitis C or hepatitis D co-infection.

Prescription of TDF therapy

TDF was prescribed in accordance with the Australian Pharmaceutical Benefit Scheme. Patients were required to satisfy the following criteria: Non-cirrhotic patients must demonstrate documented chronic liver injury confirmed *via* liver function tests or liver biopsy and must demonstrate appropriate HBV DNA levels according to HBeAg status (HBeAg positive patients HBV DNA > 20000 IU/mL; HBeAg negative patients HBV DNA > 2000 IU/mL). Patients with cirrhosis are required to demonstrate detectable HBV DNA. Patients may be NA naïve or experienced (having failed previous therapy).

HBV DNA assay

Prior to 2010, HBV DNA levels were measured using the versant HBV DNA 3.0 assay (bDNA) (Siemens Healthcare Diagnostics, Tarrytown, NY) with a lower limit of detection (LLD) of 351 IU/mL. From 2010, HBV DNA levels were measured using the Cobas Taqman assay (LLD = 20 IU/mL, Roche Molecular Systems, Pleasanton, CA, United States).

Definitions of response

Complete virological suppression was defined as plasma HBV DNA level < 20 IU/mL. Partial virological suppression was defined as plasma HBV DNA level of ⩾ 20 IU/mL and < 2000 IU/mL. Virological breakthrough (VBT) was defined as an increase in viral load > 1 $\log_{10}$ from nadir, or by a detectable HBV DNA level on two serial measures in a patient who had previously achieved an undetectable HBV DNA level. Biochemical response was defined as the normalisation of serum ALT to < 45 IU/L. Serological response was defined as the loss of detectable HBeAg and/or HBsAg from serum (HBeAg/HBsAg loss) ± the development of antibodies against these antigens (HBeAg/HBsAg seroconversion).

Clinical endpoints

The primary efficacy endpoint was complete virological suppression over time, defined by HBV DNA < 20 IU/mL. Secondary efficacy endpoints included rates of biochemical response, and HBeAg/HBsAg loss and seroconversion over time. We also measured rates of VBT and the occurrence of clinical events including hepatic decompensation and HCC. The assessment of safety was specifically focussed on renal function and, where available, bone mineral density.

Statistical analysis

All statistical analyses were performed using SAS 9.4. For descriptive statistics, continuous variables were summarised as median (25^{th}-75^{th} centile). Categorical variables were described as frequency and percentage. Comparisons between groups for demographic, clinical and virological data were performed using the Wilcoxon signed pair test for continuous data and Fisher's exact test for categorical data. Significance was defined at *P*-value < 0.05. Kaplan Meier analysis was used to determine influences on the time to virological suppression. The associations between baseline HBeAg status, baseline HBV DNA, treatment experience, age, gender, baseline ALT, fibrosis stage and end of follow-up virological suppression were tested using Cox proportional hazards regression analysis and direct multivariate analysis. Ninty-two patients were included in the analysis of demographics and on-treatment safety and efficacy. Patients who had undetectable HBV DNA levels at time of commencement of TDF were excluded from the multivariable analysis (n = 18).

This study was approved by the Human Research Ethics Committee at St Vincent's Hospital Melbourne (QA: 009/14).

RESULTS

Study population

A total of 92 patients were identified. Patient characteristics are summarised in Table 1. The majority of patients were male (70%), of Asian ethnicity (84%) and had HBeAg-negative disease (69%). Fifty-five (60%) were treatment-naive at the time TDF was commenced. Thirty-seven (40%) patients had been previously treated with NA therapy. Compared to treatment-naïve patients, treatment-experienced patients were more likely to have a lower serum HBV DNA level, and a normal serum ALT

Table 1 Baseline demographics

Baseline demographics	Total population (*n* = 92)	Treatment naïve (*n* = 55)	Treatment experienced, viraemic (*n* = 20)	Treatment experienced, non-viraemic (*n* = 17)
Age (yr)				
Mean (IQR)	46 (36-54)	42 (32-53)	48 (41-57)	55 (44-60)
Gender *n* (%)				
Male	64 (69.6)	39 (70.9)	11 (55)	14 (82.4)
Female	28 (30.4)	16 (29.1)	9 (45)	3 (17.6)
Ethnic origin *n* (%)				
African	4 (4.3)	3 (5.5)	0	1 (5.9)
Asian	77 (83.7)	48 (87.3)	16 (80)	13 (76.5)
Caucasian	5 (5.4)	3 (5.5)	0	2 (11.8)
Mediterranean	2 (2.2)	1 (1.8)	1 (5)	0
Middle Eastern	1 (1.1)	0	1 (5)	0
Duration of therapy (mo)				
Median (IQR)	24 (6-42)	24 (12-36)	24 (6-54)	24 (12-42)
HBe antigen status *n* (%)				
HBeAg positive	30 (32.6)	19 (34.5)	10 (50)	1 (5.9)
HBeAg negative	62 (67.4)	36 (65.5)	10 (50)	16 (94.1)
Treatment history *n* (%)				
Experienced	37 (40.2)	0	20 (100)	17 (100)
Adefovir	10 (27)		4 (20)	6 (35.3)
Adefovir/lamivudine	13 (35.1)		6 (30)	7 (41.2)
Lamivudine	6 (16.2)		4 (20)	2 (11.8)
Lamivudine/entecavir	1 (2.7)		1 (5)	0
Entecavir	5 (13.5)		4 (20)	1 (5.9)
Entecavir/adefovir	2 (5.4)		1 (5)	1 (5.9)
Naïve	55 (59.8)	55 (100)	0	0
HBV DNA load (IU/mL) *n* (%)				
< 20	17	-	-	17 (100)
20-2000	29 (31.5)	6 (10.9)	6 (30)	0
2000-100000	11 (12)	8 (14.5)	3 (15)	0
> 100000	52 (56.5)	41 (74.5)	11 (55)	0
Median (IQR)	1.8 × 105 (302-1.6 × 107)	9.4 × 105 (9.7 × 104-3.7 × 107)	1.8 × 105 (790-4.1 × 106)	N/A
ALT (U/L) *n* (%)				
0-20	11 (12)	2 (3.6)	4 (20)	5 (29.4)
20-40	26 (28.3)	10 (18.2)	8 (40)	8 (47.1)
40-400	51 (55.4)	39 (70.9)	8 (40)	4 (23.5)
> 400	4 (4.3)	4 (7.3)	0	0
Median (IQR)	30 (22-41.8)	73 (41-140)	34 (22.3-62.3)	24 (19-44)
Serum creatinine (IU/mL)				
Median (IQR)	70 (60-81.5)	66.5 (50.8-71.5)	71 (63.5-84.5)	83 (69-93)
Pre-treatment biopsy n (%)	69 (75)	40 (72.7)	16 (80)	14 (82.4)
Fibrosis score *n* (%)				
0	9 (9.8)	5 (9.1)	3 (15)	3 (17.6)
1	31 (33.7)	21 (38.2)	6 (30)	4 (23.5)
2	13 (14.1)	8 (14.5)	3 (15)	2 (11.8)
3	7 (7.6)	1 (1.8)	2 (10)	4 (23.5)
4	9 (9.8)	5 (9.1)	2 (10)	2 (11.8)
Genotype *n* (%)	35 (38)	6 (10.9)	9 (45)	12 (70.6)
A	3 (3.3)	2 (3.6)	0	1 (5.9)
B	7 (7.6)	2 (3.6)	1 (5)	4 (23.5)
C	13 (14.1)	2 (3.6)	7 (35)	4 (23.5)
D	3 (3.3)	0	0	2 (11.8)

"Treatment experience" refers to previous NA therapy. "Viraemia" refers to HBV DNA > 20 IU/mL. Liver biopsy was scored using the METAVIR scoring system. HBe: Hepatitis B "e"; HBV DNA: Hepatitis B viral deoxyribonucleic acid; ALT: Alanine aminotransferase; N/A: Not applicable.

at the time TDF therapy was commenced. Seventeen treatment-experienced patients had a baseline HBV DNA level less than the lower limit of detection, and had directly switched to TDF for convenience. Nity-seven percent of patients received TDF monotherapy. Median duration of follow-up was 24 mo (6-42 mo).

Virological outcomes

Virological response to TDF is detailed in Table 2 and Figure 1. Overall, 77 (83.7%) patients achieved complete virological suppression by the end-of-follow-up, with a median time to suppression of 6 mo (IQR = 3-12 mo). The rates of complete virological suppression were 71% (45/65) at 12 mo, 80% (37/46) at 24 mo and 89% (25/28) at 36 mo. Eighty-nine/ninety-two (96.7%) achieved a partial virological response (HBV DNA 20-2000 IU/mL).

Treatment-naïve individuals: Complete virological

Table 2 Virological suppression at on-treatment time-points (n = 92)

Follow-up (mo)	0	6	12	18	24	30	36
Patients with viral load n (%)	92 (100)	74 (80.4)	65 (70.7)	58 (63)	46 (50)	30 (32.6)	28 (30.4)
Virological suppression n (%)	18 (19.6)	41 (55.4)	45 (69.2)	46 (79.3)	37 (80.4)	26 (86.7)	25 (89.3)

"Patients with viral load" refers to the number of patients at each time point who had an available HBV DNA reading. "Virological suppression" refers to the number of patients with HBV DNA < 20 IU/mL. HBV: Hepatitis B virus.

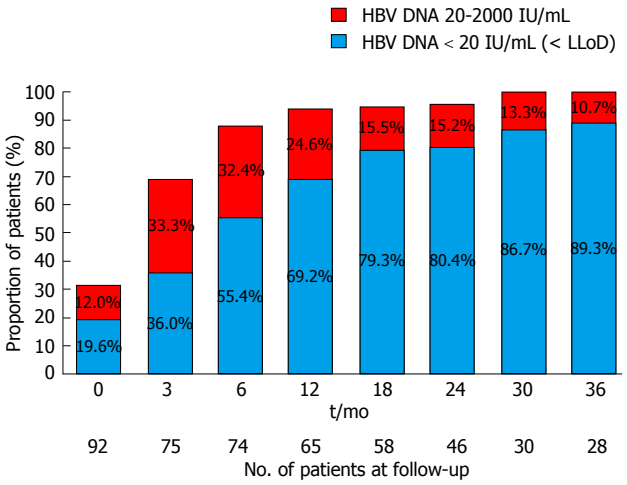

Figure 1 Complete virological suppression and partial virological suppression at on treatment time points. The proportion of patients who achieve complete virological suppression (HBV DNA < 20 IU/mL) or partial virological suppression (HBV DNA 20-2000 IU/mL) while on tenofovir therapy. The number of patients followed up at each time point is recorded below the Time axis. HBV: Hepatitis B virus.

suppression was achieved in 43/55 (78%) of patients with a median time to suppression of 6 mo (IQR = 3-12 mo). Rates of complete virological suppression were 70% (29/44) at 12 mo, 87% (26/30) at 24 mo and 100% at 36 mo (18/18). This was maintained by 50/55 (91%) of patients throughout follow-up. While a total of five patients failed to maintain complete virological suppression, only three patients experienced VBT. This was associated with reported non-compliance. In the first patient, HBV DNA levels rose from undetectable viral load at 12 mo to 55 IU/mL at 18 mo and 23 IU/mL at 24 mo. In the second patient, HBV DNA levels rose from undetectable at 18 mo to 1940 IU/mL at 24 mo and 578 IU/mL at 30 mo. In the final patient, HBV DNA levels increased from undetectable at 24 mo to 46300 IU/mL at 42 mo and 29 IU/mL at 48 mo (results for the intervening 12 mo were unavailable). A transient low level viraemia not meeting the definition for VBT (single HBV DNA level of 23 IU/mL and 21 IU/mL, respectively, following achievement of complete virological suppression) was observed in two additional patients before returning to undetectable levels.

Treatment-experienced individuals: Viraemia was seen in 54% (20/37) of treatment-experienced individuals at the time TDF therapy was commenced. Complete virological suppression was achieved among 85% (17/20) of viraemic patients with a median time to suppression of 6 mo (IQR = 3-18 mo). Rates of complete virological suppression were 64% (9/14) at 12 mo, 58% (7/12) at 24 mo and 63% (5/8) at 36 mo. While 3 patients showed persistent viraemia at 36 mo, all had an HBV DNA level < 2000 IU/mL and subsequently achieved complete virological suppression by 60 mo. This was maintained in 17/20 (85%) patients throughout follow-up. No patient met the strict definition for virological breakthrough. Two patients demonstrated a single instance of HBV DNA > 20 IU/mL (28 IU/mL and 27 IU/mL) before returning to undetectable levels, but did not meet the criteria for VBT. Among patients with an undetectable plasma HBV DNA level at baseline, 16/17 patients (94%) maintained complete virological suppression throughout follow-up. One patient experienced a single HBV DNA level of 40 IU/mL.

Predictors of virological outcome

Survival analysis of the influence of treatment experience on complete virological suppression is presented in Figure 2. Cox proportional hazards analysis was carried out on viraemic patients at baseline with the final model including baseline HBV DNA, HBeAg status treatment experience, age and baseline ALT (Table 3). Multivariate analysis showed a significant relationship between virological suppression at end of follow-up and baseline HBV DNA (OR = 0.897, 95%CI: 0.833-0.967, P = 0.0046) and HBeAg status (HR = 0.373, 95%CI: 0.183-0.762, P = 0.0069).

Serological outcomes

HBeAg loss/seroconversion: Among 30 HBeAg-positive patients at baseline, 5 (16.7%) underwent HBeAg loss and seroconversion. Median time to seroconversion was 30 mo (9-60 mo). Mean age was 38 years (24-48 mo) and median baseline HBV DNA was 1.7×10^7 IU/mL. There was no significant difference in HBeAg seroconversion rates between treatment-naïve and treatment-experienced patients (P = 0.87). Two patients showed documented HBeAg seroreversion while on TDF treatment. One patient who was HBeAg-negative at baseline underwent HBeAg seroreversion at 24 mo of TDF therapy. HBeAg seroconversion then reoccurred at 36 mo and was sustained for the remainder of follow-up. The second case showed HBeAg loss without seroconversion at 12 mo, followed by seroreversion at 36 mo of treatment. This patient had only been on therapy for 36 mo at end of follow-up.

HBsAg: One treatment-naïve male underwent HBsAg loss and seroconversion following 12 mo of TDF therapy.

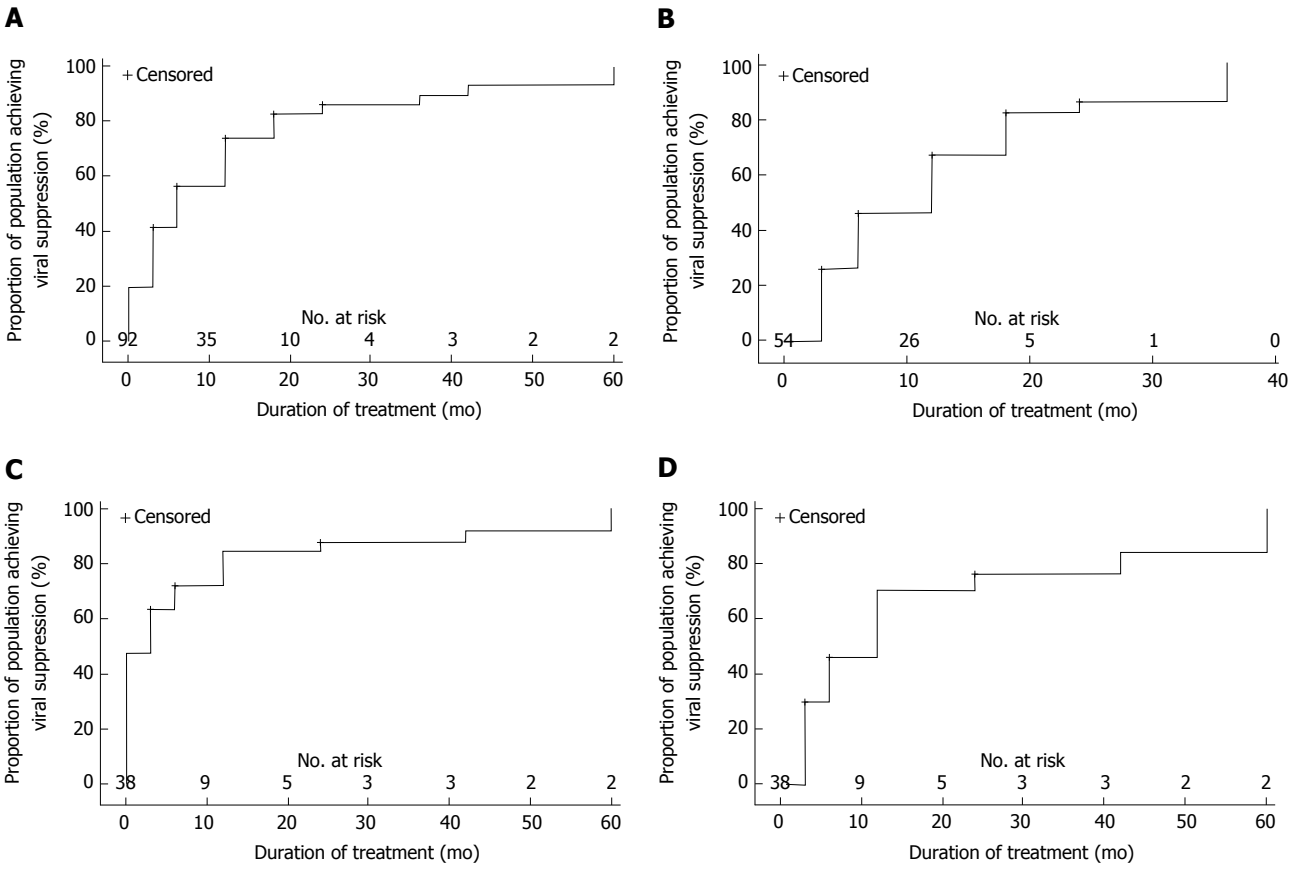

Figure 2 Survival analysis of the influence of treatment experience on complete virological suppression. A: Time to virological suppression according to duration of treatment, *n* = 92; B: Amongst treatment naïve patients *n* = 54; C: Treatment experienced patients, *n* = 37; D: Treatment experienced viraemic patients, *n* = 20. Number at risk describes the number of target group patients captured at each time period.

Table 3 Cox regression model of predictors of end of follow-up virological suppression (*n* = 74[1])

Covariates	Multivariable	
	Hazard ratio (95%CI)	*P* value
Baseline HBV DNA (log_{10} IU/mL)	0.897 (0.833-0.967)	0.0046
HBeAg status (HBeAg pos *vs* neg)	0.373 (0.183-0.762)	0.0069
Treatment experience (Naïve *vs* experienced)	1.189 (0.598-2.364)	0.6207
Age (yr)	1.018 (0.992-1.044)	0.1760
ALT (log_{10} IU/mL)	1.093 (0.816-1.465)	0.5505

[1]Excludes patients who were not viraemic at baseline. HBV: Hepatitis B virus; ALT: Alanine aminotransferase.

This individual was 28 years of age and HBeAg-negative at the time TDF was started.

Biochemical outcomes

Mean ALT at baseline was 134 ± 340 U/mL and 33 ± 13 U/mL at end of follow-up, with a mean change of -101.3 ± 340.4 U/mL. Treatment experienced patients had a lower mean baseline ALT than treatment naïve patients (52 ± 70.2 U/mL *vs* 190 ± 431.1 U/mL, *P* = 0.02). They consequently had a lower mean change in ALT at the end of follow-up (-21 ± 68 U/mL *vs* -155 ± 432 U/mL, *P* = 0.28). Baseline serum ALT levels were within the normal range in 42/92 (45.7%) patients. By the end of treatment, 76/92 (83%) patients were within the normal range. Of the 50 patients who were above the ULN at baseline, 38 (76%) achieved ALT normalisation by the end of follow-up.

Clinical outcomes

Hepatocellular cancer was diagnosed in two patients within 12 mo of starting TDF treatment. Both patients were diagnosed with cirrhosis prior to commencing TDF and one patient died as a result of their malignancy. A third patient was diagnosed with HCC 12 mo after ceasing TDF. No episodes of hepatic decompensation were recorded in the study population.

Treatment discontinuation and safety

Treatment was discontinued at the discretion of individual clinicians in 11 patients (12%). Treatment was discontinued as a result of a rise in serum creatinine levels in 3 patients (3%). All 3 patients had a peak serum creatinine < 1.5 × ULN. Two patients had only been taking TDF for 3 mo, and both had previously been treated with long-term LMV plus ADV therapy. Creatinine returned to the normal range on switch to ETV in one patient and LMV plus ADV in the other. The clinical decision to return the latter patient to LMV plus

ADV was determined by the treating physician and is not a standard treatment recommendation. One treatment-naïve patient was noted to have a rising serum creatinine at month 42 of treatment (peak creatinine = 118 μmol/L, ULN = 104). Serum phosphate levels were normal. Treatment was switched to ETV and creatinine returned to the normal range. Bone mineral density measurements were not routine and were only performed in a minority. There were 4 patients who were noted to have osteopenia or osteoporosis after treatment durations of 18-42 mo. Two of these patients were treatment naïve at the time TDF was started, one patient had previously been treated with adefovir for 5 years, and one patient had previously received LMV for 4 years. None of the 4 patients had a baseline bone mineral density measure available for comparison. Tenofovir was discontinued in another 4 patients after reports of non-specific adverse events including nausea, dizziness, fatigue, weight loss and myalgia.

DISCUSSION

Tenofovir is a potent antiviral therapy for CHB. It has been associated with high rates of virological suppression in clinical trials and virological resistance is yet to be described in clinical practice[13]. Post-registration real-world studies provide confirmation of therapy efficacy outside of the selected clinical trial situation, and monitor for rare adverse events. This is the first real-life study of TDF in an Australian setting. It validates the efficacy and safety of TDF in NA-naïve and experienced patients with CHB.

Similarly to registration trials and real-life studies, the study population was predominantly male and HBeAg negative, with 75% over the age of 40. However, while registration trials studied predominantly Caucasian populations, this population was mostly of Asian origin. Other ethnic minorities were also represented, reflecting Australian migration patterns. HBV genotype data were available for a minority of patients (35/92). Genotypes C and B were the most common genotypes, with A and D also represented. Studies from Europe and Asia are dominated by genotype A/D (Europe) and genotype B/C (Asia), limiting cross genotype comparisons. The tenofovir registration studies included mainly Western genotype A/D individuals, as have most of the real world data[13,22,23]. While this study's patient size may be limited, the population studied here are unique for the breadth of ethnicity and HBV genotypes and comprise the first dataset described in an Australian population. Liver fibrosis ranged predominately between stages 1 and 2, with 10% of patients diagnosed with cirrhosis at baseline. Forty percent of the population were NA treatment-experienced.

The efficacy of TDF therapy in our cohort largely reflects the clinical trial experience. A daily dose of 300 mg of TDF was found to achieve at least partial virological suppression in 97% of patients and complete virological suppression in 84% of patients, demonstrating robust efficacy. Complete virological suppression was sustained by 94% of patients over time. Patients with persistent viraemia had HBV DNA levels < 2080 IU/mL, except for two patients who had a viral load 1.2-2.6 × 10^5 IU/mL after 3 mo on therapy. Virological breakthrough was only observed in one patient with documented non-compliance. The clinical variables that were independently associated with time to suppression were high HBV DNA level at baseline, and HBeAg seropositivity. Previous NA therapy was not associated with reduced response rate. HBeAg seroconversion was achieved in 17% of HBeAg positive patients, with median duration of follow-up of 24 mo. One patient underwent HBsAg loss and seroconversion after 12 mo of treatment. The efficacy data are therefore broadly consistent with the experience in the registration studies[13,22,24].

Our findings are also in keeping with "real life" international studies. Pol *et al*[23] reviewed safety and efficacy data from two real-life cohorts in the United Kingdom and Europe. The cohorts had a combined sample size of 362 NA-naïve patients with a median follow-up of 9-28 mo. Virological suppression was achieved in 80%-89% of patients with breakthrough identified in 2% of patients, without any corresponding resistance mutations. HBeAg seroconversion occurred in 7%-18% of patients and HBsAg loss occurred in 2% of the European cohort. Eighty-seven percent of patients achieved ALT normalisation by 30 wk[5]. Pan *et al*[21] analysed the real-life safety and efficacy of TDF in 90 Asian-American patients over 48 wk. Ten percent of the population had a history of prior treatment with lamivudine or adefovir. Virological suppression was achieved in 82% of patients, 12% of patients underwent HBeAg seroconversion and 66% of patients showed ALT normalisation by the end of follow-up. No resistance to TDF was detected and the treatment was considered well-tolerated with few related adverse events. While our results reflect those of other "real life" data, few studies have included treatment-experienced patients and if so they compose only a small minority. This is an area for future focus considering clinical practice of switching patients over to TDF from older less effective NAs.

Therapy was ceased in 12% of patients at the discretion of individual clinicians due to concern about renal (3%) and bone impairment. Tenofovir was self-ceased by 4% of patients due to non-specific adverse events. It was not possible to establish causality for these events; all possible renal events were mild and reversible with discontinuation. No confirmed cases of proximal tubular dysfunction were observed. Isolated cases of osteomalacia and osteopenia concurrent with TDF therapy have also been reported in the HBV literature[25]; there are more numerous reports in the HIV literature. In our cohort, although cases of osteopaenia and osteoporosis were noted, the absence of baseline bone mineral density scans meant that causality could not be speculated. Chronic liver disease itself is a risk factor for osteoporosis. We now perform routine monitoring of renal function and fasting serum phosphate levels every

six months, as well as bone mineral densitometry at baseline and every 3 years to screen for osteoporosis. This approach needs prospective validation.

In conclusion, our Australian experience shows TDF to be an effective and safe therapy for patients with CHB. Rates of sustained virological suppression were very high. Elevated baseline HBV DNA level and HBeAg-positive disease were associated with slower time to suppression, but TDF resistance was not observed, and most patients achieved complete virological suppression with continued therapy. Tenofovir was generally well tolerated. This study supports the findings of other real-life experience into the efficacy and safety of TDF in the treatment of CHB.

COMMENTS

Background

Chronic hepatitis B (CHB) affects 240-400 million people around the world. It is estimated that 218000 people in Australia live with CHB, a population prevalence of approximately 1%. CHB is associated with the long-term complications of cirrhosis, liver failure and hepatocellular carcinoma (HCC), in 15%-40% of patients. CHB is one of the most common causes of HCC, the fastest increasing cause of cancer death in Australia.

Research frontiers

Tenofovir is a nucleotide analogue recommended as first-line treatment for CHB. The safety and efficacy of tenofovir disoproxil fumarate (TDF) for the treatment of chronic HBV infection has been confirmed in two phase-Ⅲ clinical trials. There are limited data that describe the safety and efficacy of TDF in the "real world". The few studies that have been published describe populations in Europe and North America. There have been no reports of the experience with TDF in Australia.

Innovations and breakthroughs

Out of 92 patients, 89 (96.7%) achieved partial virological response and 77 (83.7%) achieved complete virological suppression by the end-of-follow-up. Predictors of virological suppression included lower baseline HBV DNA and HBeAg negative disease.

Applications

The authors' Australian experience shows that TDF is an effective and safe therapy for patients with CHB. Rates of sustained virological suppression were very high and most patients achieved complete virological suppression with continued therapy. TDF resistance was not observed and treatment was generally well tolerated. This study supports the findings of other real-life experience into the efficacy and safety of TDF in the treatment of CHB.

Terminology

The hepatitis B virus (HBV) is transmitted vertically, parenterally or *via* mucosal exposure to infected blood or bodily fluids. CHB is associated with long-term complications of cirrhosis, liver failure and hepatocellular carcinoma. They carry high rates of morbidity and mortality and affect 15%-40% of patients at some point in their life. Tenofovir disoproxil fumarate is a nucleotide analogue used in the treatment of CHB. Prior to its role in CHB, TDF was used in the treatment of HIV type 1 infection.

Peer-review

This is a well-designed and well-written real life data study of tenofovir treatment for hepatitis B.

REFERENCES

1 **Ott JJ**, Stevens GA, Groeger J, Wiersma ST. Global epidemiology of hepatitis B virus infection: new estimates of age-specific HBsAg seroprevalence and endemicity. *Vaccine* 2012; **30**: 2212-2219 [PMID: 22273662 DOI: 10.1016/j.vaccine.2011.12.116]

2 **MacLachlan JH**, Allard N, Towell V, Cowie BC. The burden of chronic hepatitis B virus infection in Australia, 2011. *Aust N Z J Public Health* 2013; **37**: 416-422 [PMID: 24090323 DOI: 10.1111/1753-6405.12049]

3 **MacLachlan JH**, Cowie BC. Liver cancer is the fastest increasing cause of cancer death in Australians. *Med J Aust* 2012; **197**: 492-493 [PMID: 23121582]

4 **Lok AS**. Chronic hepatitis B. *N Engl J Med* 2002; **346**: 1682-1683 [PMID: 12037146 DOI: 10.1056/NEJM200205303462202]

5 **Liver EAFTSOT**. EASL clinical practice guidelines: Management of chronic hepatitis B virus infection. *J Hepatol* 2012; **57**: 167-185 [PMID: 22436845 DOI: 10.1016/j.jhep.2012.02.010]

6 **Lok AS**, McMahon BJ. Chronic hepatitis B: update 2009. *Hepatology* 2009; **50**: 661-662 [PMID: 19714720 DOI: 10.1002/hep.23190]

7 **Liaw YF**, Sung JJ, Chow WC, Farrell G, Lee CZ, Yuen H, Tanwandee T, Tao QM, Shue K, Keene ON, Dixon JS, Gray DF, Sabbat J. Lamivudine for patients with chronic hepatitis B and advanced liver disease. *N Engl J Med* 2004; **351**: 1521-1531 [PMID: 15470215 DOI: 10.1056/NEJMoa033364]

8 **Realdi G**, Fattovich G, Hadziyannis S, Schalm SW, Almasio P, Sanchez-Tapias J, Christensen E, Giustina G, Noventa F. Survival and prognostic factors in 366 patients with compensated cirrhosis type B: a multicenter study. The Investigators of the European Concerted Action on Viral Hepatitis (EUROHEP). *J Hepatol* 1994; **21**: 656-666 [PMID: 7814813]

9 **Chen CJ**, Yang HI, Su J, Jen CL, You SL, Lu SN, Huang GT, Iloeje UH. Risk of hepatocellular carcinoma across a biological gradient of serum hepatitis B virus DNA level. *JAMA* 2006; **295**: 65-73 [PMID: 16391218 DOI: 10.1001/jama.295.1.65]

10 **Iloeje UH**, Yang HI, Su J, Jen CL, You SL, Chen CJ. Predicting cirrhosis risk based on the level of circulating hepatitis B viral load. *Gastroenterology* 2006; **130**: 678-686 [PMID: 16530509 DOI: 10.1053/j.gastro.2005.11.016]

11 **Chen LP**, Zhao J, Du Y, Han YF, Su T, Zhang HW, Cao GW. Antiviral treatment to prevent chronic hepatitis B or C-related hepatocellular carcinoma. *World J Virol* 2012; **1**: 174-183 [PMID: 24175223 DOI: 10.5501/wjv.v1.i6.174]

12 **Liaw YF**, Chu CM. Hepatitis B virus infection. *Lancet* 2009; **373**: 582-592 [PMID: 19217993 DOI: 10.1016/s0140-6736(09)60207-5]

13 **Marcellin P**, Heathcote EJ, Buti M, Gane E, de Man RA, Krastev Z, Germanidis G, Lee SS, Flisiak R, Kaita K, Manns M, Kotzev I, Tchernev K, Buggisch P, Weilert F, Kurdas OO, Shiffman ML, Trinh H, Washington MK, Sorbel J, Anderson J, Snow-Lampart A, Mondou E, Quinn J, Rousseau F. Tenofovir disoproxil fumarate versus adefovir dipivoxil for chronic hepatitis B. *N Engl J Med* 2008; **359**: 2442-2455 [PMID: 19052126 DOI: 10.1056/NEJMoa0802878]

14 **Lee JM**, Ahn SH, Kim HS, Park H, Chang HY, Kim DY, Hwang SG, Rim KS, Chon CY, Han KH, Park JY. Quantitative hepatitis B surface antigen and hepatitis B e antigen titers in prediction of treatment response to entecavir. *Hepatology* 2011; **53**: 1486-1493 [PMID: 21520167 DOI: 10.1002/hep.24221]

15 **Gordon SC**, Krastev Z, Horban A, Petersen J, Sperl J, Dinh P, Martins EB, Yee LJ, Flaherty JF, Kitrinos KM, Rustgi VK, Marcellin P. Efficacy of tenofovir disoproxil fumarate at 240 weeks in patients with chronic hepatitis B with high baseline viral load. *Hepatology* 2013; **58**: 505-513 [PMID: 23364953 DOI: 10.1002/hep.26277]

16 **Pipili C**, Cholongitas E, Papatheodoridis G. Review article: nucleos(t)ide analogues in patients with chronic hepatitis B virus infection and chronic kidney disease. *Aliment Pharmacol Ther* 2014; **39**: 35-46 [PMID: 24299322 DOI: 10.1111/apt.12538]

17 **Carr A**, Hoy J. Low bone mineral density with tenofovir: does statistically significant mean clinically significant? *Clin Infect Dis* 2010; **51**: 973-975 [PMID: 20828303 DOI: 10.1086/656418]

18 **Grund B**, Peng G, Gibert CL, Hoy JF, Isaksson RL, Shlay JC, Martinez E, Reiss P, Visnegarwala F, Carr AD. Continuous antiretroviral therapy decreases bone mineral density. *AIDS* 2009;

23: 1519-1529 [PMID: 19531929 DOI: 10.1097/QAD.0b013e32832c1792]

19 **Carey I**, Nguyen DorothyJoe H, Al-Freah M, Knighton S, Bruce M, Suddle A, Harrison PM, Agarwal K. P47 De-novo antiviral therapy with nucleos(t)ide analogues in 'real-life' patients with chronic hepatitis B infection: comparison of virological responses between lamivudine adefovir vs entecavir vs tenofovir therapy. *Gut* 2011; **60**: A22-A23 [DOI: 10.1136/gutjnl-2011-300857a.47]

20 **Lampertico P**, Soffredini R, Viganò M, Yurdaydin C, Idilman R, Papatheodoris G, Margheriti K, Buti M, Esteban R, Zaltron S, Vavassori A, Carosi G, Minola E, Vinci M, Pinzello G, Giorgini A, Zuin M, Salmi A, Del Poggio P, De Filippi F, Bruno S, Pasulo L, Fagiuoli S, Andreoletti M, Colli A, Maldini FF, Milanese M, Colombo AE, Bellati GA, Angeli E, Magni C, Gubertini G, Rizzardini G, Fasano M, Santantonio T, Terreni N, Spinzi G, Facchetti F, Invernizzi F, Colombo M. Oc.07.1 2-Year Effectiveness and Safety of Tenofovir in 302 Nuc-Naive Patients with Chronic Hepatitis B: A Multicenter European Study in Clinical Practice. *Digestive and Liver Disease* 2012; **44**: S70 [DOI: 10.1016/s1590-8658(12)60186-8]

21 **Pan CQ**, Trinh H, Yao A, Bae H, Lou L, Chan S. Efficacy and safety of tenofovir disoproxil fumarate in Asian-Americans with chronic hepatitis B in community settings. *PLoS One* 2014; **9**: e89789 [PMID: 24594870 DOI: 10.1371/journal.pone.0089789]

22 **Heathcote EJ**, Marcellin P, Buti M, Gane E, De Man RA, Krastev Z, Germanidis G, Lee SS, Flisiak R, Kaita K, Manns M, Kotzev I, Tchernev K, Buggisch P, Weilert F, Kurdas OO, Shiffman ML, Trinh H, Gurel S, Snow-Lampart A, Borroto-Esoda K, Mondou E, Anderson J, Sorbel J, Rousseau F. Three-year efficacy and safety of tenofovir disoproxil fumarate treatment for chronic hepatitis B. *Gastroenterology* 2011; **140**: 132-143 [PMID: 20955704 DOI: 10.1053/j.gastro.2010.10.011]

23 **Pol S**, Lampertico P. First-line treatment of chronic hepatitis B with entecavir or tenofovir in 'real-life' settings: from clinical trials to clinical practice. *J Viral Hepat* 2012; **19**: 377-386 [PMID: 22571899 DOI: 10.1111/j.1365-2893.2012.01602.x]

24 **Marcellin P**, Gane E, Buti M, Afdhal N, Sievert W, Jacobson IM, Washington MK, Germanidis G, Flaherty JF, Aguilar Schall R, Bornstein JD, Kitrinos KM, Subramanian GM, McHutchison JG, Heathcote EJ. Regression of cirrhosis during treatment with tenofovir disoproxil fumarate for chronic hepatitis B: a 5-year open-label follow-up study. *Lancet* 2013; **381**: 468-475 [PMID: 23234725 DOI: 10.1016/S0140-6736(12)61425-1]

25 **Parsonage MJ**, Wilkins EG, Snowden N, Issa BG, Savage MW. The development of hypophosphataemic osteomalacia with myopathy in two patients with HIV infection receiving tenofovir therapy. *HIV Med* 2005; **6**: 341-346 [PMID: 16156882 DOI: 10.1111/j.1468-1293.2005.00318.x]

P- Reviewer: Kadayifci A, Pai CG, Silva LD **S- Editor**: Qiu S
L- Editor: A **E- Editor**: Li D

World Journal of Hepatology

Submit a Manuscript: http://www.wjgnet.com/esps/
Help Desk: http://www.wjgnet.com/esps/helpdesk.aspx
DOI: 10.4254/wjh.v9.i1.57

World J Hepatol 2017 January 8; 9(1): 57-63
ISSN 1948-5182 (online)

ORIGINAL ARTICLE

Retrospective Study

Clinical usefulness of ursodeoxycholic acid for Japanese patients with autoimmune hepatitis

Yuichi Torisu, Masanori Nakano, Keiko Takano, Ryo Nakagawa, Chisato Saeki, Atsushi Hokari, Tomohisa Ishikawa, Masayuki Saruta, Mikio Zeniya

Yuichi Torisu, Masanori Nakano, Keiko Takano, Ryo Nakagawa, Chisato Saeki, Atsushi Hokari, Tomohisa Ishikawa, Masayuki Saruta, Division of Gastroenterology and Hepatology, Department of Internal Medicine, the Jikei University School of Medicine, Tokyo 105-8461, Japan

Yuichi Torisu, Masanori Nakano, Department of Internal Medicine, Fuji City General Hospital, Shizuoka 417-8567, Japan

Mikio Zeniya, Department of Internal Medicine, Sanno Medical Center, Tokyo 107-0052, Japan

Author contributions: Torisu Y and Zeniya M designed the research; Torisu Y collected and analyzed the data; Nakano M, Takano K, Nakagawa R, Saeki C, Hokari A, Ishikawa T and Saruta M revised the manuscript for important intellectual content; Torisu Y and Zeniya M wrote the paper; all authors have read and approved the final version to be published.

Institutional review board statement: The study was reviewed and approved by the Jikei University School of Medicine Institutional Review Board; IRB Protocol No: 26-321(7827).

Informed consent statement: Written, informed consent for participation in this study was not obtained from the patients, because this study did not report on a clinical trial and the data were retrospective in nature and analyzed anonymously.

Conflict-of-interest statement: We have no financial relationships to disclose.

Data sharing statement: No additional data are available.

Manuscript source: Unsolicited manuscript

Correspondence to: Yuichi Torisu, MD, Division of Gastroenterology and Hepatology, Department of Internal Medicine, the Jikei University School of Medicine, 3-25-8 Nishishinbashi, Minato-ku, Tokyo 105-8461, Japan. torisu@yb4.so-net.ne.jp
Telephone: +81-03-34331111
Fax: +81-03-34350569

Received: July 10, 2016
Peer-review started: July 14, 2016
First decision: September 12, 2016
Revised: September 25, 2016
Accepted: November 21, 2016
Article in press: November 22, 2016
Published online: January 8, 2017

Abstract

AIM

To evaluate the therapeutic effects of ursodeoxycholic acid (UDCA) on autoimmune hepatitis (AIH).

METHODS

A total 136 patients who were diagnosed with AIH were included in our study. All of the patients underwent a liver biopsy, and had at least a probable diagnosis on the basis of either the revised scoring system or the simplified scores. Initial treatment included UDCA monotherapy (Group U, *n* = 48) and prednisolone (PSL) monotherapy (Group P, *n* = 88). Group U was further classified into two subgroups according to the effect of UDCA: Patients who had achieved remission induction with UDCA monotherapy and showed no sign of relapse (Subgroup U1, *n* = 34) and patients who additionally received PSL during follow-up (Subgroup U2, *n* = 14). We compared the clinical and histological findings between each groups, and investigated factors

contributing to the response to UDCA monotherapy.

RESULTS

In Group U, 34 patients (71%) achieved and maintained remission over 49 (range: 8-90) mo (Subgroup U1) and 14 patients (29%) additionally received PSL (Subgroup U2) during follow-up. Two patients in Subgroup U2 achieved remission induction once but additionally required PSL administration because of relapse (15 and 35 mo after the start of treatment). The remaining 12 patients in Subgroup U2 failed to achieve remission induction during follow-up, and PSL was added during 7 (range: 2-18) mo. Compared with Subgroup U2, Subgroup U1 had significantly lower alanine aminotransferase (ALT) levels at onset (124 IU/L *vs* 262 IU/L, $P = 0.023$) and a significantly higher proportion of patients with mild inflammation (A1) on histological examination (70.6% *vs* 35.7%, $P = 0.025$). When multivariate analysis was performed to identify factors contributing to the response to UDCA monotherapy, only a serum ALT level of 200 IU/L or lower was found to be associated with a significant difference ($P = 0.013$).

CONCLUSION

To prevent adverse events related to corticosteroids, UDCA monotherapy for AIH needs to be considered in patients with a serum ALT level of 200 IU/L or lower.

Key words: Autoimmune hepatitis; Japanese patients; Adverse events; Corticosteroids; Ursodeoxycholic acid

Core tip: Autoimmune hepatitis (AIH) is generally responsive to immunosuppressive treatment, and corticosteroids are commonly used for the initial and maintenance treatments. However, corticosteroid treatment must be discontinued in some patients because of several side effects. This study aimed to evaluate the therapeutic effects of ursodeoxycholic acid (UDCA), which has high tolerability and no severe side effects, on AIH. Our results suggest that to prevent adverse events related to corticosteroids, treatment with UDCA alone for AIH needs to be considered in selected patients, especially those with an alanine aminotransferase level of 200 IU/L or lower. This utility of UDCA must be confirmed in a prospective study.

Torisu Y, Nakano M, Takano K, Nakagawa R, Saeki C, Hokari A, Ishikawa T, Saruta M, Zeniya M. Clinical usefulness of ursodeoxycholic acid for Japanese patients with autoimmune hepatitis. *World J Hepatol* 2017; 9(1): 57-63 Available from: URL: http://www.wjgnet.com/1948-5182/full/v9/i1/57.htm DOI: http://dx.doi.org/10.4254/wjh.v9.i1.57

INTRODUCTION

Autoimmune hepatitis (AIH) is an unresolving progressive liver disease that affects females preferentially and is characterized by interface hepatitis, hypergammaglobulinemia, circulating autoantibodies, and a favorable response to immunosuppression. The aim of treatment in AIH is to obtain complete remission of the disease and to prevent further progression of liver disease, which generally requires permanent maintenance therapy. Corticosteroids have been widely used as the first choice drug treatment of AIH[1,2]. However, long-term treatment with a generous corticosteroid dosage may induce predictable side effects, such as cosmetic changes (facial rounding, dorsal hump formation, striae, weight gain, acne, alopecia, and facial hirsutism) or even more dreadful complications, such as osteopenia, brittle diabetes, psychosis, pancreatitis, opportunistic infections, labile hypertension, and malignancy[3-7]. Consequently, corticosteroid treatment must be discontinued in 13% of patients. Of those withdrawn from therapy, most have intolerable cosmetic changes or obesity (47%), osteoporosis with vertebral compression (27%), and/or difficult-to-control diabetes (20%)[4,8]. Because AIH predominantly affects middle-aged women, the presence of cosmetic issues is one of the key factors for maintaining drug compliance. Cosmetic issues may lead to emotional problems that result in treatment failure and a poor prognosis. Thus, a strategy to reduce the adverse effects of corticosteroid treatment is needed.

Ursodeoxycholic acid (UDCA) has been widely used as the first choice for treating primary biliary cirrhosis (PBC) and has been established as clinically useful[9-11]. No severe side effects have been reported during UDCA therapy for PBC[12]. Although there are reports that UDCA is also useful for treating similar autoimmune liver diseases, its clinical value has not as yet been established[13-15]. In this study, patients with a confirmed diagnosis of AIH who started treatment with UDCA alone were analyzed, and the results are reported.

MATERIALS AND METHODS

Patients

The present study included 136 patients who were diagnosed with AIH between 1975 and 2011 at the Division of Gastroenterology and Hepatology, Department of Internal Medicine, The Jikei University Hospital (Tokyo, Japan). All of the patients had at least a probable diagnosis on the basis of either the revised scoring system, as proposed by the International Autoimmune Hepatitis Group in 1999[16], or the simplified scores[17]. All of the patients underwent a liver biopsy. In this study, patients with no histological fibrosis (F0) were excluded. Chronic viral hepatitis B and C were excluded by serological testing in all of the patients. Patients with an overlapping syndrome or a coexistent liver disease (*e.g.*, primary biliary cirrhosis, primary sclerosing cholangitis, nonalcoholic fatty liver disease, or alcohol-induced liver injury) were also excluded by medical history, serological data and histological finding. So, patients with positive antimitochondrial antibody were excluded. Of the 136

Table 1 Clinical features of the two groups classified according to the therapeutic agent

	Group U (n = 48)	Group P (n = 88)	P
Age (yr)	45 (17-74)	51 (15-78)	ns
Sex (female)	45 (93.8%)	65 (73.9%)	< 0.01
Acute presentation	5 (10.4%)	31 (36.5%)	< 0.01
Laboratory data			
AST (IU/L)	104 (46-1234)	303 (31-2215)	< 0.001
ALT (IU/L)	149 (52-1000)	431 (38-2801)	< 0.001
T.Bil (mg/dL)	0.8 (0.3-18)	1.3 (0.4-19.3)	< 0.05
ALP (U/L)	300 (144-1184)	369 (145-4420)	ns
γ-GTP (U/L)	82 (13-875)	183 (12-1256)	< 0.05
IgG (mg/dL)	1954 (1096-3793)	2336 (1051-5776)	< 0.01
ANA (≥ 1 : 40)	46 (95.8%)	83 (94.3%)	ns
SMA (≥ 1 : 40)	11/23 (47.8%)	35/45 (77.8%)	< 0.05
HLA DR4	6/16 (37.5%)	33/57 (57.9%)	ns
Histological finding			
Grading			
A1	29 (60.4%)	25 (28.4%)	< 0.01
A2	18 (37.5%)	44 (50%)	
A3	1 (2.1%)	19 (21.6%)	
Staging			
F1	35 (72.9%)	43 (48.9%)	< 0.05
F2	6 (12.5%)	28 (31.8%)	
F3	6 (12.5%)	10 (11.4%)	
F4	1 (2.1%)	7 (8.0%)	
AIH score			
Revised score	15 (10-20)	16 (7-23)	ns
Simplified score	6 (4-8)	6 (3-8)	ns

Continuous variables are expressed as median (range) values. The Mann-Whitney *U* test was used to evaluate differences in continuous variables between two groups. Dichotomous variables were compared by Pearson's χ^2 test. Values of $P < 0.05$ were considered significant. ALT: Alanine aminotransferase; AIH: Autoimmune hepatitis; AST: Aspartate transaminase; HLA: Human leukocyte antigen; ANA: Antinuclear antibody; ALP: Alkaline phosphatase; γ-GTP: γ-glutamyltransferase; SMA: Smooth muscle antibody; ns: No significant difference; T.Bil: Total bilirubin; IgG: Immunoglobulin G.

Table 2 Clinical features of the two subgroups classified according to the effect of ursodeoxycholic acid

	Subgroup U1[1] (n = 34)	Subgroup U2[2] (n = 14)	P
Age (yr)	42 (17-74)	48 (21-66)	ns
Sex (female)	33 (97.1%)	12 (85.7%)	ns
Acute presentation	4 (11.8%)	1 (7.1%)	ns
Laboratory data			
AST (IU/L)	93 (46-505)	144 (50-1234)	0.024
ALT (IU/L)	124 (52-742)	262 (65-1000)	0.023
T.Bil (mg/dL)	0.7 (0.3-18)	1.0 (0.3-2)	ns
ALP (U/L)	300 (144-1184)	300 (168-924)	ns
γ-GTP (U/L)	86 (16-875)	67 (13-405)	ns
IgG (mg/dL)	1959 (1096-3800)	1960 (1476-3793)	ns
ANA (≥ 1 : 40)	32 (94.1%)	14 (100%)	ns
SMA (≥ 1 : 40)	8/17 (47.1%)	3/6 (50%)	ns
HLA DR4	4/11 (36.4%)	2/5 (40%)	ns
Histological finding			
Grading			
A1	24 (70.6%)	5 (35.7%)	0.025
A2	10 (29.4%)	8 (57.1%)	
A3	0 (0%)	1 (7.1%)	
Staging			
F1	25 (73.5%)	10 (71.4%)	ns
F2	4 (11.8%)	2 (14.3%)	
F3	5 (14.7%)	1 (7.1%)	
F4	0 (0%)	1 (7.1%)	
AIH score			
Revised score	15 (10-19)	17 (12-20)	ns
Simplified score	6 (4-8)	6 (6-7)	ns

[1]Subgroup U1, normalized ALT and sustained remission; [2]Subgroup U2, non-normalized ALT or relapse. Continuous variables are expressed as median (range) values. The Mann-Whitney *U* test was used to evaluate differences in continuous variables between two groups. Dichotomous variables were compared by Pearson's χ^2 test. Values of $P < 0.05$ were considered significant. ALT: Alanine aminotransferase; AIH: Autoimmune hepatitis; AST: Aspartate transaminase; HLA: Human leukocyte antigen; ANA: Antinuclear antibody; ALP: Alkaline phosphatase; γ-GTP: γ-glutamyltransferase; SMA: Smooth muscle antibody; T.Bil: Total bilirubin; IgG: Immunoglobulin G; ns: No significant difference.

patients, 48 received UDCA (Group U) after diagnosis, and the remaining 88 received prednisolone (PSL) (Group P). Furthermore, Group U was divided into the following subgroups: Subgroup A, consisting of 33 patients with a serum alanine aminotransferase (ALT) level of 200 IU/L or lower at the start of treatment; Subgroup B, consisting of 29 patients in whom histological activity on liver biopsy before the start of treatment was determined to be A1 on the basis of the classification of Desmet *et al*[18]; Subgroup C, consisting of 24 patients who were included in both Subgroups A and B; Subgroup D consisting of 15 patients with a serum ALT level of 200 IU/L or higher at the start of treatment; Subgroup E consisting of 19 patients in whom histological activity was A2 or A3 before the start of treatment; and Subgroup F consisting of 10 patients who were included in both Subgroups D and E. The clinical characteristics of the study subjects are presented in Table 1.

In each group and subgroup described above, subsequent clinical courses, changes in treatment, and histological findings at the time of diagnosis were evaluated. Moreover, Group U was divided into Subgroup U1, consisting of patients who had achieved remission induction with UDCA monotherapy and showed no sign of relapse, and Subgroup U2, consisting of patients who additionally received PSL during follow-up. Laboratory test results and histopathological findings at the time of diagnosis were compared between Subgroups U1 and U2 (Table 2).

This study complied with the standards of the Declaration of Helsinki and the current ethical guidelines, and was approved by the institutional ethics board. Written, informed consent for participation in this study was not obtained from the patients, because this study did not report on a clinical trial and the data were retrospective in nature and analyzed anonymously.

Treatment

PSL was used as the standard initial treatment. Taking into account body weight, the initial dose was set between 30 and 40 mg/d, with subsequent reduction after improvement in liver function had been confirmed.

In mild clinical cases with both histological low-grade inflammatory activity and adequate residual capacity of

liver function, the initial treatment was UDCA alone. The initial dose of UDCA was set at 600 mg/d (10-13 mg/kg per day) in accordance with Japanese guideline for the treatment of PBC. The dosage was neither increased nor decreased during the treatment period. PSL was also administered, as described above, when an incomplete response to UDCA monotherapy or relapse was observed.

Follow-up

Each patient underwent a comprehensive clinical review and physical examination at each follow-up visit. Conventional laboratory blood tests were performed every 1-3 mo.

Criteria for the remission and relapse of AIH

Remission was defined as a normalization of serum ALT levels after the start of treatment. The judgement of remission for UDCA monotherapy was carried out within at least 18 mo after initiation of therapy. Relapse was defined as an increase in serum ALT levels to more than twice the upper normal limit following the normalization of serum ALT levels with medical treatment.

Statistical analysis

Statistical analysis was performed using the SPSS statistical program (release 16.0.1 J, SPSS, Inc., Chicago, IL). Continuous variables are expressed as medians and ranges. The Mann-Whitney *U* test was used to evaluate differences in continuous variables between two groups. Dichotomous variables were compared by Pearson's χ^2 test. Multivariate analyses by logistic regression were used to identify independent factors contributing to the response to UDCA monotherapy. Values of $P < 0.05$ were considered significant.

RESULTS

Comparison of clinical features among two groups classified according to initial treatment

As the initial treatment, of the 136 patients, 48 received UDCA monotherapy (Group U) and 88 received PSL monotherapy (Group P). There were no differences between Groups U and P in age, serum levels of alkaline phosphatase, the frequencies of positivity for antinuclear antibody or human leukocyte antigen DR4, and scores derived from either the old or the new scoring system. However, compared with Group P, Group U had significantly lower serum levels of aspartate transaminase (AST) (104 IU/L *vs* 303 IU/L, $P < 0.001$), ALT (149 IU/L *vs* 431 IU/L, $P < 0.001$), total bilirubin (0.8 mg/dL *vs* 1.3 mg/dL, $P < 0.05$), γ-glutamyltransferase (82 U/L *vs* 182 U/L, $P < 0.05$), and immunoglobulin G (1954 mg/dL *vs* 2336 mg/dL, $P < 0.01$), and lower frequencies of male sex, acute presentation, and positivity for smooth muscle antibody at the onset. Additionally, Group U had a significantly higher proportion of patients with mild inflammation and fibrosis (A1 and F1) on histological examination (28.4% *vs* 60.4%, $P < 0.01$, and 48.9% *vs* 72.9%, $P < 0.05$) (Table 1). Cumulative incidence of the normalization of serum ALT levels was 80% in Group P.

UDCA monotherapy as initial treatment

The follow-up durations were 49 (range: 8-156) mo in Group U. In Group U, 34 patients (71%) achieved and maintained remission over 49 (range = 8-90) mo (Subgroup U1), and 14 patients (29%) additionally received PSL during follow-up (Subgroup U2). Two patients in Subgroup U2 achieved remission induction once but additionally required PSL administration because of relapse (15 and 35 mo after the start of treatment). The remaining 12 patients in Subgroup U2 failed to achieve remission induction during follow-up, and PSL was added during 7 (range: 2-18) mo.

Comparison of clinical features among two subgroups classified according to the effect of UDCA

The rate of numbers was 73% in Subgroup U1 and 27% in Subgroup U2. Compared with Subgroup U2, Subgroup U1 had significantly lower ALT levels at onset (124 IU/L *vs* 262 IU/L, $P = 0.023$) and a significantly higher proportion of patients with mild inflammation (A1) on histological examination (70.6% *vs* 35.7%, $P = 0.025$) (Table 2). However, there were no differences between Subgroups U1 and U2 in other clinical features, as shown in Table 2.

Predictive factors associated with normalized ALT and sustained remission with UDCA monotherapy in AIH patients

When multivariate analysis was performed to identify factors contributing to the response to UDCA monotherapy, a serum ALT level of 200 IU/L or lower was found to be associated with a significant difference (Table 3).

On subgroup analysis, remission was induced and maintained by UDCA in 85%, 83% and 92% of patients in Subgroups A, B, and C, respectively. In these subgroups, high rates of remission induction and successful maintenance were achieved by UDCA. On the other hand, the rates of remission induction and successful maintenance in Subgroups D, E and F were low, at 40%, 53%, and 50%, respectively (Figure 1).

DISCUSSION

UDCA has been widely used as the first choice drug for the treatment of PBC[9-11]. This is because of its efficacy for cholestasis, exerted through its choleretic action which is well understood[19]. In addition to its choleretic action, UDCA reportedly has a protective action on hepatocytes and an immunomodulatory action[20]. In fact, it has also been reported that the administration of UDCA reduces elevated serum immunoglobulin levels in patients with PBC, which is one of the clinical characteristics of PBC[9,21]. *In vitro* studies have also shown that UDCA inhibits immunoglobulin production by peripheral lymphocytes in a concentration-dependent manner[22]. Although the

Table 3 Multivariate logistic regression analysis of factors associated with normalized alanine aminotransferase and sustained remission of ursodeoxycholic acid monotherapy in autoimmune hepatitis patients

Factor	Category	Odds ratio (95%CI)	*P*
ALT (IU/L)	> 200	1	
	≤ 200	10.8 (1.64-71.0)	0.013
Age	> 50	1	
	≤ 50	1.16 (0.21-6.38)	0.86
IgG	> 2000	1	
	≤ 2000	0.65 (0.10-4.32)	0.66
Acute presentation	No	1	
	Yes	4.13 (0.15-110.5)	0.4
Histological Grading	A2 or A3	1	
	A1	0.76 (0.10-5.88)	0.8
Histological Staging	F2 or F3 or F4	1	
	F1	0.41 (0.04-4.44)	0.46
AIH score (International diagnostic criteria)	> 15	1	
	≤ 15	2.66 (0.43-16.48)	0.29
AIH score (Simplified criteria)	> 6	1	
	≤ 6	5.46 (0.37-81.3)	0.22

ALT: Alanine aminotransferase; AIH: Autoimmune hepatitis.

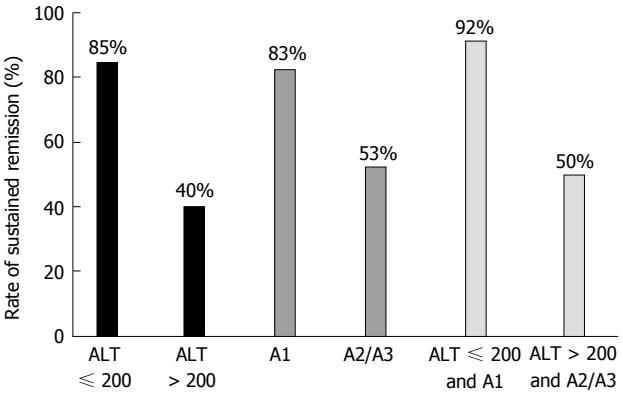

Figure 1 Remission rate of each subgroup with ursodeoxycholic acid therapy. Remission was induced and maintained by ursodeoxycholic acid in 85%, 83% and 92% of patients in Subgroups A, B and C, respectively. On the other hand, the rates of remission induction and successful maintenance in Subgroups D, E, and F are low, at 40%, 53% and 50%, respectively. ALT: Alanine aminotransferase.

UDCA level required to inhibit immunoglobulin production is approximately 10 times the blood concentration after administration of UDCA at routine doses[22], similarly high levels apparently exist in hepatocytes secreting bile, in other words, in the liver. Thus, UDCA may exert a liver-specific immunosuppressive action. This indicates that UDCA can be administered to achieve immunosuppression in patients with AIH. Miyake *et al*[13] demonstrated in a small-scale study that UDCA is effective for AIH. Moreover, the administration of UDCA has also been shown to allow corticosteroid doses to be tapered[14].

In this study, 71% of the UDCA group achieved and maintained the normalization of serum ALT levels with UDCA monotherapy. Especially, the present study also identified that in 85% of the patients with ALT levels of 200 IU/L or lower at the start of treatment, AIH remission could be induced and maintained by UDCA monotherapy. So, UDCA monotherapy will be effective in some Japanese AIH patients. However, in this study, patients treated with UDCA monotherapy had lower serum ALT levels and milder histological activity and fibrosis at presentation than those treated with PSL as shown in Table 1. Hence, it is necessary to consider that usefulness of UDCA was presented in mild AIH group. In the future, utility of UDCA must be confirmed in a prospective study.

On the other hand, among these mild AIH patients, the proportion indicated for UDCA monotherapy was low. On the bases of this finding, the patients in Group U can be considered to have no indications for treatment. In fact, 10-year survival in untreated patients with mild disease was reported to be 67%-90%[23,24], and in an uncontrolled study, untreated asymptomatic patients had similar survival to those receiving immunosuppression[25]. However, it also has to be acknowledged that untreated AIH has a fluctuating, unpredictable disease behavior, and a substantial proportion of asymptomatic patients become symptomatic during the course of their disease follow-up[25,26], and progression towards end-stage liver disease with liver failure and development of HCC is possible[24]. Muratori *et al*[27] also reported that patients with asymptomatic *vs* symptomatic AIH have similar courses of disease progression and responses to immu-nosuppressive agents, and should therefore receive the same treatment. Additionally, to exclude patients with transient liver damage that may not have required treatment, patients with no histological fibrosis (F0) were not enrolled in the present study.

According to the AIH Guidelines issued by the American Association for the Study of Liver Diseases in 2010, no treatment is needed for patients with AST and ALT levels close to or below the standard levels[1]. The patients included in the present study did not meet these criteria, but largely met the indications for treatment. While the efficacy of corticosteroids for the treatment of AIH has been established, treatment with corticosteroids is currently the first choice only in patients with appropriate indications[1,2]. However, corticosteroids are associated with adverse events, such that there is often reluctance to administer these drugs. In patients with AIH in Japan, the age at onset and diagnosis has been increasing annually[28]. Particularly in elderly women, many of whom are postmenopausal, there is actually considerable concern regarding osteoporosis. Moreover, in the treatment of AIH, prevention of relapse is the most important issue, and maintenance therapy is thus important. However, because many patients are women, drug compliance can actually be poor due to cosmetic issues. In addition, it has also been pointed out that the incidence of other adverse events is high in elderly patients. The present study subjects had an age distribution between 17 and 74 years, demonstrating that elderly patients with AIH associated

with mild liver disorders could be treated with UDCA. Moreover, when the therapeutic effects of UDCA become inadequate, treatment can be continued by switching to corticosteroids, as shown in the present study. Furthermore, treatment with UDCA also has the benefit of eventually allowing the corticosteroid dose to be tapered[14]. A recent nationwide survey on AIH in Japan showed that UDCA monotherapy is administered as the initial treatment in 20% of patients[28], so it is reasonable to assume that the treatment of AIH with UDCA is becoming clinically established. While Czaja *et al*[15] found UDCA to be effective in a double-blind study, it is important to define criteria for UDCA treatment indications, as in the present study. Although the present study had a retrospective design, the results allow the conclusion to be drawn that UDCA use may be considered in patients with a serum ALT level of 200 IU/L at the time of diagnosis, especially in those who are elderly. Prospective studies on the long-term outcomes of patients receiving UDCA monotherapy are needed.

COMMENTS

Background

Autoimmune hepatitis (AIH) is an unresolving progressive liver disease that affects females preferentially and is characterized by interface hepatitis, hypergammaglobulinemia, circulating autoantibodies, and a favorable response to immunosuppression. The aim of treatment in AIH is to obtain complete remission of the disease and to prevent further progression of liver disease, which generally requires permanent maintenance therapy. Corticosteroids have been widely used as the first choice drug treatment of AIH. However, long-term treatment with a generous corticosteroid dosage may induce side effects. Ursodeoxycholic acid (UDCA) has been widely used as the first choice for treating primary biliary cirrhosis (PBC) and has been established as clinically useful. No severe side effects have been reported during UDCA therapy for PBC. Although there are reports that UDCA is also useful for treating similar autoimmune liver diseases, its clinical value has not as yet been established. In this study, patients with a confirmed diagnosis of AIH who started treatment with UDCA alone were analyzed.

Research frontiers

There are few reports that UDCA monotherapy is effective for treating AIH. Moreover, the administration of UDCA has also been shown to allow corticosteroid doses to be tapered. However, its clinical value has not as yet been established.

Innovations and breakthroughs

Few prior reports showed that UDCA is effective in some AIH patients. However, there is no report which showed independent predictive factors associated with normalized ALT and sustained remission of UDCA monotherapy in AIH patients. The present study showed that ALT levels of 200 IU/L or lower associated with to response to UDCA monotherapy. The results of the authors' study contribute to predict the therapeutic effect of UDCA for patients with AIH.

Applications

This study suggests that that to prevent adverse events related to corticosteroids, treatment with UDCA alone for AIH needs to be considered in selected patients, especially those with an ALT level of 200 IU/L or lower.

Terminology

UDCA: One of the secondary bile acids, which are metabolic byproducts of intestinal bacteria. It has been widely used as the first choice drug for the treatment of PBC. This is because of its efficacy for cholestasis, exerted through its choleretic action which is well understood. In addition to its choleretic action, UDCA reportedly has a protective action on hepatocytes and an immunomodulatory action.

Peer-review

This is a very interesting cut off point for future prospective studies to confirm these retrospective results.

REFERENCES

1 **Mayo MJ**. Management of autoimmune hepatitis. *Curr Opin Gastroenterol* 2011; **27**: 224-230 [PMID: 21451411 DOI: 10.1097/MOG.0b013e3283457ce0]
2 **European Association for the Study of the Liver**. EASL Clinical Practice Guidelines: Autoimmune hepatitis. *J Hepatol* 2015; **63**: 971-1004 [PMID: 26341719 DOI: 10.1016/j.jhep.2015.06.030]
3 **Summerskill WH**, Korman MG, Ammon HV, Baggenstoss AH. Prednisone for chronic active liver disease: dose titration, standard dose, and combination with azathioprine compared. *Gut* 1975; **16**: 876-883 [PMID: 1104411 DOI: 10.1136/gut.16.11.876]
4 **Czaja AJ**. Safety issues in the management of autoimmune hepatitis. *Expert Opin Drug Saf* 2008; **7**: 319-333 [PMID: 18462189 DOI: 10.1517/14740338.7.3.319]
5 **Uribe M**, Go VL, Kluge D. Prednisone for chronic active hepatitis: pharmacokinetics and serum binding in patients with chronic active hepatitis and steroid major side effects. *J Clin Gastroenterol* 1984; **6**: 331-335 [PMID: 6481116]
6 **Lebovics E**, Schaffner F, Klion FM, Simon C. Autoimmune chronic active hepatitis in postmenopausal women. *Dig Dis Sci* 1985; **30**: 824-828 [PMID: 3875463]
7 **Wright SH**, Czaja AJ, Katz RS, Soloway RD. Systemic mycosis complicating high dose corticosteroid treatment of chronic active liver disease. *Am J Gastroenterol* 1980; **74**: 428-432 [PMID: 7234820]
8 **Czaja AJ**, Davis GL, Ludwig J, Taswell HF. Complete resolution of inflammatory activity following corticosteroid treatment of HBsAg-negative chronic active hepatitis. *Hepatology* 1984; **4**: 622-627 [PMID: 6745850]
9 **Poupon RE**, Balkau B, Eschwège E, Poupon R. A multicenter, controlled trial of ursodiol for the treatment of primary biliary cirrhosis. UDCA-PBC Study Group. *N Engl J Med* 1991; **324**: 1548-1554 [PMID: 1674105 DOI: 10.1056/NEJM199105303242204]
10 **Poupon RE**, Lindor KD, Cauch-Dudek K, Dickson ER, Poupon R, Heathcote EJ. Combined analysis of randomized controlled trials of ursodeoxycholic acid in primary biliary cirrhosis. *Gastroenterology* 1997; **113**: 884-890 [PMID: 9287980]
11 **Shi J**, Wu C, Lin Y, Chen YX, Zhu L, Xie WF. Long-term effects of mid-dose ursodeoxycholic acid in primary biliary cirrhosis: a meta-analysis of randomized controlled trials. *Am J Gastroenterol* 2006; **101**: 1529-1538 [PMID: 16863557 DOI: 10.1111/j.1572-0241.2006.00634.x]
12 **Lindor KD**, Dickson ER, Baldus WP, Jorgensen RA, Ludwig J, Murtaugh PA, Harrison JM, Wiesner RH, Anderson ML, Lange SM. Ursodeoxycholic acid in the treatment of primary biliary cirrhosis. *Gastroenterology* 1994; **106**: 1284-1290 [PMID: 8174890]
13 **Miyake Y**, Iwasaki Y, Kobashi H, Yasunaka T, Ikeda F, Takaki A, Okamoto R, Takaguchi K, Ikeda H, Makino Y, Ando M, Sakaguchi K, Yamamoto K. Efficacy of ursodeoxycholic acid for Japanese patients with autoimmune hepatitis. *Hepatol Int* 2009; **3**: 556-562 [PMID: 19847577 DOI: 10.1007/s12072-009-9155-9]
14 **Nakamura K**, Yoneda M, Yokohama S, Tamori K, Sato Y, Aso K, Aoshima M, Hasegawa T, Makino I. Efficacy of ursodeoxycholic acid in Japanese patients with type 1 autoimmune hepatitis. *J Gastroenterol Hepatol* 1998; **13**: 490-495 [PMID: 9641646]
15 **Czaja AJ**, Carpenter HA, Lindor KD. Ursodeoxycholic acid as adjunctive therapy for problematic type 1 autoimmune hepatitis: a randomized placebo-controlled treatment trial. *Hepatology* 1999;

30: 1381-1386 [PMID: 10573515 DOI: 10.1002/hep.510300603]
16 **Alvarez F**, Berg PA, Bianchi FB, Bianchi L, Burroughs AK, Cancado EL, Chapman RW, Cooksley WG, Czaja AJ, Desmet VJ, Donaldson PT, Eddleston AL, Fainboim L, Heathcote J, Homberg JC, Hoofnagle JH, Kakumu S, Krawitt EL, Mackay IR, MacSween RN, Maddrey WC, Manns MP, McFarlane IG, Meyer zum Büschenfelde KH, Zeniya M. International Autoimmune Hepatitis Group Report: review of criteria for diagnosis of autoimmune hepatitis. *J Hepatol* 1999; **31**: 929-938 [PMID: 10580593 DOI: 10.1016/S0168-8278(99)80297-9]
17 **Hennes EM**, Zeniya M, Czaja AJ, Parés A, Dalekos GN, Krawitt EL, Bittencourt PL, Porta G, Boberg KM, Hofer H, Bianchi FB, Shibata M, Schramm C, Eisenmann de Torres B, Galle PR, McFarlane I, Dienes H, Lohse AW. Simplified criteria for the diagnosis of autoimmune hepatitis. *Hepatology* 2008; **48**: 169-176 [PMID: 18537184DOI: 10.1002/hep.22322]
18 **Desmet VJ**, Gerber M, Hoofnagle JH, Manns M, Scheuer PJ. Classification of chronic hepatitis: diagnosis, grading and staging. *Hepatology* 1994; **19**: 1513-1520 [PMID: 8188183]
19 **Jazrawi RP**, de Caestecker JS, Goggin PM, Britten AJ, Joseph AE, Maxwell JD, Northfield TC. Kinetics of hepatic bile acid handling in cholestatic liver disease: effect of ursodeoxycholic acid. *Gastroenterology* 1994; **106**: 134-142 [PMID: 8276175]
20 **Lazaridis KN**, Gores GJ, Lindor KD. Ursodeoxycholic acid 'mechanisms of action and clinical use in hepatobiliary disorders'. *J Hepatol* 2001; **35**: 134-146 [PMID: 11495032 DOI: 10.1016/S0168-8278(01)00092-7]
21 **Kisand KE**, Karvonen AL, Vuoristo M, Färkkilä M, Lehtola J, Inkovaara J, Kisand KV, Miettinen T, Krohn K, Uibo R. Ursodeoxycholic acid treatment lowers the serum level of antibodies against pyruvate dehydrogenase and influences their inhibitory capacity for the enzyme complex in patients with primary biliary cirrhosis. *J Mol Med* (Berl) 1996; **74**: 269-272 [PMID: 8773263]
22 **Yoshikawa M**, Tsujii T, Matsumura K, Yamao J, Matsumura Y, Kubo R, Fukui H, Ishizaka S. Immunomodulatory effects of ursodeoxycholic acid on immune responses. *Hepatology* 1992; **16**: 358-364 [PMID: 1639344]
23 **De Groote J**, Fevery J, Lepoutre L. Long-term follow-up of chronic active hepatitis of moderate severity. *Gut* 1978; **19**: 510-513 [PMID: 680585]
24 **Czaja AJ**. Features and consequences of untreated type 1 autoimmune hepatitis. *Liver Int* 2009; **29**: 816-823 [PMID: 19018980 DOI: 10.1111/j.1478-3231.2008.01904.x]
25 **Feld JJ**, Dinh H, Arenovich T, Marcus VA, Wanless IR, Heathcote EJ. Autoimmune hepatitis: effect of symptoms and cirrhosis on natural history and outcome. *Hepatology* 2005; **42**: 53-62 [PMID: 15954109 DOI: 10.1002/hep.20732]
26 **Kogan J**, Safadi R, Ashur Y, Shouval D, Ilan Y. Prognosis of symptomatic versus asymptomatic autoimmune hepatitis: a study of 68 patients. *J Clin Gastroenterol* 2002; **35**: 75-81 [PMID: 12080231]
27 **Muratori P**, Lalanne C, Barbato E, Fabbri A, Cassani F, Lenzi M, Muratori L. Features and Progression of Asymptomatic Autoimmune Hepatitis in Italy. *Clin Gastroenterol Hepatol* 2016; **14**: 139-146 [PMID: 26192146 DOI: 10.1016/j.cgh.2015.07.017]
28 **Abe M**, Mashiba T, Zeniya M, Yamamoto K, Onji M, Tsubouchi H. Present status of autoimmune hepatitis in Japan: a nationwide survey. *J Gastroenterol* 2011; **46**: 1136-1141 [PMID: 21597932 DOI: 10.1007/s00535-011-0421-y]

P- Reviewer: Castiella A, Maroni L **S- Editor**: Qiu S **L- Editor**: A
E- Editor: Li D

World Journal of Hepatology

Submit a Manuscript: http://www.wjgnet.com/esps/
Help Desk: http://www.wjgnet.com/esps/helpdesk.aspx
DOI: 10.4254/wjh.v9.i1.64

World J Hepatol 2017 January 8; 9(1): 64-68
ISSN 1948-5182 (online)

ORIGINAL ARTICLE

Prospective Study

Shear wave elastography in hepatitis C patients before and after antiviral therapy

Toshikuni Suda, Osamu Okawa, Rion Masaoka, Yoshinori Gyotoku, Naohiko Tokutomi, Yasumi Katayama, Masaya Tamano

Toshikuni Suda, Osamu Okawa, Rion Masaoka, Yoshinori Gyotoku, Naohiko Tokutomi, Yasumi Katayama, Masaya Tamano, Department of Gastroenterology, Dokkyo Medical University Koshigaya Hospital, Saitama 343-8555, Japan

Author contributions: Tamano M designed the research; Suda T, Okawa O, Masaoka R, Gyoutoku Y and Tokutomi N performed the research; Suda T and Katayama Y analyzed the data; Suda T and Tamano M wrote the paper.

Institutional review board statement: This prospective study was reviewed and approved by the Ethics Committee of Dokkyo Medical University Koshigaya Hospital in Japan.

Informed consent statement: Written, informed consent was obtained from all participants and healthy volunteers in this study.

Conflict-of-interest statement: The authors have no conflicts of interest with regard to this research.

Data sharing statement: No additional data are available.

Manuscript source: Invited manuscript

Correspondence to: Masaya Tamano, Professor, Department of Gastroenterology, Dokkyo Medical University Koshigaya Hospital, 2-1-50 Minami-Koshigaya, Koshigaya-shi, Saitama 343-8555, Japan. mstamano@dokkyomed.ac.jp
Telephone: +81-48-9651111
Fax: +81-48-9651169

Received: August 10, 2016
Peer-review started: August 11, 2016
First decision: September 13, 2016
Revised: September 26, 2016
Accepted: November 1, 2016
Article in press: November 2, 2016
Published online: January 8, 2017

Abstract

AIM

To investigate shear wave (SW) propagation velocity in patients with untreated hepatitis C and patients with sustained virological response (SVR).

METHODS

A total of 136 hepatitis C patients [85 patients who had not received antiviral therapy (naïve group) and 51 patients who had received antiviral therapy and subsequently achieved SVR of at least 24 wk (SVR group)] and 58 healthy volunteers and outpatients without liver disease (control group) underwent evaluation of liver stiffness by SW elastography (SWE). Various parameters were evaluated in the chronic hepatitis C patients at the time of SWE.

RESULTS

SW propagation velocity (Vs) was 1.23 ± 0.14 m/s in the control group, 1.56 ± 0.32 m/s in the SVR group, and 1.69 ± 0.31 m/s in the naïve group. Significant differences were seen between the control group and the SVR group (P = 0.0000) and between the SVR group and the naïve group (P = 0.01417). All four fibrosis markers were higher in the naïve group than in the SVR group. In the naïve group, Vs was positively correlated with alanine aminotransferase (ALT) (r = 0.5372), α feto protein (AFP) (r = 0.4389), type Ⅳ collagen (r = 0.5883), procollagen Ⅲ peptide (P-Ⅲ-P) (r = 0.4140), hyaluronic acid (r = 0.4551), and Mac-2 binding protein glycosylation isomer (M2BPGi) (r = 0.6092) and negatively correlated with albumin (r = -0.4289), platelets (r = -0.5372), and prothrombin

activity (r = -0.5235). On multiple regression analysis, Vs was the most strongly correlated with ALT (standard partial regression std β = 0.4039, P = 0.00000). In the SVR group, Vs was positively correlated with AFP (r = 0.6977), type IV collagen (r = 0.5228), P-Ⅲ-P (r = 0.5812), hyaluronic acid (r = 0.5189), and M2BPGi (r = 0.6251) and negatively correlated with albumin (r = -0.4283), platelets (r = -0.4842), and prothrombin activity (r = -0.4771). On multiple regression analysis, Vs was strongly correlated with AFP (standard partial regression std β = 0.5953, P = 0.00000) and M2BPGi (standard partial regression std β= 0.2969, P = 0.03363).

CONCLUSION

In hepatitis C patients, liver stiffness is higher in treatment-naïve patients than in those showing SVR. SWE may be a predictor of hepatocarcinogenesis in SVR patients.

Key words: Hepatocarcinogenesis; Sustained virological response; Antiviral therapy; Shear wave elastography; Hepatitis C

Core tip: This study is the first to compare liver stiffness in a group of hepatitis C patients in whom the virus was eliminated with antiviral therapy and a group of untreated hepatitis C patients using shear wave elastography. The liver stiffness value was higher in the untreated group than in the group in which the virus had been eliminated, which is thought to be due hepatitis activity. This study also suggests the possibility that liver stiffness measurements with shear wave elastography can be used as predictors of hepatocarcinogenesis in patients in whom the virus has been eliminated.

Suda T, Okawa O, Masaoka R, Gyotoku Y, Tokutomi N, Katayama Y, Tamano M. Shear wave elastography in hepatitis C patients before and after antiviral therapy. *World J Hepatol* 2017; 9(1): 64-68 Available from: URL: http://www.wjgnet.com/1948-5182/full/v9/i1/64.htm DOI: http://dx.doi.org/10.4254/wjh.v9.i1.64

INTRODUCTION

Shear wave elastography (SWE) is a new technology that gauges liver stiffness by measuring the propagation velocity of shear waves generated in liver tissue. At the same time, images are observed in real time using a normal B-mode ultrasound probe. The velocity of laterally propagated shear waves (lateral waves) is measured. SWE is useful for a diagnosis of breast tumor[1], thyriod tumor[2], muscle stiffness[3] as well as liver stiffness. SWE resembles acoustic radiation force impulse[4], but it is new another technology.

Liver stiffness measurements with SWE are reported to be useful in diagnosing fibrosis in hepatitis C[5]. In studies using transient elastography, liver stiffness was affected not only by liver fibrosis but also by necroinflammatory activity[6,7]. Therefore, the meaning of liver stiffness is predicted to differ in untreated patients with hepatitis activity and patients whose hepatitis has subsided with antiviral therapy.

The purpose of this study was to investigate the significance of SW propagation velocity in patients with untreated hepatitis C and patients with sustained virological response.

MATERIALS AND METHODS

Patients

This prospective study was reviewed and approved by the Ethics Committee of Dokkyo Medical University Koshigaya Hospital, and written, informed consent was obtained from all participants and healthy volunteers. This study conformed to the ethical guidelines of the 2008 Declaration of Helsinki.

The subjects were 136 chronic hepatitis C patients who were diagnosed in the Department of Gastroenterology of Dokkyo Medical University Koshigaya Hospital from April to October, 2015. The 136 patients included 85 patients in a naïve group who had not received antiviral therapy and 51 patients who had received antiviral therapy, either interferon-based therapy or direct-acting antiviral agent therapy (daclatasvir/asunaprevir), and subsequently achieved sustained virological response (SVR) of at least 24 wk (SVR group). Patients with decompensated liver cirrhosis, hepatocellular carcinoma, autoimmune disease, collagen disease, or chronic heart disease were excluded. Patients with a history of drinking $\geqslant$ 20 g alcohol per day and those diagnosed with obvious fatty liver on abdominal ultrasound were also excluded.

To obtain a standard liver stiffness value, SWE was performed in a total of 58 people including healthy volunteers and outpatients without liver disease (control group).

Measurement of SWE

Measurement of liver stiffness by shear wave elastography was performed using a LOGIQ E9 (GE Healthcare, Milwaukee, WI). The right lobe of the liver was visualized through an intercostal space while the patient was lying in a supine position with the right arm in maximum abduction. Measurements were taken while subjects held their breath during spontaneous breathing. The visual depth of the system was fixed at 8 cm, and the region of interest was 1-2 cm below the surface of the liver. The system was adjusted so that sample volume depth was 4 cm or less. Liver stiffness was automatically calculated by the apparatus, and the results are expressed as the velocity of shear wave velocity (Vs) (m/s). Measurements were performed by two investigators (Suda T and Tamano M) who have measurement experience of SWE more than 100 patients. They shot 10 to 12 times on liver segment 5, and the result was considered reliable only when 10

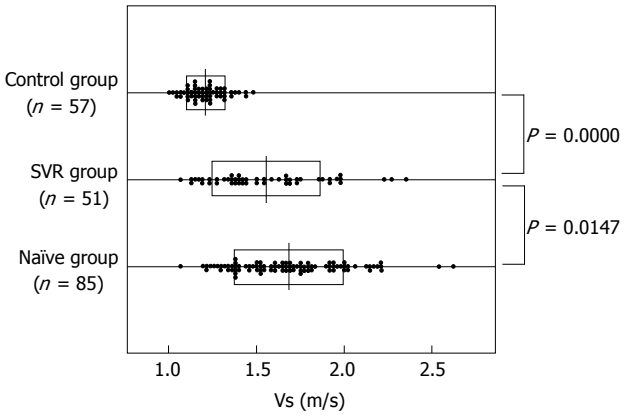

Figure 1 Velocity based on shear wave elastography is shown for each group. Vs is 1.23 ± 0.14 m/s in the control group, 1.56 ± 0.32 m/s in the sustained virological response (SVR) group, and 1.69 ± 0.31 m/s in the naïve group. Significant differences are seen between the control group and the SVR group (P = 0.0000) and between the SVR group and the naïve group (P = 0.01417). Vs: Velocity.

successful shots and a measurement success rate > 80% were obtained.

Clinical parameters

The following clinical parameters were determined in chronic hepatitis C patients at the time SWE was performed: Age; aspartate aminotransferase (AST); alanine aminotransferase (ALT); total bilirubin, serum albumin; white blood cell (WBC) count; platelet count; prothrombin activity; α fetoprotein (AFP); hyaluronic acid; type Ⅳ collagen; procollagen Ⅲ peptide (P-Ⅲ-P); Mac-2 binding protein glycosylation isomer (M2BPGi) measurements; and the Fib-4 index.

Statistical analysis

Continuous data for Vs and other clinical parameters are expressed as means ± SD. The Mann-Whitney *U* test was used for between-group comparisons. Correlations between Vs and other parameters were assessed using Spearman's rank correlation coefficient and multiple regression analysis. Values of $P < 0.05$ were regarded as statistically significant.

RESULTS

Figure 1 shows Vs (m/s) measured by SWE in each group. Vs was 1.23 ± 0.14 m/s in the control group, 1.56 ± 0.32 m/s in the SVR group, and 1.69 ± 0.31 m/s in the naïve group. Significant differences were seen between the control group and the SVR group (P = 0.0000) and between the SVR group and the naïve group (P = 0.01417).

Table 1 shows the characteristics of the naïve group and the SVR group. Compared with the SVR group, the naïve group had significantly higher AST and ALT values (P = 0.00001) and a significantly lower serum albumin value (P = 0.01049). No significant differences were seen between the two groups in total bilirubin, WBC, platelet count, or prothrombin activity. AFP was significantly higher in the naïve group than in the SVR group (P = 0.00773). All four fibrosis markers were higher in the naïve group than in the SVR group. No significant differences were seen in type Ⅳ collagen or hyaluronic acid, but significant differences were seen in P-Ⅲ-P (P = 0.00215) and M2BPGi (P = 0.00546). The FIB-4 index tended to be higher in the naïve group than in the SVR group, but the difference was not significant (P = 0.37443).

Table 1 Clinical characteristics in the Naïve and sustained virological response group

Characteristics	Naïve group (n = 85)	SVR group (n = 51)	P value
Age (yr)	63.5 ± 13.7	64.9 ± 10.2	0.9726
Sex (male/female)	43/42	27/24	0.79039
AST (IU/L)	55.4 ± 38.7	29.2 ± 16.8	0.00001
ALT (IU/L)	61.9 ± 50.1	23.9 ± 18.0	0.00001
Total bilirubin (mg/dL)	0.89 ± 0.36	0.95 ± 0.33	0.14736
Serum albmin (g/dL)	4.10 ± 0.46	4.32 ± 0.44	0.01049
WBC (× 10^3/mm^3)	5.21 ± 1.83	5.24 ± 1.56	0.79015
Hb (g/dL)	13.9 ± 1.6	14.1 ± 1.5	0.47879
Platelet (× 10^4/mm^3)	14.5 ± 6.4	14.5 ± 5.7	0.89078
Prothrombin activity (%)	97.5 ± 12.1	96.9 ± 13.1	0.98341
AFP (g/dL)	9.6 ± 10.6	5.1 ± 3.3	0.00773
Type Ⅳ collagen (ng/mL)	180.5 ± 71.8	179.2 ± 71.6	0.62913
P-Ⅲ-P (U/mL)	0.92 ± 0.27	0.81 ± 0.31	0.00215
Hyaluronic acid (ng/mL)	191.5 ± 290.3	102.1 ± 93.5	0.24908
M2BPGi (COI)	3.67 ± 4.41	2.03 ± 2.49	0.00546
FIB-4 index	4.44 ± 4.21	3.39 ± 2.63	0.37443

AST: Aspartate aminotransferase; ALT: Alanine aminotransferase; WBC: White blood cell; P-Ⅲ-P: Procollagen Ⅲ peptide; M2BP: Mac-2 binding protein; COI: Cut-off index.

Correlation between Vs and each parameter in the naïve group (n = 85)

Vs was positively correlated with ALT (r = 0.5372), AFP (r = 0.4389), type Ⅳ collagen (r = 0.5883), P-Ⅲ-P (r = 0.4140), hyaluronic acid (r = 0.4551), and M2BPGi (r = 0.6092). Vs was negatively correlated with albumin (r = -0.4289), platelets (r = -0.5372), and prothrombin activity (r = -0.5235). A multiple regression analysis was performed with the five parameters of ALT, platelets, prothrombin activity, type Ⅳ collagen, and M2BPGi that had correlation coefficients (r) ≥ 0.5, and the results showed that Vs was the most strongly correlated with ALT in the naïve group (standard partial regression std β = 0.4039, P = 0.00000) (Table 2).

Correlation between Vs and each parameter in the SVR group (n = 51)

Vs was positively correlated with AFP (r = 0.6977), type Ⅳ collagen (r = 0.5228), P-Ⅲ-P (r = 0.5812), hyaluronic acid (r = 0.5189), and M2BPGi (r = 0.6251). Vs was negatively correlated with albumin (r = -0.4283), platelets (r = -0.4842), and prothrombin activity (r = -0.4771). A multiple regression analysis was performed with the five parameters of AFP, type Ⅳ collagen, P-Ⅲ-P, hyaluronic acid, and M2BPGi that had correlation coefficients (r) ≥ 0.5, and the results showed that Vs was strongly correlated with two parameters, AFP

Table 2 Multiple regression analysis in the Naïve group

	Coefficient (β)	SE(β)	Std β	*t*-value	df	*P* value
ALT	0.00261	0.00052	0.4069	5.02998	62	0.00000
Plt	-0.0121	0.00436	-0.27300	0.27300	62	0.00740
PT %	-0.0044	0.00245	-0.1712	1.79923	62	0.07685
Type Ⅳ collagen	0.00061	0.00040	0.1578	1.51030	62	0.13605
M2BPGi	0.00844	0.00709	0.1361	1.19098	62	0.23820

ALT: Alanine aminotransferase; Plt: Blood platelet; PT: Prothrombin time; M2BP: Mac-2 binding protein.

(standard partial regression std β = 0.5953, *P* = 0.00000) and M2BPGi (standard partial regression std β = 0.2969, *P* = 0.03363) (Table 3).

DISCUSSION

The extent of hepatic fibrosis has classically been evaluated by histological procedures. However, the accuracy of this evaluation of hepatic fibrosis is limited by both sampling variability and inter-observer variability between pathologists[8,9]. In addition, liver biopsy is associated with patient discomfort and a risk of serious complications[10].

Transient elastography (TE) has attracted attention as a noninvasive, objective diagnostic tool, and liver stiffness measured by TE is reported to be useful in diagnosing fibrosis in hepatitis C[11]. TE is useful in diagnosing nonalcoholic fatty liver disease[12] and in predicting carcinoma development in viral hepatitis patients[13]. However, TE is a test that is done blindly using a special probe in the right hepatic lobe confirmed with B mode, as a result of which measurement results are imprecise if vessels or other structures are present in the measured region. SWE is built into ultrasonic diagnostic equipment, and reliable measurements are possible in a short time under observation with normal B mode[14].

The results of SWE measurements are expressed as the SW propagation velocity Vs (m/s). In this investigation, the Vs was 1.23 ± 0.14 m/s in healthy livers, 1.69 ± 0.31 m/s in the naïve group, and 1.56 ± 0.32 m/s in the SVR group. The naïve group had a significantly higher Vs than the SVR group, suggesting that Vs decreases with virus elimination in hepatitis C patients. In this study, however, the naïve group and SVR group were different populations, and Vs measurements over time in the same population will be needed to accurately compare Vs before and after treatment.

Vs is determined not only by tissue elasticity (fibrosis), but it is also affected by viscosity. Thus, in cases of active hepatitis, propagation is expected to become faster due to increased tissue viscosity from increased exudate into the interstitium and cell infiltration, and in acute hepatitis that trend is marked[15,16]. In the naïve group, Vs was most strongly correlated with ALT. This is thought to be because the naïve group included many patients with active hepatitis with high ALT levels. Good positive correlations were seen between Vs and the liver fibrosis markers of hyaluronic acid, type Ⅳ collagen, P-Ⅲ-P, and M2BPGi in the naïve group. Thus, in the naïve group, Vs is thought to reflect both hepatic activity (viscosity) and fibrosis (elasticity).

Table 3 Multiple regression analysis in the sustained virological response group

	Coefficient (β)	SE (β)	Std β	*t*-value	df	*P* value
AFP	0.05564	0.0098	0.5953	5.6797	28	0.00000
Type Ⅳ Collagen	-0.0003	0.00066	-0.0626	0.42483	28	0.67420
P-Ⅲ-P	0.13859	0.17013	0.146	0.81462	28	0.42217
Hyaluronic acid	0.00053	0.00053	0.1658	0.99713	28	0.32724
M2BPGi	0.03554	0.01591	0.2969	2.23421	28	0.03363

AFP: α feto protein; P-Ⅲ-P: Procollagen Ⅲ peptide; M2BP: Mac-2 binding protein.

In the SVR group, hepatitis had subsided for six months or more, and, in fact, the correlation between Vs and ALT in the SVR group in this study was very low. Therefore, Vs in the SVR group is presumed to almost purely reflect liver fibrosis (elasticity), and thus it is thought to have better correlations with fibrosis markers. Among the four different fibrosis markers, M2BPGi had the strongest positive correlation with Vs. M2BPGi is a new liver fibrosis marker that quantitatively measures changes in the carbohydrate structure of Mac-2 binding protein[17], and it is also considered useful in predicting carcinogenesis in hepatitis C patients[18-20].

In hepatitis C patients, AFP is a useful indicator of hepatocarcinogenesis following interferon therapy[21]. Although AFP had positive correlations in both the naïve group and the SVR group, a stronger correlation was seen in the SVR group. In the naïve group, AFP reflects inflammation and necrosis of hepatocytes and the accompanying hepatocyte regeneration. In the SVR group, on the other hand, AFP has a strong element as a surrogate marker of hepatocellular carcinoma, as mentioned previously. A very interesting finding in the SVR group in the present study was the strong correlations between Vs and AFP and between Vs and M2BPGi, which suggest the possibility that liver stiffness measurements with SWE may be used as predictors of hepatocarcinogenesis in hepatitis C patients following SVR.

In hepatitis C patients, liver stiffness with SWE was higher in the naïve group than in the SVR group, presumably due to hepatitis activity. In the SVR group, liver stiffness measurements with SWE may be a predictor of hepatocarcinogenesis.

COMMENTS

Background

Shear wave elastography (SWE) is a new technology that gauges liver stiffness by measuring the propagation velocity of shear waves generated in liver tissue. At the same time, images are observed in real time using a normal B-mode ultrasound probe. The velocity of laterally propagated shear waves (lateral waves) is measured.

Research frontiers

The results of SWE measurements are expressed as the SW propagation velocity Vs (m/s). In this investigation, the Vs was 1.23 ± 0.14 m/s in healthy livers, 1.69 ± 0.31 m/s in the naïve group, and 1.56 ± 0.32 m/s in the SVR group. The naïve group had a significantly higher Vs than the SVR group, suggesting that Vs decreases with virus elimination in hepatitis C patients. In this study, however,

the naïve group and sustained virological response (SVR) group were different populations, and Vs measurements over time in the same population will be needed to accurately compare Vs before and after treatment.

Innovations and breakthroughs

A very interesting finding in the SVR group in the present study was the strong correlations between Vs and α feto protein and between Vs and Mac-2 binding protein glycosylation isomer, which suggest the possibility that liver stiffness measurements with SWE may be used as predictors of hepatocarcinogenesis in hepatitis C patients following SVR.

Applications

In the SVR group, liver stiffness measurements with SWE may be a predictor of hepatocarcinogenesis.

Peer-review

This manuscript by Suda *et al* points to assess the changes of shear wave velocity in patients with untreated chronic hepatitis C and patients who received antiviral therapy and obtained SVR. The authors found significant differences between shear wave velocity between patients with SVR and those untreated.

REFERENCES

1 **Zhang Q**, Xiao Y, Dai W, Suo J, Wang C, Shi J, Zheng H. Deep learning based classification of breast tumors with shear-wave elastography. *Ultrasonics* 2016; **72**: 150-157 [PMID: 27529139 DOI: 10.1016/j.ultras.2016.08.004]

2 **Gangadhar K**, Hippe DS, Thiel J, Dighe M. Impact of Image Orientation on Measurements of Thyroid Nodule Stiffness Using Shear Wave Elastography. *J Ultrasound Med* 2016; **35**: 1661-1667 [PMID: 27335441 DOI: 10.7863/ultra.15.10016]

3 **Du LJ**, He W, Cheng LG, Li S, Pan YS, Gao J. Ultrasound shear wave elastography in assessment of muscle stiffness in patients with Parkinson's disease: a primary observation. *Clin Imaging* 2016; **40**: 1075-1080 [PMID: 27408992 DOI: 10.1016/j.clinimag.2016.05.008]

4 **Osakabe K**, Ichino N, Nishikawa T, Sugiyama H, Kato M, Shibata A, Asada W, Kawabe N, Hashimoto S, Murao M, Nakano T, Shimazaki H, Kan T, Nakaoka K, Takagawa Y, Ohki M, Kurashita T, Takamura T, Yoshioka K. Changes of shear-wave velocity by interferon-based therapy in chronic hepatitis C. *World J Gastroenterol* 2015; **21**: 10215-10223 [PMID: 26401087 DOI: 10.3748/wjg.v21.i35.10215]

5 **Tada T**, Kumada T, Toyoda H, Ito T, Sone Y, Okuda S, Tsuji N, Imayoshi Y, Yasuda E. Utility of real-time shear wave elastography for assessing liver fibrosis in patients with chronic hepatitis C infection without cirrhosis: Comparison of liver fibrosis indices. *Hepatol Res* 2015; **45**: E122-E129 [PMID: 25580959 DOI: 10.1111/hepr.12476]

6 **Lupşor M**, Badea R, Stefănescu H, Grigorescu M, Sparchez Z, Serban A, Branda H, Iancu S, Maniu A. Analysis of histopathological changes that influence liver stiffness in chronic hepatitis C. Results from a cohort of 324 patients. *J Gastrointestin Liver Dis* 2008; **17**: 155-163 [PMID: 18568136]

7 **Coco B**, Oliveri F, Maina AM, Ciccorossi P, Sacco R, Colombatto P, Bonino F, Brunetto MR. Transient elastography: a new surrogate marker of liver fibrosis influenced by major changes of transaminases. *J Viral Hepat* 2007; **14**: 360-369 [PMID: 17439526 DOI: 10.1111/j.1365-2893.2006.00811.x]

8 **Regev A**, Berho M, Jeffers LJ, Milikowski C, Molina EG, Pyrsopoulos NT, Feng ZZ, Reddy KR, Schiff ER. Sampling error and intraobserver variation in liver biopsy in patients with chronic HCV infection. *Am J Gastroenterol* 2002; **97**: 2614-2618 [PMID: 12385448 DOI: 10.1111/j.1572-0241.2002.06038.x]

9 **Bedossa P**, Dargère D, Paradis V. Sampling variability of liver fibrosis in chronic hepatitis C. *Hepatology* 2003; **38**: 1449-1457 [PMID: 14647056 DOI: 10.1016/j.hep.2003.09.022]

10 **Piccinino F**, Sagnelli E, Pasquale G, Giusti G. Complications following percutaneous liver biopsy. A multicentre retrospective study on 68,276 biopsies. *J Hepatol* 1986; **2**: 165-173 [DOI: 10.1016/S0168-8278(86)80075-7 PMID: 3958472]

11 **Sandrin L**, Fourquet B, Hasquenoph JM, Yon S, Fournier C, Mal F, Christidis C, Ziol M, Poulet B, Kazemi F, Beaugrand M, Palau R. Transient elastography: a new noninvasive method for assessment of hepatic fibrosis. *Ultrasound Med Biol* 2003; **29**: 1705-1713 [PMID: 14698338 DOI: 10.1016/j.ultrasmedbio.2003.07.001]

12 **Yoneda M**, Yoneda M, Fujita K, Inamori M, Tamano M, Hiriishi H, Nakajima A. Transient elastography in patients with non-alcoholic fatty liver disease (NAFLD). *Gut* 2007; **56**: 1330-1331 [PMID: 17470477 DOI: 10.1136/gut.2007.126417]

13 **Akima T**, Tamano M, Hiraishi H. Liver stiffness measured by transient elastography is a predictor of hepatocellular carcinoma development in viral hepatitis. *Hepatol Res* 2011; **41**: 965-970 [DOI: 10.1111/j.1872-034X.2011.00846.x]

14 **Ferraioli G**, Parekh P, Levitov AB, Filice C. Shear wave elastography for evaluation of liver fibrosis. *J Ultrasound Med* 2014; **33**: 197-203 [PMID: 24449721 DOI: 10.7863/ultra.33.2.197]

15 **Kim SU**, Han KH, Park JY, Ahn SH, Chung MJ, Chon CY, Choi EH, Kim DY. Liver stiffness measurement using FibroScan is influenced by serum total bilirubin in acute hepatitis. *Liver Int* 2009; **29**: 810-815 [PMID: 19018979 DOI: 10.1111/j.1478-3231.2008.01894.x]

16 **Arena U**, Vizzutti F, Corti G, Ambu S, Stasi C, Bresci S, Moscarella S, Boddi V, Petrarca A, Laffi G, Marra F, Pinzani M. Acute viral hepatitis increases liver stiffness values measured by transient elastography. *Hepatology* 2008; **47**: 380-384 [PMID: 18095306 DOI: 10.1002/hep.22007]

17 **Kuno A**, Ikehara Y, Tanaka Y, Ito K, Matsuda A, Sekiya S, Hige S, Sakamoto M, Kage M, Mizokami M, Narimatsu H. A serum "sweet-doughnut" protein facilitates fibrosis evaluation and therapy assessment in patients with viral hepatitis. *Sci Rep* 2013; **3**: 1065 [PMID: 23323209 DOI: 10.1038/srep01065]

18 **Tamaki N**, Kurosaki M, Kuno A, Korenaga M, Togayachi A, Gotoh M, Nakakuki N, Takada H, Matsuda S, Hattori N, Yasui Y, Suzuki S, Hosokawa T, Tsuchiya K, Nakanishi H, Itakura J, Takahashi Y, Mizokami M, Narimatsu H, Izumi N. Wisteria floribunda agglutinin positive human Mac-2-binding protein as a predictor of hepatocellular carcinoma development in chronic hepatitis C patients. *Hepatol Res* 2015; **45**: E82-E88 [PMID: 25559682 DOI: 10.1111/hepr.12466]

19 **Sasaki R**, Yamasaki K, Abiru S, Komori A, Nagaoka S, Saeki A, Hashimoto S, Bekki S, Kugiyama Y, Kuno A, Korenaga M, Togayachi A, Ocho M, Mizokami M, Narimatsu H, Ichikawa T, Nakao K, Yatsuhashi H. Serum Wisteria Floribunda Agglutinin-Positive Mac-2 Binding Protein Values Predict the Development of Hepatocellular Carcinoma among Patients with Chronic Hepatitis C after Sustained Virological Response. *PLoS One* 2015; **10**: e0129053 [PMID: 26070204 DOI: 10.1371/journal.pone.0129053]

20 **Yamasaki K**, Tateyama M, Abiru S, Komori A, Nagaoka S, Saeki A, Hashimoto S, Sasaki R, Bekki S, Kugiyama Y, Miyazoe Y, Kuno A, Korenaga M, Togayachi A, Ocho M, Mizokami M, Narimatsu H, Yatsuhashi H. Elevated serum levels of Wisteria floribunda agglutinin-positive human Mac-2 binding protein predict the development of hepatocellular carcinoma in hepatitis C patients. *Hepatology* 2014; **60**: 1563-1570 [PMID: 25042054 DOI: 10.1002/hep.27305]

21 **Asahina Y**, Tsuchiya K, Nishimura T, Muraoka M, Suzuki Y, Tamaki N, Yasui Y, Hosokawa T, Ueda K, Nakanishi H, Itakura J, Takahashi Y, Kurosaki M, Enomoto N, Nakagawa M, Kakinuma S, Watanabe M, Izumi N. α-fetoprotein levels after interferon therapy and risk of hepatocarcinogenesis in chronic hepatitis C. *Hepatology* 2013; **58**: 1253-1262 [PMID: 23564522 DOI: 10.1002/hep.26442]

P- Reviewer: Pawlowska M, Pekgoz M, Stanciu C **S- Editor**: Qi Y
L- Editor: A **E- Editor**: Li D

Published by **Baishideng Publishing Group Inc**
8226 Regency Drive, Pleasanton, CA 94588, USA
Telephone: +1-925-223-8242
Fax: +1-925-223-8243
E-mail: bpgoffice@wjgnet.com
Help Desk: http://www.wjgnet.com/esps/helpdesk.aspx
http://www.wjgnet.com